Characterization of the persisting HIV-1 reservoir in early treated children on long-term suppressive ARV regimens

By

Mary Grace Kato Katusiime

Dissertation presented for the Degree of Doctor of Philosophy in the Faculty of Health Sciences, at Stellenbosch University

Supervisor: Prof. Gert van Zyl

Co-supervisor: Prof. John Mellors

Co-supervisor: Prof. Susan Engelbrecht

December 2019

Declaration

By submitting this dissertation electronically, I declare that the entirety of the work contained therein is my own, original work, that I am the sole author thereof (save to the extent explicitly otherwise stated), that reproduction and publication thereof by Stellenbosch University will not infringe any third party rights and that I have not previously in its entirety or in part submitted it for obtaining any qualification.

Mary Grace Kato Katusiime

December 2019

Abstract

Introduction:

The major barrier to curing HIV-1 infection is a latent reservoir of long-lived, replication-competent proviruses that persists despite suppressive antiretroviral therapy (ART). Initiating ART during acute infection limits the development of phylogenetically diverse reservoirs. Novel approaches for reservoir elimination are emerging, providing hope for a cure. Perinatally infected, early-treated children, are likely good candidates for cure interventions as they have low immune activation states and a low proportion of central memory T-cells. We studied the post-CHER cohort of perinatally infected children, who initiated ART during acute infection and are in long-term follow-up. To inform cure interventions, we aimed to: (i) quantify latently infected cells and describe longitudinal genetic diversity, (ii) describe mechanisms that enable long-term reservoir persistence, (iii) describe the extent to which early therapy shapes the proviral landscape.

Methods:

In Aim I, we used a sensitive quantitative PCR assay for HIV-1 cell associated DNA (iCAD), followed by cell-associated DNA-single genome sequencing (CAD-SGS) of 1200bp in HIV-1 *gag-pol* to investigate genetic evolution in the reservoir during long-term ART. We performed 3 tests for evolution: (i) average pairwise distance (APD) for intra-patient viral population diversity, (ii) panmixia for probability of shifts in viral population structure, (iii) maximum likelihood (ML) root-to-tip distances to detect emergence of new viral populations.

In Aim II, we performed integration site analysis (ISA) on samples from close to therapy initiation (baseline) and after 6-9 years on ART to investigate clonal expansion as a mechanism for reservoir persistence despite early, suppressive therapy.

In Aim III, near full length- proviral amplification and sequencing (NFL-PAS) was performed to determine the proportion of genetically intact vs defective proviruses after 6-9 years on ART.

Findings:

We found low iCAD levels (median iCAD:22.45cp/10^6) in 16 children who initiated ART within the first 18 months of life. No significant changes in intra-patient proviral diversity, shifts in viral population structure or emergence of new viral populations were detected in children who were fully suppressed on ART, suggesting that ART prevents ongoing replication that replenishes the reservoir.

ISA detected expanded clones in baseline samples of 6 children treated as early as 2 months of age, suggesting that infected cells begin clonally expanding before ART. Furthermore, there was a significant increase in the proportion of expanded clones after several years.

A total of 738 NFL amplicons were generated from 9 children. Of these, 72.9% had large internal deletions, 23.7% were hypermutated, 1.4% had small internal deletions, and 1% had deletions in the *gag*-leader region. Intact proviruses were detected at a frequency of 1%.

This study showed that early therapy and long-term suppression in children leads to limited reservoir size and genetic diversity, factors that are favourable for cure interventions. The reservoir appears to be maintained by clonal expansion that begins before therapy is initiated. Although a large proportion of proviral DNA in long-term suppressed children is defective, genetically intact variants persist and likely form part of expanded clones. This suggests the need for novel approaches that target HIV reservoirs by reducing proliferation of cells that harbour replication-competent proviruses.

Opsomming

Inleiding:

Die groot hindernis in die soektog na ’n geneesmiddel vir MIV-1-infeksie is ’n latente reservoir langlewende, replikasievaardige provirusse wat ondanks doeltreffende antiretrovirale terapie (ART) oorleef. Die aanvang van ART gedurende akute infeksie beperk die saaiing en ontwikkeling van filogeneties diverse reservoirs. Namate die vakgebied verder ontwikkel, kom nuwe benaderings aan die lig om dié reservoir uit te wis, wat hoop bied vir ’n geneesmiddel. Kinders wat perinataal geïnfekteer is en vroeg reeds met behandeling begin, is waarskynlik goeie kandidate vir genesingsintervensies omdat hulle laer immuunaktiveringstoestande en minder sentralegeheue-T-selle as volwassenes het. Die CHER-kohort (“Children with HIV Early Antiretroviral Therapy”) is ’n groep perinataal geïnfekteerde kinders van wie sommige gedurende akute infeksie reeds met ART begin het en die afgelope dekade deur middel van opvolgbesoeke gemoniteer is. Om die soektog na ’n geneesmiddel te ondersteun, was die doel van hierdie studie (i) om latent geïnfekteerde selle te kwantifiseer en provirale genetiese diversiteit oor tyd te beskryf, (ii) om meganismes te beskryf wat die reservoir in staat stel om op lang termyn te oorleef, en (iii) om te beskryf watter invloed vroeë terapie op die provirale landskap by ’n substel van die CHER-kohort het.

Metodes:

Vir doelwit I is ’n sensitiewe kwantitatiewe PCR-toets vir MIV-1-selverwante DNS (CAD) by 16 kinders gebruik, gevolg deur selverwante DNS-enkelgenoomreeksvorming (CAD-SGS) van ’n 1 200 bp-fragment wat oor MIV-1-gag-pol strek, om die genetiese evolusie in die reservoir ná ses tot nege jaar op behandeling te ondersoek. Daarna is drie sensitiewe evolusietoetse uitgevoer: (i) gemiddelde paarsgewyse afstand (APD) om virale populasiediversiteit binne pasiënte te bepaal, (ii) panmiksie (lukrake paring) om die waarskynlikheid van verskuiwings in virale populasiestruktuur vas te stel, en (iii) maksimumaanneemlikheids- (ML-)afstande van wortel tot punt om die ontwikkeling van nuwe virale populasies op te spoor.

Vir doelwit II is integrasiesetelontleding (ISA) op monsters van 12 kinders uitgevoer na aan terapieaanvang (basislyn) en weer ná ses tot nege jaar op ART. Die doel hiermee was om klonale uitbreiding te ondersoek as ’n meganisme vir reservoir-oorlewing ondanks vroeë, langdurige onderdrukkingsterapie.

Vir doelwit III is byna-vollengte- provirale versterking en reeksvorming (NFL-PAS) op nege kinders uitgevoer om die MIV-1- provirale landskap te beskryf en die hoeveelheid geneties ongeskonde teenoor disfunksionele provirusse ná ses tot nege jaar op ART te bepaal.

Bevindinge:

CAD-ladings was laag (mediaan: 22,45 cp/106) vir die 16 kinders wat binne die eerste 18 maande ná geboorte met ART begin het, wat daarop dui dat vroeë behandeling die frekwensie van latent-geïnfekteerde selle beperk. Geen beduidende veranderinge in provirale diversiteit binne pasiënte, verskuiwings in virale

populasiestruktuur óf ontwikkeling van nuwe virale populasies is opgemerk by kinders wie se toestand ten volle onderdruk is op ART nie. Dít gee te kenne dat ART voortdurende replikasiesiklusse, wat die reservoir kan aanvul, voorkom.

ISA het op uitgebreide klone afgekom in voor-ART-monsters van ses kinders wat op so jonk as twee maande met terapie begin het, wat daarop dui dat geïnfekteerde selle klonaal begin uitbrei reeds voordat ART kort ná geboorte by kinders aangevoor word. Daarbenewens het die hoeveelheid uitgebreide klone ná ’n aantal jaar beduidend toegeneem.

Van die 738 NFL-amplikone wat van nege kinders verkry is, het 72,9% groot interne delesies gehad, 23,7% hipermutasie, 1,4% klein interne delesies, en 1% delesies in die verpakkingsein/groot splitsskenkersetel. Seldsame ongeskonde provirusse is teen ’n frekwensie van 1% opgespoor, wat soortgelyk is aan volwassenes wat gedurende akute infeksie behandel word.

Acknowledgements

I would like to acknowledge the following individuals for their invaluable contributions throughout this journey:

My supervisor Prof van Zyl, thank you for being reliable, enthusiastic, available and involved, for all the opportunities to grow as a researcher, for your insights, guidance and constant support.

My co-supervisor Prof John Mellors and his team at the University of Pittsburgh, thank you for your expert training, valuable insights, and the opportunity to learn and apply new skills to my research.

My co-supervisor Prof Susan Engelbrecht, thank you for always being available to provide guidance and support.

Prof Mark Cotton, the entire Reservoir study team and all study participants from the CHER and post CHER cohorts without whom none of this would have been possible.

Our collaborators Dr Mary Kearney, Dr Wei Shao, Michael Bale, Dr Imogen Wright, your expert contributions have made all the findings of this study possible.

The National Research Foundation (NRF), the Poliomyelitis Research Foundation (PRF), the Margaret McNamara Education Grant (MMEG), and the National Institute of Health (NIH), thank you for your financial support.

My colleagues in the division of Medical Virology, thank you for the camaraderie, your friendship and support.

My friends Bronwyn, Hilory, Don, Dora, Jos, Hannah, Tammy, Amo, Ntho, Johéan and so many others, thank you for walking this road with me, for bringing the balance, you make life colourful and meaningful.

My brothers Benjamin and Emmanuel, thank you for motivating me, encouraging and believing in me.

My Godmother Aunty Di, I am so thankful for you and all you do.

My dad, I am thankful for every sacrifice seen and unseen, every prayer, every word of encouragement, for believing in me, I take none of it for granted.

My mother and hero, I know that I stand on the shoulders of giants, you never got the chance to see me reach this season, but you always said I would, and I hope that I have made you proud.

My Heavenly Father I owe you everything, you have walked me through the highest highs and lowest valleys, I can confidently say:

"**I have known and relied on the love that God has for me**". – 1 John 4:16

Research Outputs

Peer reviewed publications:

Van Zyl, G.U., Katusiime, M.G., Wiegand, A., McManus, W.R., Bale, M.J., Halvas, E.K., Luke, B., Boltz, V.F., Spindler, J., Laughton, B., Engelbrecht, S., Coffin, J.M., Cotton, M.F., Shao, W., Mellors, J.W., Kearney, M.F., 2017. No evidence of HIV replication in children on antiretroviral therapy. Journal of Clinical Investigation. 127, 3827–3834.

Conference Presentations:

Katusiime, M.G., Van Zyl, G.U., Wiegand, A., McManus, W.R., Bale, M.J., Halvas, E.K., Luke, B., Boltz, V.F., Spindler, J., Laughton, B., Engelbrecht, S., Coffin, J.M., Cotton, M.F., Shao, W., Mellors, J.W., Kearney, M.F., 2017. Characterizing the persisting reservoir in post-CHER patients on long-term suppressive regimens. Pathology Research Day, Stellenbosch University, 9 June 2016.

Katusiime, M.G., Van Zyl, G.U., Wiegand, A., McManus, W.R., Bale, M.J., Halvas, E.K., Luke, B., Boltz, V.F., Spindler, J., Laughton, B., Engelbrecht, S., Coffin, J.M., Cotton, M.F., Shao, W., Mellors, J.W., Kearney, M.F., 2017. Characterizing the persisting reservoir in post-CHER patients on long-term suppressive regimens. Annual Academic Year Day, Stellenbosch University, 11 August 2016.

Katusiime, M.G., Van Zyl, G.U., Wiegand, A., McManus, W.R., Bale, M.J., Halvas, E.K., Luke, B., Boltz, V.F., Spindler, J., Laughton, B., Engelbrecht, S., Coffin, J.M., Cotton, M.F., Shao, W., Mellors, J.W., Kearney, M.F., 2017. No Evidence of Ongoing HIV Replication in children after 7 Years on ART. Conference on Retroviruses and Opportunistic infections (CROI), Seattle, USA, 13-16 February 2017.

Katusiime, M.G., Van Zyl, G.U., Wiegand, A., McManus, W.R., Bale, M.J., Halvas, E.K., Luke, B., Boltz, V.F., Spindler, J., Laughton, B., Engelbrecht, S., Coffin, J.M., Cotton, M.F., Shao, W., Mellors, J.W., Kearney, M.F., 2017. No Evidence of Ongoing HIV Replication in children after 7 Years on ART. Annual Academic Day, Stellenbosch University, 30 August 2017.

Katusiime, M.G, Bale M.J., Wright, I., Shao, W., Shau, W., Cotton, M., Mellors, J.W., Kearney, M.F., van Zyl, G.U. Intact HIV proviruses are detectable 7-9 years later when ART starts after 3 months. Conference on Retroviruses and Opportunistic infections (CROI), Seattle, USA, 4-7 March 2019.

Table of Contents

List of Figures

List of Tables

List of Abbreviations

Abbreviation	Full Text
3TC	Lamivudine
AML	Acute myeloid leukemia
APCs	Antigen presenting cells
APD	Average pairwise distance
ART	Antiretroviral therapy
ATI	Analytical treatment interruption
AU_log_VLC	Area under log viral load curve
AZT	Zidovudine
bNabs	Broadly neutralising antibodies
bp	Base pairs
CAD-SGS	Cell associated DNA-single genome sequencing
CAR	Cell associated ribonucleic acid
cART	Combination antiretroviral therapy
CCR5	Chemokine receptor type 5
CD4	Cluster of differentiation 4
cDNA	Complementary Deoxyribonucleic acid
CHER	Children with early antiretroviral therapy cohort
CMV	Cytomegalovirus
CNS	Central nervous system
CRF	Circulating recombinant forms
CRS	Cis-acting repressive sequences
CSF	Cerebrospinal fluid
ct	Cycle threshold
CTL	Cytotoxic T-Lymphocyte
DNA	Deoxyribonucleic Acid
dNTP	Deoxyribonucleotides
dPCR	Digital polymerase chain reaction
DTT	Dithiothreitol
EDTA	Ethylenediaminetetraacetic acid
EFV	Efavirenz
Eg	Example
ET	Early therapy
FISH	Fluorescent in-situ hybridisation
GALT	Gut- associated lymphoid tissue
gDNA	Genomic Deoxyribonucleic Acid
HDAC	Histone deacetylases
HDACi	Histone deacetylase inhibitors
HIV	Human immunodeficiency virus
HMT	Histone methyltransferases
HSCT	Hematopoietic stem cell transplantation0
HSPC	Hematopoietic stem/progenitor cells
iCAD	Integrase cell-associated Deoxyribonucleic Acid
IE	Integration Event

IN	Integrase
IS	Integration site
ISA	Integration site analysis
IUPM	Infectious units per million
Kb	Kilo base pairs
KIDCRU	Children's Infectious Diseases Clinical Research Unit of Tygerberg Hospital
KLT	Kalentra
LLV	Low level viremia
LPV	Lopinavir
LRA	Latency reversal agents
LTR	Long terminal repeats
mgCl	Magnesium chloride
MHC-1	Major histocompatibility complex-1
min	Minutes
ML	Maximum Likelihood
mM	Mili-molar
mRNA	Messenger ribonucleic Acid
ms RNA	Multiply spliced Ribonucleic Acid
MSD	Major splice donor site
NFL-PAS	Near full length-Proviral amplification and sequencing
NHP	Non-human primates
NK	Natural killer
nM	Nano-molar
Nt	Nucleotide
ORF	Open reading frame
PBMC	Peripheral blood mononuclear cells
PBS	Primer binding site
PCR	Polymerase chain reaction
PD-1	Programmed cell death protein-1
PD-L1	Programmed cell death ligand-1
PIC	Pre-integration complex
PID	Patient identification
PKC	Protein kinase agonists
PPT	Polypurine tract
PR	Protease
psi	Packaging signal
qPCR	Quantitative polymerase chain reaction
qVOA	Quantitative viral outgrowth assay
Rev	Regulator of viral expression
RNA	Ribonucleic Acid
RRE	Rev responsive element
RT	Reverse transcriptase
RT-PCR	Real time-Polymerase Chain Reaction
rxn	Reaction
s	Seconds
SB	Sodium borate

SGS	Single genome sequencing
siRNA	Small interfering Ribonucleic Acid
SIV	Simian immunodeficiency virus
SNPs	Single nucleotide polymorphisms
SOP	Standard operating procedure
TALENS	Transcription activator-like effector nucleases
Tat	Trans-activator of transcription
T_{CM}	Central memory T-lymphocytes
TILDA	Tat/rev-induced limiting dilution assay
TLR7	Toll-like receptor 7
T_{SCM}	Stem cell-like CD4 T cells
T_{TM}	Transitional memory CD4 T cells
URF	Unique recombinant forms
usRNA	Un-spliced Ribonucleic Acid
USA	United states of America
USD	US dollars
UV	Ultraviolet
Vif	Viral infectivity factor
Vpu	Viral protein u
WHO	World health organisation
ZDV	Zidovudine
ZFN	Zinc finger nucleases

Chapter 1

1.1 Introduction

1.1.1 Global HIV burden and the need for a cure

As of 2017, 36.9 million people worldwide are living with the Human Immunodeficiency Virus (HIV) (UNAIDS, 2018a). Of these, 1.8 million are children below the age of 15 years (UNAIDS, 2018a). The highest HIV rates globally are in sub-Saharan Africa where 19.6 million people are currently infected (UNAIDS, 2018a). Since the introduction of antiretroviral therapy (ART), several studies have reported a significant decline in morbidity and mortality as well as an improved life expectancy among infected children and adults (Brady et al., 2010; Gona et al., 2006; Gortmaker et al., 2001; Judd et al., 2007; Palella et al., 1998; Walensky et al., 2006). ART has been effective in limiting sexual transmissions by reducing the plasma viral loads of well-suppressed individuals to below the detection limit of commercial assays (Castilla et al., 2005; Granich et al., 2010). There has also been great success in using ART as prophylaxis to prevent mother to child transmissions (Teasdale et al., 2011). With 80% of pregnant women worldwide now having access to ART, there is a continued decline in new infections among children (UNAIDS, 2018a).

Despite this, a cure is still warranted. South Africa has the largest ART programme in the world. Between 2014 and 2015, 350 million US dollars (USD) was spent on ART programmes (Venter et al., 2017). The recent change in treatment guidelines to accommodate all infected people regardless of CD4 threshold, coupled with the increase in the life expectancy of people on effective ART means that the national budget must cater for several millions of infected people who will need ART for many decades (Sabin, 2013). The high cost of providing life-long ART for over 36 million individuals (and counting) is not economically sustainable.

Women of child bearing age in sub-Saharan are a major risk group for acquiring the infection and of concern because of the potential for continued mother to child transmissions (UNAIDS, 2018b). In addition, drug toxicities, psychological and socio-economic factors still have a significant impact on ART adherence (Mellins et al., 2004; Williams et al., 2006). The lack of proper adherence could lead to development of drug resistance to current regimens as well as the possible spread of infection to others (Bangsberg et al., 2004; Sethi et al., 2003). Treatment adherence is of particular concern in perinatally infected children and adolescents from resource limited settings. While there is evidence to suggest that disclosure of HIV status may have a positive impact on ART adherence (Bikaako-Kajura et al., 2006; Corneli et al., 2009; Fetzer et al., 2011; Montalto et al., 2017) there is an increased risk of non-adherence to ART above the age of 15 years (Bygrave et al., 2012; Mellins et al., 2011). Challenges such as the poor palatability of liquidate ART formulations, gastro-intestinal intolerance to the drugs, co-morbidities (e.g malaria), low nutritional status, cultural/environmental factors, and psychosocial changes during adolescence all influence paediatric adherence (Agwu and Fairlie, 2013; Davies et al., 2008; Phelps and Rakhmanina, 2011; Schlatter et al., 2016).

Furthermore, the drug toxicities associated with life-long ART, especially in children who have been treated since birth are largely unknown. In older people living with HIV, some ART related morbidities have been reported. The use of some nucleoside reverse transcriptase inhibitors (NTRI) can cause loss of bone mineral density increasing the risk of osteoporotic fractures (Borges et al., 2017). Long-term ART use has been associated with an increased risk of developing kidney disease and liver toxicity (Fernandez-Fernandez et al., 2011; Kovari and Weber, 2011; Scherzer et al., 2012). Efavirenz and dolutegravir have been associated with impaired neurocognitive functioning and adverse neuropsychiatric events (Hoffmann et al., 2017; Ma et al., 2016; Treisman and Kaplin, 2002) and protease inhibitors (PI) have been reported to increase the risk of myocardial infarction (Lai et al., 2009; Sabin et al., 2016). The search for a cure is therefore high priority in the HIV research community (Barré-Sinoussi et al., 2013). Increasing global efforts are now focused on understanding the mechanisms that allow the virus to persist despite effective ART and developing strategies to overcome these barriers.

1.1.2 HIV genome and the active replication cycle:

HIV belongs to the Lentivirus genus from the *Retroviridae* family and is classified under two species that infect humans, namely HIV-1 and HIV-2. HIV-1 is the predominant species and is further divided into groups M (main), O (Outlier) and N (new). Under group M are nine subtypes (ranging from A-D, F-H and J-K) as well as several Circulating recombinant forms (CRFs) and Unique recombinant forms (URFs) (Robertson et al., 2000). The HIV genome is 9.7kb in length and consists of 9 genes that encode 15 viral proteins. The translated gene products result in structural proteins of the viral exterior and core, polymerases that enable viral replication, and regulatory as well as accessory proteins that enhance entry and viral reproduction. Each virion has an outer envelope derived from the *env* gene precursor which gives rise to the gp120 surface membrane and gp41 transmembrane (Freed, 1998). Within the envelope are the matrix protein (p17), capsid protein (p24), and nucleocapsid (p7) encoded by the *gag* gene. The capsid encloses two copies of unspliced, positive sense, single stranded viral RNA genomes (Freed, 1998). Also within the viral core are three enzymes essential for infection and replication namely *Protease (PR*), *Reverse transcriptase (RT*) and *Integrase (IN*), all derived from the *pol* gene (Hill et al., 2005). In addition, the viral genome encodes proteins with regulatory function namely *tat* (trans-activator of transcription) and *rev* (regulator of viral expression) as well as four accessory proteins namely *nef* (negative factor), *vpr* (viral protein r)*, vif* (viral infectivity factor)*,* and *vpu* (viral protein u) (Ranki et al., 1994). The viral genome also includes non-coding regions known as the 5' and 3' long terminal repeats (LTR) that are duplicated on both ends of the genome when it is in DNA form (Kao et al., 1987). The other non-coding regions are the primer binding site (PBS), packaging signal (ψ), polypurine tract (PPT), Rev-responsive element (RRE) and cis-acting repressive sequences (CRSs) (Paillart et al., 1996).

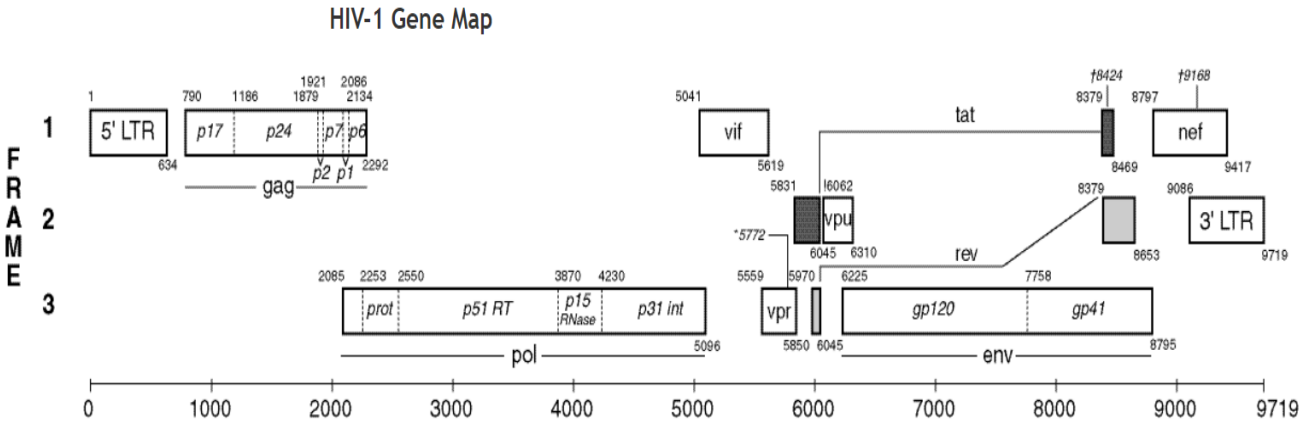

Figure 1.1: HIV-1 Gene map (HXB2): Image taken from (https://www.hiv.lanl.gov/content/sequence/HIV/MAP/landmark.html); accessed 01/06/2017.

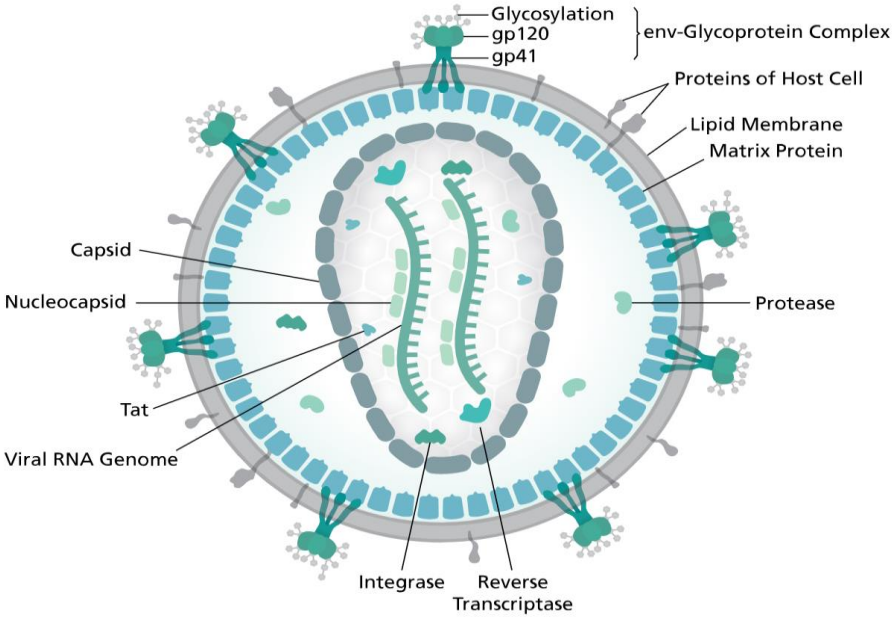

Figure 1.2: HIV Virion. Image by Thomas Splettstoesser (www.scistyle.com) https://commons.wikimedia.org/w/index.php?curid=38751738; accessed 09/09/2017.

The HIV-1 replication cycle begins when viral glycoprotein receptors bind to CD4 molecules and chemokine co-receptors CCR5 or CXCR4 on the surface of CD4 T cells (Chan and Kim, 1998). The fusion of viral and cellular membranes follows and leads to partial uncoating of the virion. Reverse transcription of the viral RNA by the *RT* enzyme occurs in the cytoplasm and results in a double stranded DNA product that together with viral and cellular proteins forms a nucleoprotein called the pre-integration complex (PIC). The PIC is transported through the cytoplasm to the nucleus. Following nuclear entry, integration of the viral DNA into the host cell's chromosomal DNA is mediated by the viral encoded *Integrase* enzyme (Ciuffi and Bushman, 2006). The integrated provirus serves as the template for transcription by the host cell's DNA-dependent RNA polymerase II and remains as part of the host cell's genome for the lifespan of the infected cell. HIV integrates preferentially in actively transcribed cellular genes and its expression depends on the host cell's metabolism and activation state (Craigie and Bushman, 2012; Mitchell et al., 2004; Wu et al., 2003). If the infected cell is activated, viral replication is efficient and rapid due to the expression of *tat*, increased nucleotide pools, and

the availability of host transcription factors that bind to the viral *LTR* region to initiate transcription (Frankel, 1992). Transcription results in the production of messenger RNA (mRNA) some of which are spliced and transported into the cytoplasm where they are translated into proteins while others are packaged as genomic RNA for progeny virions. *Gag-pol* poly proteins are transported to the cell's plasma membrane where mature virions are assembled and budd from the host cell (Park and Morrow, 1991). Following budding, viral *protease* performs proteolysis and enables the formation of mature viral particles (Park and Morrow, 1991).

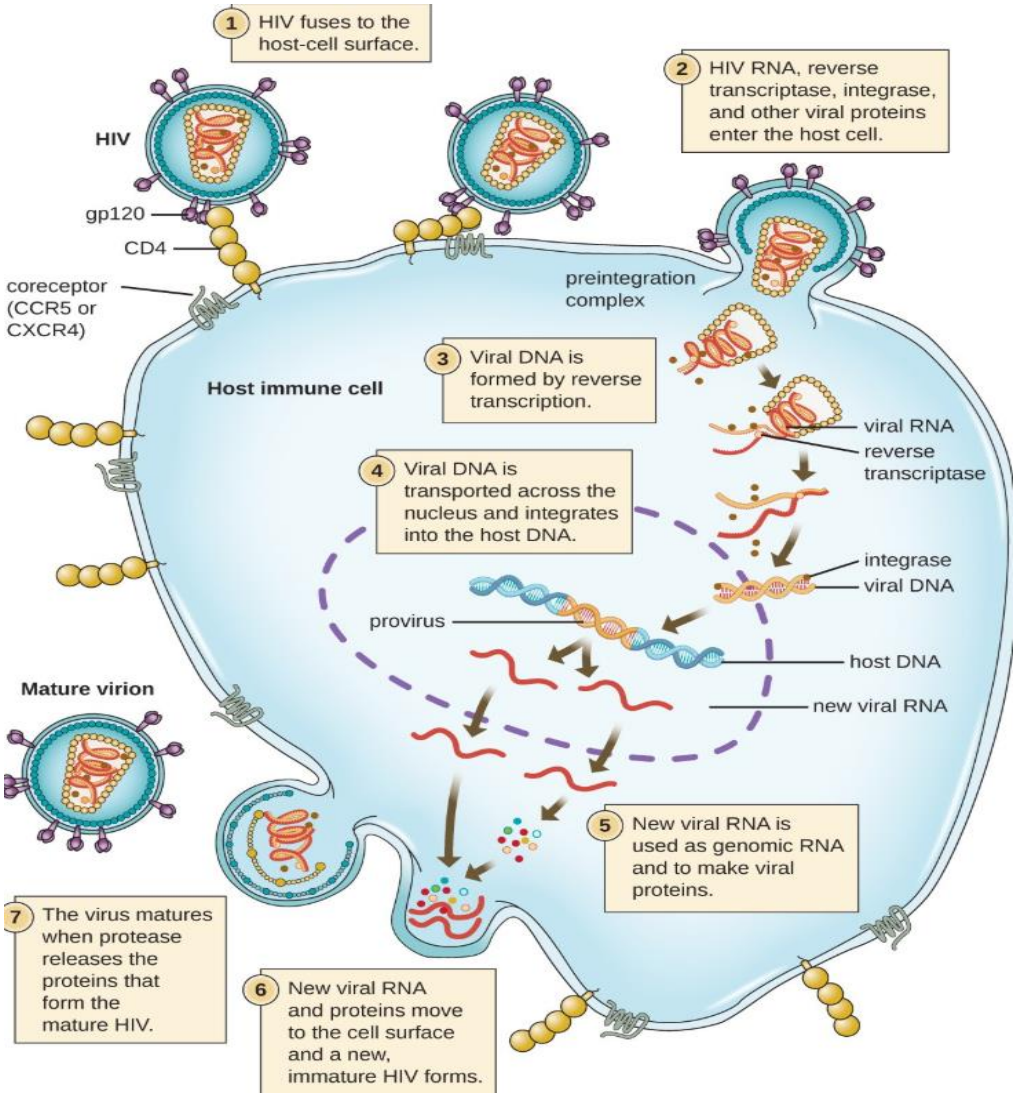

Figure 1.3: The HIV-1 viral life cycle. Image taken from: https://courses.lumenlearning.com, modified from work by NIAID, NIH; accessed 20/09/2017.

1.1.3 Latent reservoirs of HIV and their maintenance at a cellular level:

In most cells, HIV infection leads to active replication which results in the release of new virions and the destruction of the infected cell by viral cytopathic effects. However in a small subset, replication-competent proviruses remain dormant within the host cell's genome and HIV is able to persist in this form for the duration of the life-span of the infected cell (Brooks et al., 2001; Siliciano and Greene, 2011).These cells remain hidden from effects of the immune response, are unaffected by antiretroviral drugs (which target various stages of viral replication in an actively infected cell) and are capable of reactivating to produce new

cycles of replication when therapy is interrupted. Such cells are referred to as latent reservoirs (Chun et al., 1997b). Research shows that reservoir seeding occurs very early during infection (Chun et al., 1998). Although the exact mechanism by which a reservoir is established in these cells is not entirely understood, multiple mechanisms have been proposed:

I. Latent infections are thought to occur in cells that are entering a resting state where the down regulation of coactivating factors such as NF-kB and P-TEFb in the nucleus prevent transcription (Brooks et al., 2001; Finzi et al., 1999).
II. Because HIV mostly integrates within introns of actively transcribed genes, ongoing transcription from an upstream host promoter could interfere with viral transcription and result in latency (Han et al., 2008; Lenasi et al., 2008).
III. Histone modifications due to the recruitment of histone deacetylases (HDACs) at the site of insertion can result in repressive chromatin structure and reduce the accessibility of DNA templates to transcription factors leading to the downregulation of HIV expression (Coull et al., 2000; Jenuwein and Allis, 2001; Verdin et al., 1993; Ylisastigui et al., 2004).
IV. Histone CpG methylation (methylation of CG rich DNA) in the LTR region of the integrated viral genome can cause the winding of LTR chromatin structure blocking the binding of transcription factors and consequently expression of the viral genome (Blazkova et al., 2009).
V. Cellular micro RNAs that are upregulated in latent cells can directly target viral transcripts or indirectly repress translation of transcripts thus interfering with protein synthesis and inhibiting viral production (Chiang et al., 2012; Huang et al., 2007; Wang et al., 2015).
VI. Immune checkpoint molecules such as PD-1, TIGIT and LAG-3 that are highly expressed on the surface of latently infected memory CD4 T cells, serve to down-regulate the immune response and have been shown to play a role in the establishment and maintenance of latency (Evans et al., 2018; Fromentin et al., 2016).

1.1.4 Cellular and anatomical locations of the reservoir

Several cell types are susceptible to HIV infection and have the potential to harbour latent forms of the virus. CD4 T cells, particularly the central memory (T_{CM}) and transitional memory (T_{TM}) subsets have been identified as the main cellular reservoirs of HIV. These cells are able to survive for several years through cellular proliferation and have the capacity to reactivate when they encounter a cognate antigen making them ideal reservoirs (Chomont et al., 2010; Chun et al., 1997b; Chun et al., 1998; Siliciano and Greene, 2011; Whitney et al., 2014). More recently, stem cell-like CD4 T cells (T_{SCM}) with relatively longer lifespans and enhanced proliferative capacity have been reported to make an increasing contribution to the total cellular reservoir over time on ART (Buzon et al., 2014b; Gattinoni et al., 2012). Follicular helper CD4 T-cells, another subset of

the T_{CM} CD4 T cell compartment, have also been implicated as major reservoirs that serve as a source of HIV persistence in chronically infected individuals (Pallikkuth et al., 2016).

CD4 T cells are found in lymphoreticular tissues - predominantly the gut associated lymphoid tissues, peripheral blood and in low concentrations at many anatomic sites. Although most studies describing cellular reservoirs are conducted on peripheral blood due to ease of sampling, circulating CD4 T cells comprise <2% of total body CD4 T cells (Mascio et al., 2009; Westermann and Pabst, 1992). During HIV infection, CD4 T cells disseminate throughout the body and establish reservoirs in tissue compartments. Tissue reservoirs are thought to be immunologically sheltered and lack sufficient drug penetration making them potential sites of ongoing viral replication and latent reservoir persistence. The detection of viral RNA in tissue despite being undetectable in peripheral blood during ART was thought to be an indication of ongoing compartmentalized viral replication (Fletcher et al., 2014). However, there has been no evidence of compartmentalization of viral populations in the lymph nodes of long-term ART suppressed individuals suggesting that there is circulation of virus and/or infected cells between lymphoid tissues and peripheral blood (Kearney et al., 2015; McManus et al., 2018) . Compartmentalization and ongoing replication on ART are further discussed in section 1.1.8.2 below.

The gut mucosa plays a critical role in HIV pathogenesis. It is the earliest site of infection, has high expression of CCR5 and CD4 (Brenchley et al., 2004; Li et al., 1999; Mehandru et al., 2004; Veazey et al., 1998), and contains 40-60% of the body's lymphocyte population (Olivares-Villagómez and Van Kaer, 2018). Most CD4 T cells in the gut mucosa are of the activated memory phenotype and therefore readily infected (Olivares-Villagómez and Van Kaer, 2018). CD4 T cells in the gut associated lymphoid tissue (GALT) have been shown to harbour HIV DNA (Yukl et al., 2013) at levels that remain constant even after long-term ART making it the most significant tissue reservoir.

Cells of the myeloid lineage including monocytes, macrophages and dendritic cells have been implicated as cellular reservoirs of HIV. Macrophages are a key target for infection (Koenig et al., 1986; Sharova et al., 2005) but differ from CD4 T cells in that they are already terminally differentiated, have longer persistence of unintegrated virus and are more resistant to viral cytopathic effects (Coleman and Wu, 2009; Ho et al., 1986; Kelly et al., 2008). Although their relative contribution to the latent reservoir appears smaller than CD4 T cells, they are found in almost all tissues and potentially transmit virus to different anatomic sites (Groot et al., 2008; Kumar and Herbein, 2014). As antigen presenting cells (APCs), macrophages transfer virus to by stander CD4 T cells through cell to cell contact (Groot et al., 2008; Kumar and Herbein, 2014). They also engulf infected CD4 T cells thus increasing their chance of infection and latency formation (Baxter et al., 2014). Natural killer (NK) cells have also been implicated as possible reservoirs (Coleman and Wu, 2009; Crowe et al., 2003; Valentin et al., 2002).

The central nervous system (CNS) is major tissue reservoir of HIV. Reservoir establishment in this compartment occurs early after peripheral infection and is maintained due to limited ART penetration as a

result of the 'blood-brain barrier'. Microglial and perivascular macrophages are critical cellular reservoirs in the CNS where they are resistant to viral cytopathic effects and are able to sustain the infection for long periods of time (Cassol et al., 2006; Churchill et al., 2006; Thompson et al., 2011; Williams et al., 2001). Astrocytes are another cell type that play a role in spreading the virus across the blood brain barrier (Churchill et al., 2006; Eugenin and Berman, 2013; Narasipura et al., 2012). A recent study detected viral immune escape populations in cerebrospinal fluid (CSF) of patients on long-term suppressive ART further implicating the CNS as a site of viral persistence (Joseph et al., 2018).

Studies in SIV infected animals have shown that lymph nodes are a site for reservoir formation (Horiike et al., 2012). Macrophages and dendritic cells play significant roles in spreading and sustaining the infection within secondary lymphoid tissues (Baxter et al., 2014; Kumar and Herbein, 2014; Zhang and Perelson, 2013). Dendritic cells are capable of retaining infectious virions on their cell surfaces and transmit virus via cell to cell spread (Burton et al., 2002; Spiegel et al., 1992). Also more recently described are follicular helper CD4 T cells within B cell follicles in lymphoid tissue that are highly susceptible to infection and comprise the main reservoir in this compartment (Perreau et al., 2013).

Several other anatomic sites harbour latent reservoirs. The detection of HIV DNA in T lymphocytes and macrophages from semen implicate the genital tract as a site for HIV reservoirs (Coombs et al., 2003; Diem et al., 2008; Quayle et al., 1997). HIV has also been recovered from alveolar lymphocytes and alveolar macrophages (Costiniuk et al., 2018; Cribbs et al., 2015) pointing to potential reservoirs in the lungs.

1.1.5 Current Cure approaches:

Current cure strategies aim to either eliminate all latently infected cells (sterilizing cure) or induce a state of viral remission where viral replication is suppressed, and patients are non-infectious for prolonged periods in the absence of ART (functional cure). Viremia typically rebounds 2-3 weeks after ART interruption (Davey et al., 1999; García et al., 1999) and the 'time to rebound' has been shown to correlate with the size of the reservoir (Li et al., 2016; Williams et al., 2014). As a result, the gold standard to evaluate the efficacy of any cure intervention is to perform an analytical treatment interruption (ATI) of ART followed by frequent viral load testing to monitor the time to detectable viral loads. However, a functional cure response may exhibit an initial viral rebound followed by immune mediated suppression as is the case in therapeutic vaccine approaches (Borducchi et al., 2016).

1.1.5.1 Early ART

Studies in non-human primates (NHP) have shown high levels of integrated SIV DNA in resting CD4 T cells as early as 3 days post infection, suggesting very rapid reservoir establishment (Nishimura et al., 2009; Whitney et al., 2014). There are several benefits of initiating ART during acute infection (Ananworanich et al., 2015). Early ART limits the establishment of reservoirs particularly in long-lived CD4 T cell subsets (Archin et al., 2012). Strain et al and others have shown that over time on therapy, HIV DNA in CD4 T cells of individuals

who initiate ART in acute infection decays faster than those initiating in chronic infection (Buzon et al., 2014; Chun et al., 2007; Strain et al., 2005). Early therapy also preserves HIV specific B and T cell responses and reverses the chronic mucosal and systemic immune activation that contributes to reservoir spread (Ananworanich et al., 2014; Jain et al., 2013; Schuetz et al., 2014). Furthermore, early ART can lead to functional cure. During the VISCONTI and SPARTAC trials, a small percentage of the individuals who initiated ART during acute infection were able to maintain undetectable viral loads after ART was interrupted (Frange et al., 2016; Sáez-Cirión et al., 2013). Post treatment control has also been reported in a South African child from the CHER cohort who was diagnosed with HIV at 32 days of age and initiated ART at 8.5 weeks of age for up to 1 year (Violari et al., 2019). The child was later interrupted as per the trial and has remained aviremic for 9 years (Violari et al., 2019). The immune mediated mechanisms by which post treatment viral control is achieved in such cases are yet to be understood. Other recent cases of paediatrics who following very early ART, had delayed viral rebound with no detectable virus in peripheral blood despite no evidence of immune mediated control further highlight the role of early ART in limiting reservoir establishment (Frange et al., 2016; Luzuriaga et al., 2015; Persaud et al., 2013). However, early therapy alone is not sufficient to prevent the establishment of reservoirs or lead to their eradication (Luzuriaga et al., 2000). Furthermore, the implementation of early ART at a population level especially in resource limited settings may not always be feasible. Early therapy therefore needs to be used in combination with other approaches to eliminate the persisting reservoir.

1.1.5.2 'Shock and Kill' approach

Certain compounds referred to as latency reversing agents (LRAs) have been shown to reactivate latently infected cells. These include protein kinase agonists (PKC) that initiate transcription (e.g PMA), histone deactylase inhibitors (HDACi/s) which inhibit cellular histone deactylases, histone methlytranferases (HMT) inhibitors, DNA methlytranferase inhibitors (Rasmussen and Lewin, 2016), agonists of innate immune receptors TLR7 or TLR9, inhibitors of the PI3/Akt pathway that influences cell survival, and others (Offersen et al., 2016; Tsai et al., 2017). The 'shock and kill approach' uses LRAs in combination with ART such that latently infected cells are reactivated to induce viral production and cleared by immune effector cells or virus mediated cytolysis while ART prevents further spread of the released virions to new cells. Several LRAs have been tested in clinical trials, these include: vorinostat (Archin et al., 2017; Archin et al., 2012; Elliott et al., 2014), panobinostat (Rasmussen et al., 2014), romidepsin (Søgaard et al., 2015), disulfiram (Elliott et al., 2015; Spivak et al., 2014; Xing et al., 2011), bryostatin-1 (Gutierrez et al., 2016), and the TLR9 agonist MGN1703 (Vibholm et al., 2017). All except byrostatin-1 have shown an increase in plasma HIV RNA but none has shown a reduction in infected cells. This is thought to be due to the lack of effective 'killing' of reactivated cells. There are multiple potential mechanisms that prevent the clearance of reactivated cells including: (i) the over expression of cellular pro-survival protein Bcl-2 that inhibits virus mediated killing (Cummins et al., 2016) (ii) immune escape mutations in latently infected cells of individuals treated during chronic infection

(Deng et al., 2015), (iii) direct inhibition of CD8 + T-cells and natural killer (NK) cells by HDACis (Pace et al., 2016), (iv) inherent resistance of reservoir cells to killing by CD8 effector cells (Huang et al., 2018). These data collectively highlight the fact that more effective approaches to 'kill' reactivated cells are required. Furthermore, the potential for global activation of immune cells, cellular toxicity, and tumor inducing potential of LRAs remain of concern with the 'shock and kill' approach (Rasmussen and Lewin, 2016).

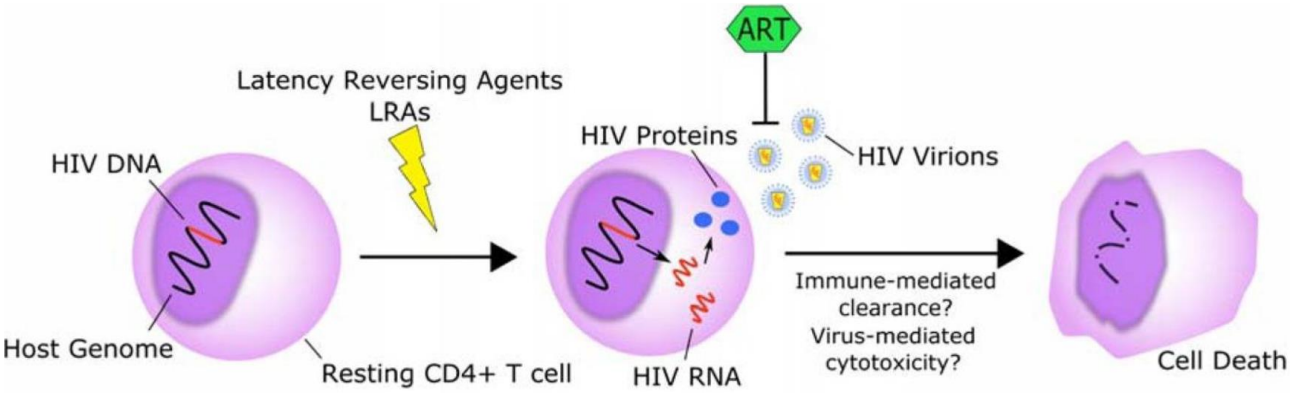

Figure 1.4: Shock and Kill approach to reactivate and eliminate latently infected cells. Image taken from Kim et al., 2017. (https://www.ncbi.nlm.nih.gov/pubmed/29324227); accessed 05/02/2018.

1.1.5.3 'Block and Lock' approach

More recently, an alternative to the 'shock and kill' approach referred to as 'block and lock' is aimed at inducing a state of deep latency using latency promoting strategies. In one study, mice treated with small interfering RNAs (siRNA) that target conserved promoter regions of the integrated provirus have shown a reduction in HIV RNA levels in serum (Suzuki et al., 2013). In another cell-culture study, a new compound (L-HIPPO) captures the HIV Pr55 protein that mediates virion budding and blocks it from translocating from the cytoplasm to plasma membrane thus inducing cellular apoptosis (Tateishi et al., 2017). Yet another approach uses a novel drug didehydro-cortistatin A to bind to promoter regions and restrict the recruitment of *tat* and other host factors required for transcription (Kessing et al., 2017). In a mouse model this approach showed delayed viral rebound off ART. Lastly, small molecule inhibitors called LEDGINS have been shown to interfere with integration site selection and shift viral integrations to inner nuclear compartments away from active genes (Debyser et al., 2018).

1.1.5.4 Gene editing approaches

The cases of the 'Berlin' and 'London' patients who to-date are the only individuals to be cured of HIV suggested that reduced or no cell surface expression of CCR5 could be protective and have served as proof of concept that long-term remission/cure is possible if the reservoir size is sufficiently reduced (Gupta et al., 2019; Hutter et al., 2009). The 'Berlin patient' received hematopoietic stem cell transplantation (HSCT) as treatment for acute myeloid leukemia (AML) from a donor who was homozygous for the Δ32 mutation in the CCR5 gene that makes cells resistant to HIV infection (Hutter et al., 2009). The patient has remained off ART for over 10 years without evidence of residual virus even after extensive tissue sampling (Hutter et al., 2009).

However, the Berlin patient scenario was high risk and may not be a scalable approach for cure. Multiple attempts to replicate this model have been unsuccessful with exception of the 'London patient'. All other recipients of HSCT from a homozygous Δ32 donor developed fatal complications due to the transplant or failed to maintain long-term viral remission (Henrich et al., 2014; Kordelas et al., 2014). Alternative approaches to block viral entry by knocking out the CCR5 gene in hematopoietic stem/progenitor cells (HSPCs) using zinc finger nucleases (ZFN) or CRISPR/Cas9 have been tested in HIV infected individuals (Cannon and June, 2011; Tebas et al., 2014). All patients eventually had viral rebound following ATI due to the low frequency of modified CD4 T cells that were adoptively transferred (Cannon and June, 2011; Tebas et al., 2014). However, a patient heterozygous for the CCR5 Δ32 mutation experienced better control of viral replication post-treatment interruption suggesting that the reduction of cell surface CCR5 expression might be protective (Tebas et al., 2014). HSCs have also been used in vivo to generate HIV specific cytotoxic T cells that inhibit viral replication (Kitchen et al., 2012). Another approach is the direct excision of HIV proviruses from cellular genomes using gene-editing enzymes such as zinc finger nucleases (ZFNs), homing endonucleases, transcription activator-like effector nucleases (TALENS) and CRISPR/Cas9 (Ebina et al., 2015, 2013; Kaminski et al., 2016; Qu et al., 2013; Sarkar et al., 2007; Yin et al., 2017). This approach has been effective in culture with primary cell lines and humanized mouse models but has not proceeded to clinical trials due to poor efficacy of gene delivery, off target effects, the low frequency of latently infected cells and the challenge of targeting multiple sites of proviral integration in the host cell genome (Ebina et al., 2015, 2013; Kaminski et al., 2016; Qu et al., 2013; Sarkar et al., 2007; Yin et al., 2017).

1.1.5.5 Immunotherapy

Various immunotherapeutic approaches towards a cure are on-going. Therapeutic vaccines composed of attenuated viral vectors or plasmid viral DNA have been used to express HIV antigens and induce an HIV specific immune response (Katlama et al., 2013; Shan et al., 2012). Several of these vaccines appear promising. In a macaque model, an adenovirus-based vaccine used in combination with a TLR7 agonist was able to induce post-treatment control following ART interruption (Borducchi et al., 2016). Likewise, a CMV-based vaccine was able to induce a broad range of cellular immune responses resulting in control of SIV infection (Hansen et al., 2013, 2011).

The use of passively administered broadly neutralising antibodies (bnAbs) against various viral strains has shown promise with reports of delayed viral rebound following ART interruption (Barouch et al., 2013; Scheid et al., 2016).These bNabs target both cell free virus and infected cells and contribute to boosting HIV specific T cell responses (Barouch et al., 2013; Caskey et al., 2015; Lu et al., 2016; Williams et al., 2017). In humanized mouse models, bNabs have shown efficacy in reducing viral rebound when used in combination with LRAs (Halper-Stromberg et al., 2014). However, their short half-life, limited accessibility to all anatomical reservoir sites, and high cost are some of the current hurdles in their use as cure interventions.

Another immunotherapeutic approach is to enhance the CD8 T cell response by reversing chronic cell activation and exhaustion. Immune regulators such as the programmed cell death protein (PD-1), act to blunt cell activation during chronic HIV infection (Velu et al., 2015). The ligands PD-L1 and PD-L2 block the PD1 pathway and their administration has been shown to restore T cell function resulting in the reduction of viral reservoirs (Gardiner et al., 2013; Shetty et al., 2012). Studies in SIV infected macaques showed that the administration of PD-1 ligands resulted in a reduction in viral loads and immune activation (Shetty et al., 2012; Velu et al., 2009). Clinical trials to assess the efficacy of PD-L1 and PD-L2 in humans are on-going.

Other cure strategies under investigation include the use of nanocarriers and chimeric antigen receptor (CAR) T cell therapy (Lisziewicz and Toke, 2013; Zhen et al., 2015). It is becoming more apparent that the most effective approach includes a combination of reservoir reduction and immune control.

1.1.6 Paediatric HIV infection, CHER and early treated children as good candidates for cure interventions

In 2017, approximately 180 000 children aged 0-14 years were newly infected with HIV worldwide (UNAIDS, 2018a). Without the administration of ART prophylaxis, 35%–49% of children born to HIV-infected mothers become infected. Of these, 8% are estimated to be infected during pregnancy, 15% during labour and delivery, and 12%–26% during breast-feeding (Jourdain et al., 2007; Leroy et al., 1998). When a combination of maternal and infant ART prophylaxis is administered, transmission rates are reduced to below 5% (WHO, 2015).

1.1.6.1 The CHER study and post CHER cohort

High mortality rates have been reported among children who become infected and initiate ART during the symptomatic phase of infection, suggesting that earlier therapy is required to prevent disease progression (Lilian et al., 2013; Newell et al., 2004). The Children with HIV Early antiRetroviral therapy (CHER) randomised trial was conducted on HIV infected infants in South Africa to determine whether early, time-limited therapy soon after primary infection, during the time when the immune system was most immature could result in long-term benefit and delay the time to commencement of life-long ART (Cotton et al., 2013). The first line ART regimen for CHER was lopinavir, lamivudine and zidovudine (LPV/r + 3TC + ZDV). Asymptomatic infants with CD4≥25% were randomised to receive ART for either 40 (arm 2) or 96 weeks (arm 3) or deferred ART according to concurrent guidelines (arm 1). Children in arm 2 and 3 had slower disease progression compared to those in the deferred arm (Cotton et al., 2013). Moreover, children who initiated earlier were more likely to have undetectable HIV-specific antibodies by the age of 2 years and had lower HIV cell associated DNA (CAD) and RNA (CAR) compared to those who initiated later (Cotton et al., 2013; Payne et al., 2015; Van Zyl et al., 2014). Children from the CHER study were later retained in follow up cohort studies to investigate neurocognitive outcomes and HIV-1 persistence.

1.1.6.2 Early treated children as good candidates for cure interventions

The CHER study findings have been corroborated by several others showing that children who initiate treatment within days of diagnosis and maintain adherence have improved virologic and immunological outcomes compared to those who initiate based on clinical criteria (Ananworanich et al., 2014; Bitnun et al., 2014; Luzuriaga et al., 2014; Persaud et al., 2012). Treatment initiation during acute infection halts new rounds of viral replication and limits the spread and establishment of a replication competent reservoir in long-lived cells (Luzuriaga et al., 2014). Furthermore, early treatment increases the reservoir's decay rate and limits the development of phylogenetically diverse viral quasi-species which allow evasion of specific immune responses (Luzuriaga et al., 2014; Persaud et al., 2007).

The case of the 'Mississippi baby' who initiated ART within hours of life and showed no evidence of HIV replication for a period of 27months off therapy, indicates a very low reservoir and provides support that early treated infants may be ideal candidates for curative interventions (Hill et al., 2014; Persaud et al., 2013). With current international guidelines recommending early initiation of therapy for all infected infants, there is a growing number of early treated, long- term suppressed children that are surviving to adolescence and older (Department of Health Republic of South Africa, 2013; Klein et al., 2015). Thymic activity in children is significantly higher than in adults and provides the advantage of an increased capacity to restore a functional immune repertoire –which may facilitate de novo vaccine- specific responses (Lynch et al., 2011). The immune system in children is characterised by a higher number of naive CD4 T cells, lower activation states, and a lower proportion of central memory T cells – all factors that would facilitate a smaller and less diverse reservoir than would be present in adults (De Rossi et al., 2002; Klein et al., 2013). Early treated children have better CD4 T cell function than early treated adults which could mean an enhanced capacity to respond to new antigens when therapeutic T cell vaccines are administered (Adland et al., 2018). Also, most early treated children become sero-negative after 2 years on suppressive ART and therefore lack HIV-specific cellular immune responses that would likely interfere with investigating vaccine specific responses (Klein et al., 2015). To lay the ground work for therapeutic vaccine trials and other novel cure interventions, it is vital that current cohorts of early-treated, long term suppressed children be thoroughly characterised. Factors such as reservoir size, genetic diversity over time and proviral landscape of the reservoir need to be determined in order to understand the mechanisms that drive persistence in this key population.

1.1.7 Measuring the replication competent reservoir

1.1.7.1 Quantitative measurement of HIV nucleic acids

Quantitative polymerase chain reaction (qPCR) assays, namely real-time PCR (RT-PCR) and digital PCR (dPCR), have been used to quantify HIV nucleic acids in peripheral blood, tissues, plasma and other compartments (De Oliveira et al., 2015; Henrich et al., 2012; Kiselinova et al., 2014; Strain et al., 2013). Following extraction of viral DNA or RNA, these samples are reverse transcribed (in the case of RNA) and then amplified using

primers that target conserved regions of the HIV genome including *LTR*, *gag* or *pol*. During real-time PCR, the PCR cycle where fluorescence reaches a pre-determined cycle threshold (Ct) is measured in both serial dilution standards and unknown samples. RNA or DNA concentrations are then determined by log-linear regression from a standard curve. Digital PCR quantification entails limiting dilution of target RNA/DNA in miniaturized reactions, determining the proportion of reactions that are positive and estimating the original concentration by Poisson statistics (De Oliveira et al., 2015; Eriksson et al., 2013; Henrich et al., 2012; Kiselinova et al., 2014).

Different assays have been developed for the ultrasensitive quantification of either total HIV DNA, integrated HIV DNA or episomal DNA formed from failed integration attempts (i.e 1LTR and 2LTR circles) (Eriksson et al., 2013). Similarly, ultrasensitive assays are available to quantify free virion HIV RNA that persists below the limit of detection of commercial viral load assays, also referred to as residual viremia. In order to characterize transcriptional activity of HIV infected cells, assays are available to determine cell associated unspliced and multiply spliced RNA transcripts. The detection limits differ depending on the assay used but range from 150 HIV RNA copies per ml of plasma to less than 1 HIV RNA copy and have been useful in clinical trials to analyse changes in viral transcription or release of virions into plasma after administration of LRAs (Cillo et al., 2014b, 2014a; Palmer et al., 2003). Quantitative PCR approaches have the benefit of being highly sensitive, high throughput and relatively inexpensive. A big limitation however, is their inability to distinguish between genetically defective or intact proviruses due to the majority of proviral HIV being defective (Ho et al., 2013). They have been shown to overestimate the true size of the reservoir by over 300-fold (Ho et al., 2013). There is also variability and bias among the different assays (Eriksson et al., 2013). Differences in gene targets and even different labs settings have affected their reproducibility.

1.1.7.2 Quantitative Viral Outgrowth Assays

The quantitative viral outgrowth assay (qVOA) is currently the gold standard for measuring the replication competent reservoir. qVOA involves the mitogenic reactivation of resting CD4 T cells at limiting dilution in the presence of feeder cells to enable subsequent rounds of infection (Chun et al., 1997a; Eriksson et al., 2013; Siliciano and Siliciano, 2005). Maximum likelihood statistics are then used to estimate the amount of reactivated virus as infectious units per million (IUPM) (Rosenbloom et al., 2015). There are some limitations with qVOA; it is expensive, time consuming, and requires large blood volumes and thus not ideal for use in large scale clinical trials. The assay is also not ideal for quantifying tissue reservoirs and therefore does not give a true representation of the full body reservoir load. Furthermore, qVOA underestimates the reservoir size by 25-fold in patient treated during acute infection and 27-fold in chronic phase treated patients because not all genetically intact proviruses are sufficiently reactivated in-vitro and may require multiple rounds of stimulation (Bruner et al., 2016). However, there are continued improvements to the assay, a recent modified version where resting CD4 T cells are fed into a humanised mouse model followed by measurement of viral outgrowth has shown increased sensitivity (Metcalf Pate et al., 2015)

1.1.7.3 Inducible virus recovery assays

Inducible virus recovery assays measure viral induction (i.e transcriptional activity, translation and virion release) following stimulation. Resting or total CD4 T cells from suppressed individuals are reactivated in the presence of ART followed by measurement of viral RNA in supernatants or directly from cell extractions. Unlike infectious virus recovery assays, they do not require that rounds of replication take place and are therefore less cumbersome.

One such assay is the tat/rev-induced limiting dilution assay (TILDA) developed by Procopio and colleagues which measures cells that are capable of producing multiply spliced (ms) HIV RNA (Procopio et al., 2015). As opposed to unspliced (us) HIV RNA which is produced at low levels in latently infected cells, multiply spliced HIV transcripts contain *tat* and *rev* viral genes that are used as a surrogate marker for viral release and therefore show the ability of infected cells to produce virus. The assay involves T cell activation using potent mitogens at limiting dilution similar to qVOA but is followed by ultra-sensitive PCR measurement of ms HIV RNA.

Other inducible virus recovery assays have been used to describe the transcriptional profile of CD4 T cells in ART suppressed individuals using a panel of transcripts that reflect the various stages of the transcription process (Bullen et al., 2014; Yukl et al., 2016). Bullen et al compared the potency of various LRAs with PMA/ionomycin using dPCR measurement of various HIV RNA transcripts i.e poly-A transcripts (mature), tat/rev transcripts (ms), LTR transcripts (elongated) and found that vorinostat had no effect on the levels of mature polyadenylated RNA (Bullen et al., 2014).

Cillo et al and Massanella et al described the relationship between viral transcription and virion production by stimulating resting (Cillo et al., 2014a) or total CD4 T cells (Massanella et al., 2016) with anti-CD3 and ant-CD-28 antibodies at limiting dilution in the presence of ART followed by qPCR quantification of cell-free viral RNA from culture supernatants (Cillo et al., 2014a; Massanella et al., 2016).

Compared to qVOA, inducible virus recovery assays have the advantage of being high throughput, requiring fewer cells, and being relatively shorter and easier to perform. However, TILDA has been shown to measure 6-27 times less than quantitative DNA assays but 48 times more than qVOA suggesting that inducible virus recovery assays may overestimate the size of the latent reservoir (Procopio et al., 2015). Furthermore, these assays do not prove replication competence, as it is possible for defective proviruses to have intact *tat* and *rev* (Bruner et al., 2016; Ho et al., 2013).

1.1.7.4 Fluorescent In-Situ hybridization

Fluorescent in-situ RNA/DNA hybridization (FISH) assays allow for the quantification and visualization of HIV nucleic acids in blood and tissue (Deleage et al., 2016b, 2016a). During these assays, fluorescent or chromogenic probes are hybridized to HIV RNA or DNA fragments, amplified and visualized by microscopy. Improved versions of the assays use branched DNA hybridization and flow cytometry detection, which

increase sensitivity to a single cell level. This approach has been used to identify latent cells that produce mRNA also described as the 'transcriptionally active reservoir' (Grau-Expósito et al., 2017). There are variations of the assay, some combined with the detection of viral proteins (Baxter et al., 2016). FISH has also been used to visualize SIV infected cells in lymphoid tissues (Fukazawa et al., 2015). However, HIV-FISH assays are unable to discern between intact and defective viral sequences.

1.1.8 Understanding how the reservoir persists despite early, long-term suppressive ART

1.1.8.1 Clonal expansion

The half-life of the latent reservoir in patients who initiate antiretroviral therapy during chronic infection is about 44- 48 months (Finzi et al., 1999; Siliciano et al., 2003). As a result, ART alone cannot lead to its decay over the lifespan of the infected individual. The proliferation of infected cells is one mechanism that enables this remarkable stability. It is not surprising that latently infected cells are able to proliferate because HIV integrates into central memory (T_{CM}) and transitional memory (T_{TM}) T cells that proliferate in-vivo in response to homeostatic or antigen driven stimuli (Chomont et al., 2010). Studies aimed at characterising the persistent low level viremia in plasma of long-term suppressed individuals have reported the detection of identical viral sequences by single genome sequencing (Anderson et al., 2011; Bailey et al., 2006; Kearney et al., 2014). These monotypic sequences rebound after treatment interruption (Joos et al., 2008), are identical to DNA sequences from resting CD4+ T cells (Anderson et al., 2011) and can be detected in the gastrointestinal (Evering et al., 2012) and genital tracts (Bull et al., 2009). Monotypic proviral sequences have also been shown to increase in proportion over time in early-treated children (Wagner et al., 2013). Integration site analysis of these monotypic variants reveals that many latently infected cells have identical sites of HIV integration in the host cell genome providing evidence that these sequences are clonal (Simonetti, 2015; Simonetti et al., 2016). Furthermore, even though most proviral DNA is defective, expanded cell clones can harbour intact proviruses that produce infectious virions. Interestingly, a recent study reported an enrichment of intact clonally expanded cells in Th1-polarized cells which naturally have a high proliferative rate (Lee et al., 2017). The proliferation and clonal expansion of latently infected cells is now recognized as a major mechanism that drives persistence of the reservoir in early-treated long -term suppressed individuals (Reeves et al., 2018).

T cell proliferation can be driven by several factors. It has been shown in a cell model, that homeostatic stimuli such as IL-5 and IL-7 can lead to cellular proliferation without reactivation of resting cells (Hosmane et al., 2017). Latent cells also proliferate in response to antigenic stimuli (Douek et al., 2002; Simonetti et al., 2016). Also, several studies have suggested that the site of integration in the host genome, particularly in genes responsible for cell growth and survival can 'turn-on' cellular proliferation (Maldarelli et al., 2014; Wagner et al., 2014). However, a recent study suggests that antigenic stimuli rather than integrations into growth genes is a larger contributor to clonal expansion (Wang et al., 2018).

Integration site analysis (ISA) is used to detect clonally expanded cell populations because of their identical sites of proviral integration in the host cell genome (Maldarelli et al., 2014). The assay involves fragmentation of cellular genomic DNA, linker-mediated amplification, sequencing of fragments that contain the host-virus junctions and mapping of integration sites in the host genome (Maldarelli et al., 2014). Although ISA is high throughput and has the advantage of mapping the site of integration, it is unable to determine whether proviruses are genetically intact because only a short fragment of the integrated provirus is sequenced.

VOA followed by HIV-1 gag-pol RNA sequencing to identify identical RNA sequences in different positive wells and sequence confirmation by overlapping half-genome sequencing, has also been used to detect intact clonal populations (Bui et al., 2017). However, this approach is most feasible when there is a high enough proviral diversity (e.g in patients who initiate ART during chronic infection) to ensure that the identification of identical HIV-1 RNA sequences in different wells is due to outgrowth from cells belonging to the same clone rather than the detection of homogenous founder viruses.

1.1.8.2 Persistent low-level viral replication

In well-suppressed patients with clinically undetectable viral loads, persistent low-level viremia (LLV) is usually detected by ultra-sensitive assays (Hatano et al., 2011; Lorenzo-Redondo et al., 2016) and is of concern because of its potential to replenish the reservoir in long-lived cells (Bailey et al., 2006; Persaud et al., 2004; Tobin et al., 2005). There is ongoing debate in the field as to the source of this persistent viremia. On one hand, it is thought to be a result of poor ART penetration in lymphoid tissue and the subsequent trafficking of released virus into peripheral blood (Chun et al., 2005; Cory et al., 2013; Fletcher et al., 2014; Huang et al., 2016; Lorenzo-Redondo et al., 2016). Supporting this notion is a study that showed an inverse correlation between ART penetration and the amount of virus detected in lymph nodes (Fletcher et al., 2014). In another study, ART intensification by the addition of the integrase inhibitor, raltegravir, resulted in a brief increase of 2 LTR circles, thought to have been indicative of abortive integration attempts and suggestive that ongoing replication was inhibited by raltegravir (Buzon et al., 2010). More recently, a study used time-stamped phylogenetic analysis and mathematical modelling of viral sequences from various compartments to show ongoing replication in lymphoid tissues(Lorenzo-Redondo et al., 2016). However, the study included only 3 participants, sampled a very small number of non-identical sequences, and the conclusions could not be reproduced by others, even when analysing the same data (Kearney et al., 2017). Moreover samples used to measure evolution in this study were from the first 6 months after ART initiation when it is known that shorter lived subpopulations undergo rapid decay and could give a false signal of viral evolution (Rosenbloom et al., 2017).

On the other hand, sequencing of viral RNA or proviral DNA in infected individuals over time on ART has revealed a lack of evolution or the detection of drug resistant strains, suggesting that ART completely halts ongoing viral replication (Bailey et al., 2006; Dinoso et al., 2009; Gandhi et al., 2012; Joos et al., 2008; Josefsson et al., 2013; Kearney et al., 2016, 2014; Mok et al., 2018). Furthermore, several other studies have

shown that ART intensification does not reduce persistent low-level viremia (Dinoso et al., 2009; Gandhi et al., 2012; Henrich, 2018; Rasmussen et al., 2018) or have any significant effect on markers of viral persistence (Gandhi et al., 2012). In most patients, LLV is genetically identical to proviruses in resting CD4+ T cells, similar to variants which circulated shortly after infection and is likely an indication of release from a stable, early-established reservoir. The stochastic reactivation of latent cells that were infected before ART followed by release into periphery is more likely the source of persistent low-level viremia observed in long-term suppressed individuals (van Zyl et al., 2018).

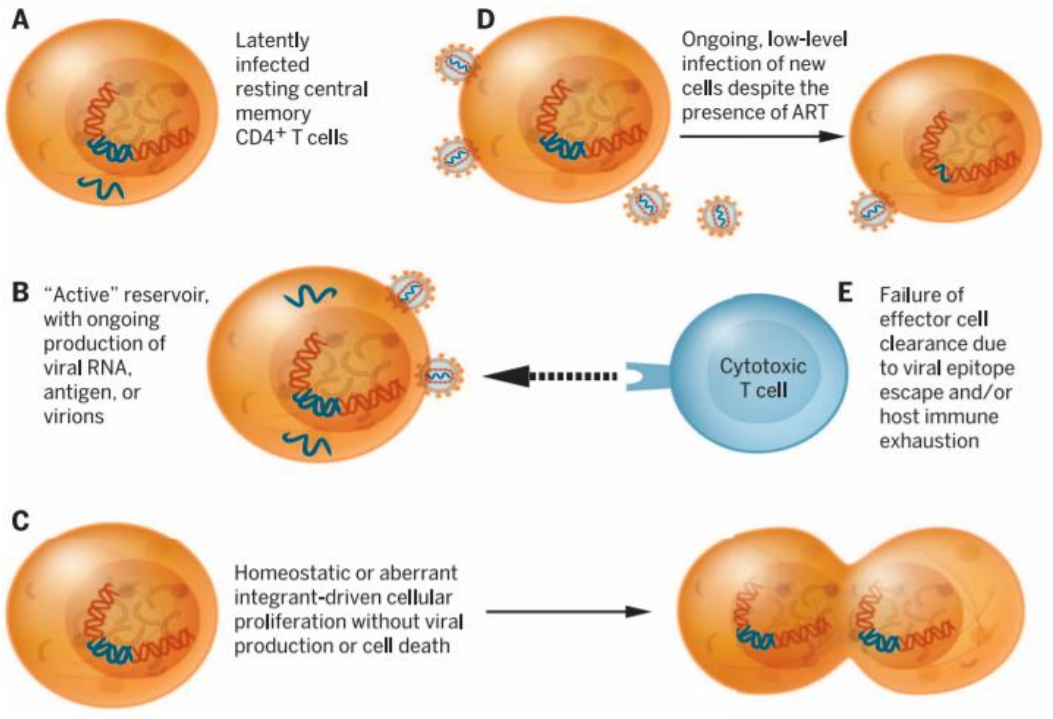

HIV latency. Potential obstacles to HIV eradication. (**A**) True virological and transcriptional latency, with little HIV RNA expression, and no detectable HIV antigen presentation. (**B**) So-called "active latency" with ongoing production of HIV RNA and antigen. (**C**) Proliferation of latently infected cells, driven by homeostatic forces, or by dysregulation of the host gene program by a viral integrant, without viral production. (**D**) The possibility that de novo infection occurs despite effective ART. (**E**) Failure of immune clearance owing to viral epitope escape or host immune exhaustion.

Figure 1.5: HIV latency. Image taken Margolis et al., 2016. (https://www.ncbi.nlm.nih.gov/pubmed/27463679); accessed 10/10/2017.

1.1.9 The HIV-1 proviral landscape during long-term ART

Describing the HIV-1 proviral landscape and understanding factors that influence its composition during long-term ART may enhance our ability to accurately measure the replication competent reservoir and provide insight on the mechanisms by which intact proviruses persist.

In adults, longitudinal qPCR measurements of proviral DNA after ART initiation reveal that different cell subsets decay at different rates. The largest decay of proviral DNA occurs in the first year on ART where there is a reported 86% decline in proviral DNA (Ananworanich et al., 2016; Archin et al., 2012; Besson et al.,

2014a; Buzon et al., 2014a; Fischer et al., 2008). This is likely due to the death of productively infected cells, decay of un-integrated virus and concurrent blocking of new infections by ART. In year 1-4 there is a slower, 23% decline per year, this is the second phase and represents decay of cells with a longer half-life (Blankson et al., 2000; Koelsch et al., 2008; Murray et al., 2012). There is eventual plateau after 4 years on ART which represents long-lived HIV-1 infected cells (Ananworanich et al., 2016; Besson et al., 2014). Measurements of the inducible, replication competent reservoir by VOA over a few years on ART also shows a slight decay of the replication competent reservoir over time with a half-life of 3.6 years (Crooks et al., 2015; Siliciano et al., 2003). The decay rate of HIV-1 DNA in children who initiate ART within days of birth however, is much more rapid. Veldsman et al showed that DNA levels in a large proportion of children who initiated ART within 8 days of birth reached undetectable levels between 6 days to 3 months on therapy (Veldsman et al., 2018).

Although it is known that the majority of proviral DNA during long-term ART is defective, a recent study showed that these defects accumulate within weeks of infection (Bruner et al., 2016). The study reported 92% of proviral DNA being defective in patients initiating ART during chronic infection and 98% in patients treated during acute infection (Bruner et al., 2016). Full length genome sequencing revealed the various mutations arising from errors during reverse transcription. These genomes contain guanine-to-adenine (G to A) hyper-mutations caused by cytidine deaminases APOBEC3F and APOBEC3G which act as HIV restriction factors, large internal deletions due to template switching during reverse transcription, frameshifts and nonsense mutations because of the error prone reverse transcriptase enzyme (Bebenek et al., 1989; Ho et al., 2013; Kieffer et al., 2005; Sanchez et al., 1997).

Pollack and colleagues recently showed that some defective proviruses, particularly those with defective major splice donor (MSD) sites, are able to use alternative novel splice sites to transcribe and produce antigens that are recognized by cytotoxic T lymphocytes (CTLs) (Pollack et al., 2017). Additionally, the lack of downregulation of MHC-1 due to the absence of functional *nef* may further allow some defective proviruses to more efficiently present antigens to CTLs (Pollack et al., 2017). CTLs can therefore exert selective pressure on these antigen producing defective cells allowing intact proviruses and those with severe mutations to persist. The HIV-1 proviral landscape is dynamic and shaped by the decay of shorter lived cell subsets, selective pressures of CTLs and clonal expansion over time on ART.

1.2 Study Rationale

The persistence of HIV-1 reservoirs in long-lived cells despite effective ART is now recognised as the main obstacle to achieving a cure. The health system costs of ART (which include treatment, personnel, facility, laboratory costs and the necessity to maintain supply), long term drug toxicities and the risk of drug resistance are some of the major challenges associated with life-long ART and point to the need for a cure (Mellins et al., 2004; Wada et al., 2015; Williams et al., 2006). As the field advances, new technologies and novel approaches to eliminate the reservoir are emerging, providing hope for a cure. Consequently, research is ongoing to describe HIV persistence in adults and several cure interventions have been tested in adult cohorts (Barouch et al., 2013; Halper-Stromberg et al., 2014; Rasmussen and Lewin, 2016; Scheid et al., 2016). On the other hand, the incidence of perinatal HIV infection has declined significantly and successful treatment of infected children has resulted in an increasing number of HIV infected children who are surviving to adolescence and older and have to remain on life-long ART (UNAIDS, 2018a). Perinatally infected, early treated children are likely better candidates for cure interventions as they have naïve immune systems and smaller reservoirs than adults (De Rossi et al., 2002; Klein et al., 2013). However, not much is known about the reservoir dynamics in early treated children, much less in the context of HIV-1 subtype C infection. In order to lay ground for cure interventions, there is need for a thorough characterization of the reservoir size, mechanisms that enable long-term persistence and the extent to which early therapy shapes the proviral landscape in this population. The post-CHER cohort is a unique population of perinatally infected children, some of whom initiated ART during acute infection and have been in follow-up for close to a decade (Cotton et al., 2013). This provides an ideal context in which to study the latent reservoir in long-term suppressed children. This study sought to characterise reservoirs in a subset of the post-CHER cohort after 6-9 years on suppressive ART. We focused on three main aspects:

- Study Aim I (Chapter 2): Using HIV-1 cell associated DNA (CAD) as a biomarker for latently infected cells, we sought to quantify latently infected cells in early treated children after 6-9 years on ART. Secondly, we described the changes in genetic diversity of latently infected cells after 6-9 years on ART.
- Study Aim II (Chapter 3): We investigated the role of clonal expansion as a mechanism by which latently infected cells persist despite early, long-term suppressive therapy.
- Study Aim III (Chapter 4): Through near full length single genome amplification and sequencing (NFL-PAS), we described the HIV-1 proviral landscape and determined the proportion of proviruses that were genetically intact vs defective after 6-9 years on ART.

Chapter 2

2.1 Introduction

Early ART in children has been shown to limit the establishment of long-lived reservoirs and accelerate their decay rate during long-term ART (Ananworanich et al., 2015; Persaud et al., 2012). Starting ART early also prevents the development of phylogenetically diverse viral quasi-species. Markers of persistence such as cell associated DNA (CAD) are used as biomarkers of reservoir size (Hong et al., 2016). In this sub-study, we quantified HIV-1 cell associated DNA after 6-9 years on ART and described the longitudinal HIV-1 genetic diversity in a subset of the post-CHER cohort. We hypothesized that in these children, the frequency of HIV-1 infected cells would be low and the HIV-1 genetic diversity over time on ART would be limited.

2.2 Study Aim I

To characterise the size and longitudinal genetic diversity of latently infected cells after 6-9 years on suppressive ART in a subset of the post CHER cohort.

2.3 Objectives

- Quantify total HIV-1 DNA as a biomarker for the frequency of latently infected cells using a cell associated HIV-1 DNA quantitative real-time PCR assay targeting the *Integrase* gene (iCAD).
- Compare iCAD values between participants who initiated ART at 0-3, 3-8 and 9-18 months of age.
- Perform single genome sequencing (SGS) to characterise HIV cell-associated DNA and plasma RNA genetic diversity close to the time of ART initiation (baseline) and after several years on ART and determine whether there is evidence of evolution in viral populations during suppressive therapy.
- Determine the clinical and virologic factors associated with low HIV-1 DNA loads and genetic diversity. Factors investigated included age at therapy initiation, duration of virologic suppression, HIV-1 cell-associated DNA load, time to viral load suppression, area under viral load curve, nadir CD4 count, CD8 count, CD4 percentages and CD4:8 ratios.

2.4 Study Population and Inclusion criteria

The study population consisted of 16 children aged 6-9 years, a subset of the post-CHER cohort. Parents or legal guardians provided consent for participation in the study. All 16 children initiated ART between 7 – 42 weeks of age and had HIV-1 RNA loads of <400 copies/ml for up to the most recent 36 months of the 6-9 year sample. This allowed us to investigate long-term HIV DNA persistence in these children. Of the 16, 10 were viral load suppressed from after therapy was initiated until the 6-9year sample. As shown in table 2.1 below, three children had isolated viremic episodes while on ART and 2 children had delayed suppression probably

due to poor adherence, evidenced by detectable viremia during consecutive visits (longitudinal viral load curves: appendix A, section 2.10). One child initiated ART at 17.1 months of age, much later than the others.

Table 2.1: Clinical characteristics of study participants

PID	Gender	CHER study Arm	Age ART Initiated (months)	ART regimen	Baseline HIV Viral load (copies/mL)	Nadir CD4 (%)	Time to Viral load suppression (years)	Longitudinal Viral loads	Age (years)	CD4 % at sample
335106	Female	2	1.8	AZT/3TC/LPV/r	510000	28	0.46	Suppressed	8.4	39
337336	Male	3	1.8	AZT/3TC/LPV/r	>750,000	25.4	0.47	Suppressed	8.5	41
337916	Male	1	1.9	AZT/3TC/LPV/r	>750,000	17	0.46	Suppressed	8.2	21
360806	Female	2	2	AZT/3TC/LPV/r	>750,000	12	3.76	Suppressed	9.3	29
341862	Female	3	2.2	AZT/3TC/LPV/r	>750,000	19	0.44	Viremic episode 2 years on ART	6.95	36
333056	Female	1	2.6	AZT/3TC/LPV/r	>750,000	26.3	0.46	Suppressed	8.8	40
332406	Male	3	2.8	AZT/3TC/LPV/r	>750,000	26	1.38	Viremic episode 6 months on ART	9	46
341146	Male	1	3.9	AZT/3TC/LPV/r	>750,000	30.1	0.92	Suppressed	8.14	37
335836	Male	1	5.1	AZT/3TC/LPV/r	277000	17	0.93	Suppressed	8.6	31
333466	Female	1	6.0	AZT/3TC/LPV/r	>750,000	29.3	0.92	Viremic for first 15 months	8.8	38
334696	Male	1	6.1	AZT/3TC/LPV/r	>750,000	16	0.47	Suppressed	8.5	41
339266	Female	1	9.2	AZT/3TC/LPV/r	635000	28	0.44	Suppressed	8.2	50
340116	Female	1	9.3	AZT/3TC/LPV/r	>750,000	28	2.29	Viremic blip 6 ½ years on ART	8.1	54
338206	Male	1	10	AZT/3TC/LPV/r	>750,000	26	0.92	Suppressed	9.7	35
334436	Female	1	11.1	AZT/3TC/LPV/r	696000	28	3	Viremic for first 3 years	8.8	47
337286	Male	1	17.7	AZT/3TC/LPV/r	654000	22	1.37	Delayed start	8.3	33

AZT – zidovudine, 3TC – lamivudine, LPV-r: Lopinavir-ritonavir, EFV – efavirenz

2.5 Sample collection and patient visits

Fifteen to 20 mL of ethylene-diamine tetra-acetic acid (EDTA) blood was collected 6-monthly at the Children's Infectious Diseases Clinical Research Unit (KIDCRU) of Tygerberg Hospital. Peripheral blood mononuclear cells (PBMC) were separated according the HANC Cross-Network PBMC processing SOP (https://www.hanc.info/labs/labresources/procedures/Pages/pbmcSop.aspx) and stored in aliquots of 2.5 million cells in liquid nitrogen. In addition, stored plasma and PBMC samples collected prior to or soon after ART initiation (a sample time point referred to as 'Baseline') were included in the study.

2.6 Ethical Considerations

For all three study aims, ethical approval was obtained from the Human Research Ethics Committee of Stellenbosch University (ethics numbers N13/04/046 and M14/07/029).

2.7 Methods

2.7.1 HIV-1 *Integrase* Cell-associated DNA (iCAD) for subtype C

Real-time PCR quantification of total HIV-1 DNA is often used as a biomarker of reservoir size. Although it does not discriminate between unintegrated, replication competent and defective proviruses it is a high throughput and affordable assay.

2.7.1.1 Preparation of an HIV-1 subtype C Integrase standard

To prepare a real-time PCR standard, the primers (table2.2) and PCR conditions (table 2.3), below were used to generate a 418 base pair (bp) amplicon (table 2.4) from within the HIV *Integrase* gene using an infectious HIV subtype C clone (PMJ4) as the template. PCR was conducted using GoTaq G2 Hot Start Polymerase (Promega, WI, USA) on an ABI Veriti thermal cycler (Applied Biosystems, CA, USA). This 418bp fragment served as a standard for the iCAD assay.

Table 2.2: HIV-1 subtype C Integrase primers for generating iCAD standard

Primer description	Primer name	Sequence (5' to 3')	HXB2 binding Position
Forward primer	HIV_Int_FP	CCCTACAATCCCCAAAGTCA	4653 → 4672
Reverse primer	HIV_Int_RP	CACAATCATCACCTGCCATC	5051 → 5070

Table 2.3: PCR reaction to generate iCAD standard

Reagent	Stock concentration	Final concentration	Volume (µL)/Rxn
Molecular Grade Water	NA	NA	25.75
GoTaq Buffer	5X	1X	10
dNTPs	40mM total	1,25mM each	1
$MgCl_2$	25mM	2mM	4
Forward Primer	10µM	0.4uM	2
Reverse Primer	10µM	0.4uM	2
GoTaq Enzyme	5U/µL	1.25U	0.25
DNA	2ng/µL	10ng	5
Total			50

Table 2.4: PCR cycling conditions for generating iCAD standard

Temperature	Time	Number of cycles
94 °C	2 min	1X
94 °C	30 s	30X
44 °C	30 s	
72 °C	30 s	
72 °C	7 min	1X
4 °C	∞	

The 418bp PCR product was visualised by loading 5µL of PCR product on a 1% agarose gel with Novel Juice™ DNA stain (Promega; WI; USA) alongside a 1 kb molecular weight marker (Promega; WI; USA).

In order to eliminate non-specific products, the amplicon was gel extracted using the QIAquick Gel Extraction Kit (Qiagen; Hilden; Germany) according to manufacturer's instructions followed by ethanol precipitation to eliminate carry-over salt contamination from the gel extraction kit. The DNA was precipitated by adding 1/10 DNA volume of 3M sodium acetate followed by adding three times DNA volume of ice-cold 100% ethanol. The mixture was incubated at -20^{o}C for 1 hour and then pelleted by centrifuging at 13 000rpm for 30 minutes. The DNA pellet was washed twice with 0.5ml of ice-cold 75% ethanol and then allowed to air-dry before re-suspending in 50µL of 5mM Tris.

2.7.1.2 Quantification of the iCAD standard

The purified standard was quantified on two instruments that use distinct technologies to determine DNA concentration; namely: the NanoDrop™ 2000 Spectrophotometer (Thermofisher Scientific; MA; USA) and the Qubit 2.0 fluorometer (Thermofisher Scientific; MA; USA). The DNA copy number was determined using an online DNA copy number calculator which uses the known DNA sequence, DNA concentration from the nanodrop/qubit and Avogadro's constant to determine the exact copy number. (http://endmemo.com/bio/dnacopynum.php). Results were as follows:

Table 2.5: Quantification of CAD standard

	NanoDrop™ 2000 Spectrophotometer	**Nanodrop A260/230 ratio#**	**Nanodrop A260/280 ratio***	**Qubit 2.0 fluorometer**
Estimated stock DNA concentration	176 ng/µL	1.9	1.75	118.8 ng/µL
Calculated copy DNA number	3.0 x10^{11} cp/µL	NA	NA	2.6 x10^{11} cp/µL

A value of ≈1.8 is acceptable and indicates the absence of protein contaminants that absorb near 280nm

***** A value in the range of 1.8 – 2.2 is acceptable and indicates the absence of organic salts and other contaminants that absorb near 230nm

Following quantification, the DNA standard was serially diluted in 5mM Tris as described elsewhere (Hong et al., 2016) according to the Qubit fluorometer readings. The standard was stored in 20 µL single use aliquots at a concentration of 1 x10^5 copies/ µL.

2.7.1.3 Optimisation of iCAD cycling conditions

To determine the optimal primer and probe concentrations for the iCAD assay, the primers and probe were titrated and the iCAD assay was performed as described elsewhere (Hong et al., 2016).

The primer titration ranged from 100nM to 900nM final concentration per reaction. 1x10^3 and 1x10^4 copies of the standard was used as template in each reaction respectively and each primer concentration was run in triplicate. This experiment was repeated three times and the optimal concentration (corresponding to the concentration with the lowest cycle threshold (Ct)) was determined to be 900nM as shown in figure 2.1 and table 2.6 below:

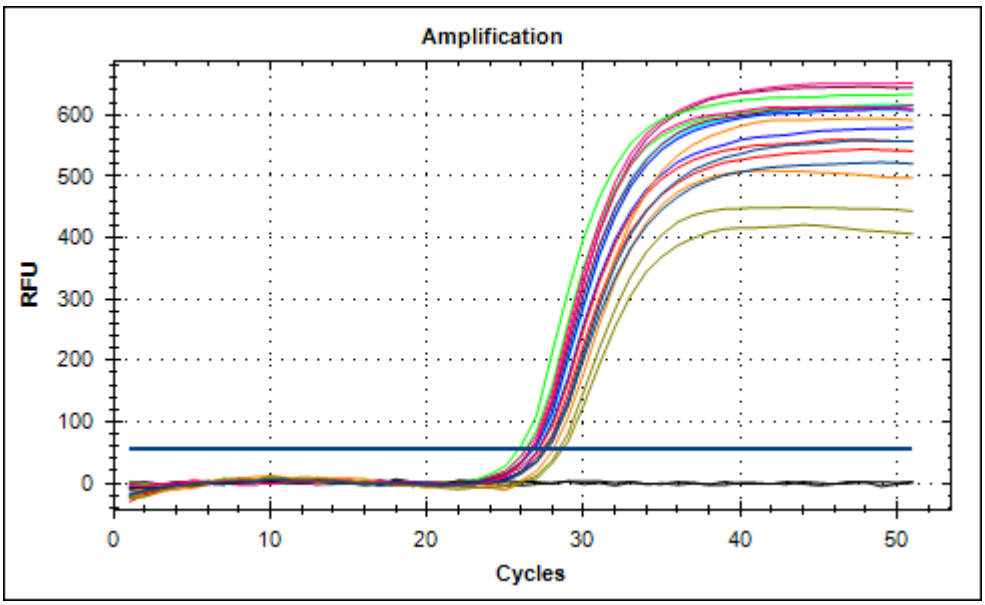

Figure 2.1: Experiment #1 primer titration ranging from 100nM to 900nM per reaction

Table 2.6: *i*CAD primer titration results

Primer concentration (nM)	Mean Cycle Threshold (Ct)	Ct Standard Deviation
100	27.23	0.179
200	27.55	0.094
300	27.79	0.356
400	28.51	0.160
500	26.92	0.244
600	26.61	0.011
700	26.46	0.216
800	26.76	0.068
900	26.04	0.326
No template control	0	-

Likewise, probe titrations ranging from 100nM to 400nM per reaction were performed in three separate experiments using $1x10^3$ and $1x10^4$ copies of the standard respectively as template. Each probe concentration was run in triplicate. The mean optimal concentration was determined to be 400nM as shown in figure 2.2 and table 2.7 below:

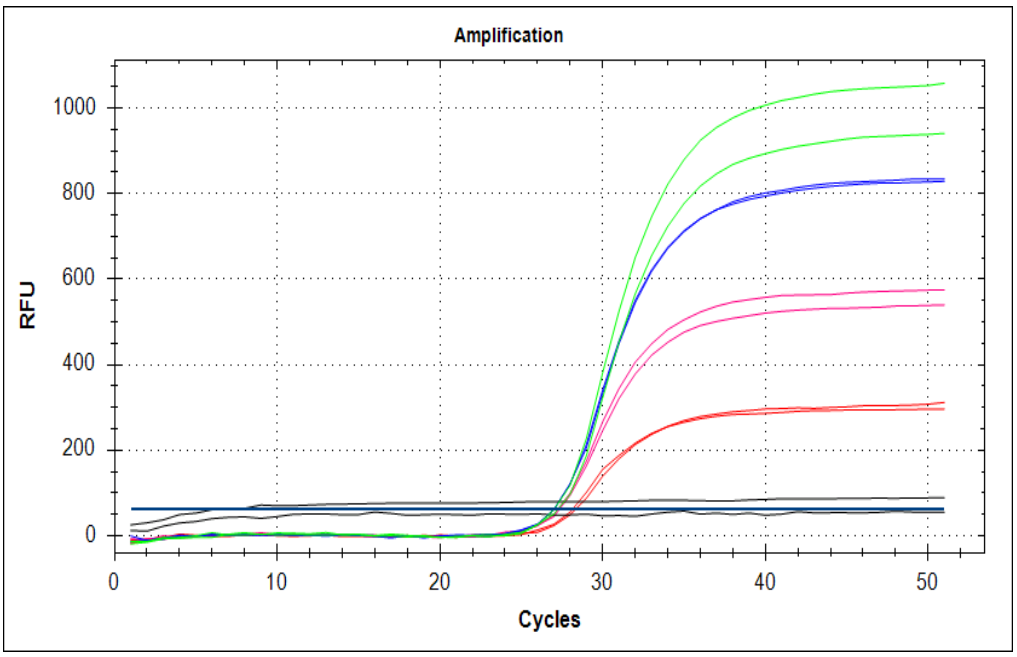

Figure 2.2: Experiment #1 probe titration ranging from 100nM to 400nM per reaction

Table 2.7: *i*CAD probe optimisation results

Probe Concentration (nM)	Mean Cycle Threshold (Ct)	Ct Standard Deviation
100	28.23	0.130
200	27.30	0.065
300	27.01	0.006
400	27.12	0.162
No template control	0	-

2.7.1.4 Optimised iCAD protocol

Below (table 2.8, 2.9 and 2.10) are the optimised iCAD reaction conditions using the LightCyler ® 480 probes master mix (Roche, Switzerland) and adapted from a published protocol (Hong et al., 2016).

Table 2.8: *i*CAD subtype C primers and probe

Primer description	Primer name	Sequence (5' to 3')	HXB2 binding Position

Forward primer	iSCA subtype C_Fwd	TTTGGAAAGGACCAGCCAA	4930 → 4948
Reverse primer	iSCA subtype C_Rev	CCTGCCATCTGTTTTCCA	5042 → 5059
Probe	iSCA subtype C_probe	6FAM- AAAGGTGAAGGGGCAGTAGTAATACA - BHQ1	4959 → 4984

Table 2.9: iCAD master mix

Reagent	**Stock concentration**	**Final concentration**	**Volume (µL)/Rxn**
Molecular Grade Water	NA	NA	1.97
2x Roche MasterMix LC480	2X	1X	12.5
Forward Primer	100µM	0.9µM	0.23
Reverse Primer	100µM	0.9µM	0.23
Probe	100µM	0.3µM	0.075
DNA	90-130ng/µL	36-52ng/µL	10
Total			25

Table 2.10: *i*CAD cycling conditions

Temperature	**Time**	**Number of cycles**
95 °C	5 min	1X
95 °C	15 s	} 50X
60 °C	1 min	
37 °C	∞	Hold

In each iCAD experiment, patient PBMC samples were simultaneously tested for the number of copies HIV-1 *integrase* and the *ccr5* gene. The *ccr5* assay was used to normalise for the number of lymphocytes tested in each sample. Below (table2.11) are *ccr5* reaction conditions:

Table 2.11: *ccr5* primers and probe

Primer description	Primer name	Sequence (5' to 3')
Forward primer	CCR5_Fwd	ATGATTCCTGGGAGAGACGC
Reverse primer	CCR5_Rev	AGCCAGGACGGTCACCTT
Probe	CCR5_probe	6FAM- AACACAGCCACCACCCAAGTGATCA - BHQ1

The *ccr5* quantitative PCR (qPCR) reaction components and cycling conditions were the same as those used for iCAD.

2.7.1.5 Endpoint dilution and Probit regression for validation of the standard

To determine the sensitivity of the assay and ascertain how accurately the standard was quantified, an endpoint dilution real-time PCR experiment was performed on the CFX 96 qPCR thermocycler (Bio-rad; CA; USA). The standard was serially diluted 3-fold with input copy numbers ranging from 3000 copies to 1 copy per reaction. Each concentration was tested in replicates of 10. Probit analysis of the data estimated the 95% hit rate to be 11.7 copies, 95% CI (4.8 – 51.7). The 50% hit rate was estimated to be 3.4 copies, 50% CI (1.64 – 6.20).

2.7.1.6 Extraction of total genomic DNA (gDNA) from patient PBMC

Total genomic DNA (gDNA) was extracted from $1.25x10^6$ PBMC as described elsewhere (Hong et al., 2016). The cells were pelleted, incubated in proteinase K and guanidine hydrochloride to facilitate the lysis of cell walls and release of nucleic acids. Guanidine thiocyanate and glycogen were then added to the nucleic acid and the solution was precipitated in absolute isopropanol followed by a wash with 70% ethanol. The nucleic acid was pelleted, air dried, resuspended in 5mM tris and stored at -80^{o}C until use.

2.7.2 HIV-1 Cell-associated DNA Single-genome sequencing (CAD-SGS) and plasma single genome sequencing (plasma-SGS)

Single genome sequencing (SGS) involves the amplification and sequencing of individual HIV genomes at limiting dilution and allows for the assessment of proviral diversity at a given time (Fig 2.3). Performing SGS within a patient across several time-points can inform about the changes in genetic diversity of HIV-1 proviral DNA, cell-associated HIV-1 RNA or plasma virus during long-term ART.

2.7.2.1 CAD-SGS Serial dilutions and nested PCR

Genomic DNA from 1.25 x 10^6PBMC was extracted as described in section 2.7.1.6 from samples at a time point of 6-9yrs after ART initiation. The extraction protocol was modified to exclude sonification of the DNA and ensure the integrity of long templates. Nested PCR (table 2.13 – 2.15) targeted a 1.5kb region of the *gag-pol* gene spanning *p6*, *protease* and the first 900 nucleotides (nt) of *reverse transcriptase* (*p6-PR-RT*; nt 1893 - 3408, HXB2 positions (Korber et al., 1998)). The primers were described elsewhere (Kearney et al., 2009, 2008; Palmer et al., 2005) but adapted for subtype C (table 2.12). The extracted DNA was then serially diluted such that each PCR reaction was seeded by a single HIV-1 DNA molecule. According to the Poisson distribution, dilutions at which 30% of all reactions are positive, are most likely derived from a single template (Kearney et al., 2009, 2008; Palmer et al., 2005). Initially, a 'screening PCR plate' was performed for each sample to determine the target dilution at which about 30% of replicates were PCR positive. Each screening plate consisted of three-fold serial dilutions ranging from 1:3 to 1:81 with multiple replicates at each dilution. Once the target dilution was determined, multiple 'expansion PCR plates' at the target dilution were performed until a sufficient number of positive PCR reactions had been obtained.

Table 2.12: Nested PCR primers for HIV gag-pol subtype C SGS

Primer description	Primer name	Sequence (5' to 3')	HXB2 binding Position
Forward outer	1849(C)+	GATGACAGCATGTCAGGGAG	1849 → 1868
Reverse outer	3500 (C)-	CTATYAAGTCTTTTGATGGGTCATAA	3500→ 3525
Forward Inner	1870(C)+	GAGTGTTGGCTGAGGCAATGAG	1870→ 1892
Reverse Inner	3410(C)-	CAGTTAGTGGTACTATGTCTGTTAGTGCTT	3410→ 3439

Table 2.13: Pre-nested and Nested PCR reactions for gag-pol SGS

Reagent	Stock concentration	Final concentration	Volume (µL)/Rxn
PCR buffer (Invitrogen)	10X	1X	1µL
MgCl2	50mM	2mM	0.4µL
dNTPs	10mM	0.2mM	0.2µL
Primers (ea)	50µM	0.2µM	0.04µL
Plat Taq Enzyme (Invitrogen)	5U/µL	0.4U	0.08µL

Molecular-grade water	-	-	6.24µL
DNA	-	-	2µL
Total			10µL

Table 2.14: Pre-nested gag-pol SGS reaction

Temperature	**Time**	**Number of cycles**
94 °C	2 min	1X
94 °C	30 s	44X
50 °C	30 s	
72 °C	1 min 30 s	
72 °C	3 min	1X
4 °C	∞	

The pre-nested PCR plate was diluted by adding 83µL of 5mM tris. After this, 2µL of the diluted pre-nested reaction was added into the corresponding PCR well in the nested plate.

Table 2.15: Nested gag-pol SGS reaction

Temperature	**Time**	**Number of cycles**
94 °C	2 min	1X
94 °C	30 s	40X
44 °C	30 s	
72 °C	1 min	
72 °C	3 min	1X
4 °C	∞	

Sanger sequencing (table 2.16 – 2.18) was performed on all PCR positive reactions using the BigDye™ Terminator v3.1 Cycle Sequencing Kit (Applied Biosystems; CA; USA).

Table 2.16: HIV gag-pol subtype C sequencing primers

Primer description	Primer name	Sequence (5' to 3')	HXB2 binding Position
Forward outer	2030(C)+	TGTTGGAAATGTGGAAAGGAAGGAC	2030 → 2055
Forward Inner	2600 (C)+	ATGGCCCAAAGGTTAAACAATGGC	2600→ 2623
Reverse Inner	2610(C)-	YTCTTCTGTCAATGGCCATTGTTTAAC	2610→ 2636
Reverse Outer	3330(C)-	TTGCCCAGTTTAATTTTCCCACTAA	3330→ 3354

Table 2.17: Big Dye Terminator sequencing master mix

Reagent	Stock concentration	Final concentration	Volume (µL)/Rxn
BigDye Ready Reaction mix	2.5X	0.25X	1 µL
BigDye Sequencing Buffer	5X	1.5X	3 µL
Primer	5µM	0.5µM	1 µL
Molecular-grade water	-	-	4 µL
DNA	-	-	1µL
Total			10 µL

Table 2.18: Sequencing cycling conditions

Temperature	Time	Number of cycles
96 °C	10 s	}
50 °C	5 s	} 25X
60 °C	4 min	
4 °C	∞	

2.7.2.2 Plasma-SGS

In patients where there was no PBMC sample available at baseline, single genome sequencing was performed on baseline plasma samples. The assay was performed by our collaborators at the 'HIV Dynamics and Replication unit' of the National Cancer Institute.

Virion RNA was extracted from plasma containing 10 000 copies as previously described but with some modifications (Hong et al., 2016). The plasma was subjected to an initial pre-spin step to remove cellular debris. This was followed by a spin at 4^{o}C for an hour at 16,000xg to pellet the virions. The virion pellet was then treated with proteinase K and incubated at 55^{o}C for 30 minutes to facilitate the release of viral nucleic acid. Guanidine thiocyanate and glycogen were added to the nucleic acid solution followed by precipitation in absolute isopropanol. A wash with 70% ethanol followed. The nucleic acid pellet was then air dried, resuspended in a 5mM tris buffer and stored at -80^{o}C until use. For each sample, 10% of the RNA suspension was removed for use as a 'no reverse transcription control' (NRT). The extracted RNA was denatured at 65^{o}C for 10 minutes in the presence of 1mM dNTPs and 0.2µM gene specific primer. The cDNA synthesis cocktail was prepared as shown in table 2.19 below and added to the denatured RNA. The incubation protocol is shown in table 2.20 below:

Table 2.19: cDNA Synthesis cocktail

Reagent	**Stock concentration**	**Final concentration**	**Volume (µL)/Rxn**
10X RT buffer (Invitrogen)	10X	1X	10µL
MgCl2	25mM	5mM	20µL
DTT	100mM	1mM	1µL
Superscript III Reverse Transcriptase (Invitrogen)	200U/µL	100U	0.5µL
Rnase-Out (Invitrogen)	40U/µL	40U	1µL
RNase-free water	-	-	17.5µL

Table 2.20: cDNA Synthesis protocol

Temperature	**Time**
45 °C	50 min
85 °C	10 min
4 °C	∞

Following cDNA synthesis, screening and expansion plates were generated followed by sanger sequencing as described for CAD-SGS in section 2.6.2.1 above.

2.7.2.3 Sequence alignments

Bidirectional sanger sequences from a region that spans HIV-1 *p6- protease – reverse transcriptase* genes were aligned to the ancestral HIV-1 subtype C reference sequence from the HIV Los Alamos database and trimmed to a length of 1200bp to exclude poor quality reads at the ends of the sequences. Sequence alignments, contigs and consensus sequences for each sample were generated using a sequence alignment pipeline developed by our collaborators at the National Cancer Institute (MD, USA). The pipeline detected and scored sequences with single nucleotide polymorphisms (SNPs) with a cut off value of <85 indicating that there was more than one template present in those reactions. Such sequences were excluded from further analysis. Each single genome sequence was analysed for the presence of drug resistance mutations to current and previous patient ART regimens (hivdb.stanford.edu). Sequences were also analysed for evidence of G to A hypermutation caused by the host restriction factor APOBEC using the 'Hypermut' program (https://www.hiv.lanl.gov/content/sequence/HYPERMUT/background.html).

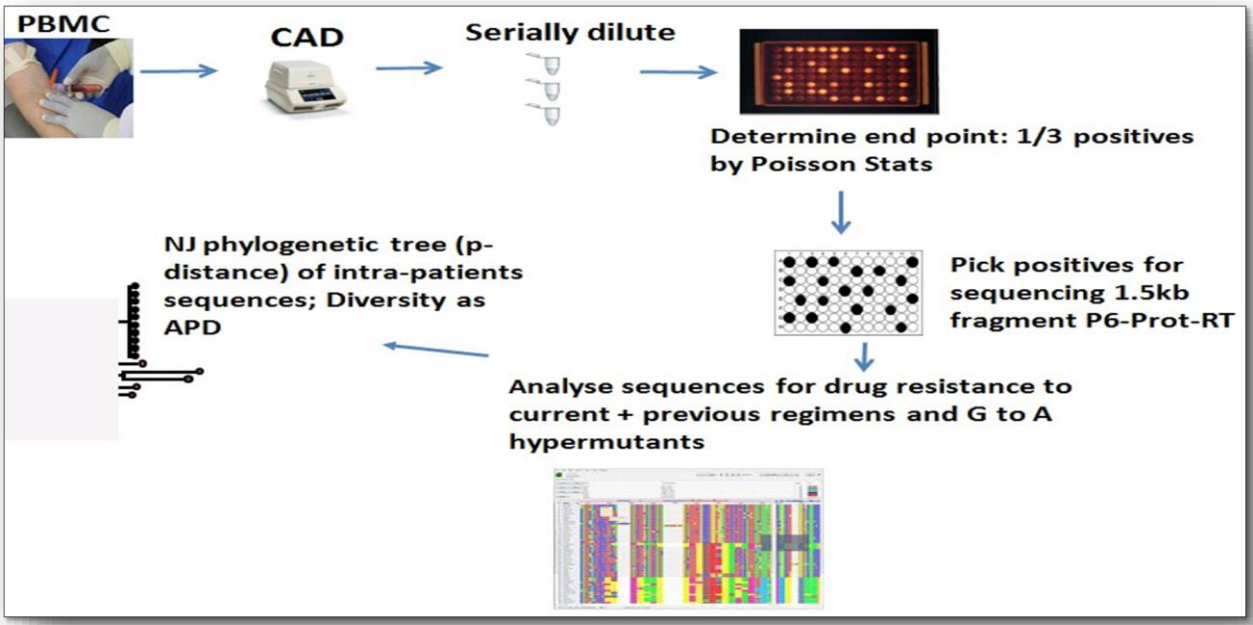

Figure 2.3: CAD-SGS Workflow

2.7.2.4 Phylogenetic tests for genetic diversity and evolution

To assess whether viral evolution occurred between the baseline and on-ART time points, the single genome sequences from each time point were included in the following analyses of population structure and evolution:

a) Calculation of the average pairwise distance (APD) as a measure of intra-patient viral genetic diversity at a given time point. This was followed by construction of neighbour joining phylogenetic trees using the Molecular Evolutionary Genetics Analysis software, version 6.0 (MEGA6) (http://www.megasoftware. net) p-distance algorithm.

b) The probability of shifts in viral population structure was determined using a subdivision test for panmixia (http://wwwabi.snv.jussieu.fr/achaz/hudsontest.html). The test was derived from a geographic population structure test proposed by Hudson et al (Hudson et al., 1992). The panmixia test compared longitudinal single genome sequences from a patient and calculated the probability that the populations were the same across the two time points. A p value of less than 10^{-3} was set as the significance cut-off (as described by the original report and other publications) to account for the high number of comparisons between sequences and nucleotide sites (Achaz et al., 2004; Hudson et al., 1992; Rouzine and Coffin, 2010) .

c) Maximum likelihood (ML) models to assess root to tip distance before and after long-term ART: PAUP4.0 (http://paup.sc.fsu.edu/) was used to construct ML trees. The model used in the tree construction was GTR+I+Γ4. HIV-1 consensus C or the majority sequence at baseline were set as the outgroup. Root-to-tip length was calculated on the basis of the ML trees with TreeStat, version 1.6.2 in the BEAST package (http://beast.bio.ed.ac.uk/) to detect the emergence of new viral populations.

2.7.3 Data Correlations

Correlation between variables was assessed with the Spearman's rank-order correlation test in R software for the following variables: "Age of ART initiation", "Time to viral load suppression", "Area under viral log load curve", "Total HIV-1 DNA", "Percent proviral diversity by SGS" and "Number of identical sequence clusters by SGS". A p value of less than 0.05 was accepted as statistically significant.

2.8 Results

2.8.1 HIV-1 Cell-associated DNA (CAD) during long-term ART:

This was a cross-sectional analysis to quantify HIV-1 cell-associated DNA as a biomarker of reservoir size after long periods on suppressive ART. The median time on ART at time of testing was 8 years (range 7-9.3 years). The cohort of 16 children was divided into three tertiles based on the age at which ART was initiated i.e ART initiated between 0-3 months, 3-8 months and 9-18 months of age respectively as shown in table 2.21 below. The median time to first viral load suppression was 0.92 years (range 0.44 – 3.76 years). HIV-1 cell-associated DNA values ranged from 0 copies/10^6 PMBC to 186.2 copies/10^6 with a median iCAD value of 22.45 copies/10^6 PBMC. Seven of the 16 patients (47%) had very low iCAD values (< 20 copies/10^6). Two children had undetectable iCAD. This could have been due to the proviral load being so low that more cells would need to be tested to determine the proviral load. Primer mismatches in the *Integrase* gene because of the high genetic diversity of HIV-1 subtype C could also have resulted in undetectable iCADs in these two patients. There was no significant difference in iCAD values among the three tertiles.

The area under the log viral load curve, measured in log10 HIV-1 RNA copy years, shown in table 2.21, is a measure of amount of exposure to HIV antigen or replication over time on therapy. It was determined by calculating the area beneath a plot of log viral load against time. A spearman's rank correlation between HIV cell associated DNA (iCAD) on long-term therapy and area under the log viral load curve showed a significant positive correlation (rho=0.8, p<0.05) figure 2.4.

Table 2.21: HIV-1 Cell-associated DNA in early-treated children after 7-9 years on ART

PID	Age ART start (months)	Time to Viral load Suppression (years)	Area Under Viral load curve (log 10 HIV copy years)	Duration of ART at sample (years)	iCAD (DNA copies /10^6 PBMC)	Total cell equivalents assayed for HIV DNA
335106	1.8	0.46	1.74	8.4	4.5	348 300
337336	1.8	0.47	1.78	9.2	0	379 350
337916	1.9	0.46	1.82	8.2	1.5	321 750
360806	2	3.76	12	9.3	186.2	770 895
341862	2.2	0.44	4.78	7	42.3	406 350
333056	2.6	0.46	1.88	8.6	0	345 150
332406	2.8	1.38	6.35	9	23.6	997 500
341146	3.9	0.92	2.61	7.8	32.5	483 300
335836	5.1	0.93	3.14	8.6	11.9	331 200
333466	6.0	0.92	4.77	8.3	2.2	762 300
334696	6.1	0.47	3.53	8.5	9.2	520 650
339266	9.2	0.44	5.11	8.2	46.7	701 550
340116	9.3	2.29	10.34	8.1	181.5	454 050
338206	10	0.92	6.31	9.7	21.3	360 900
334436	11.1	3	13.01	8.8	86.3	333,900

337286	17.7	1.37	9.74	8.3	32.8	391 050
Median	4.5	0.92	4.8	8.45	22.5	398 700

ART initiated between 0 - 3 month

ART initiated between 3 – 9 months

ART initiated between 9 – 18 months

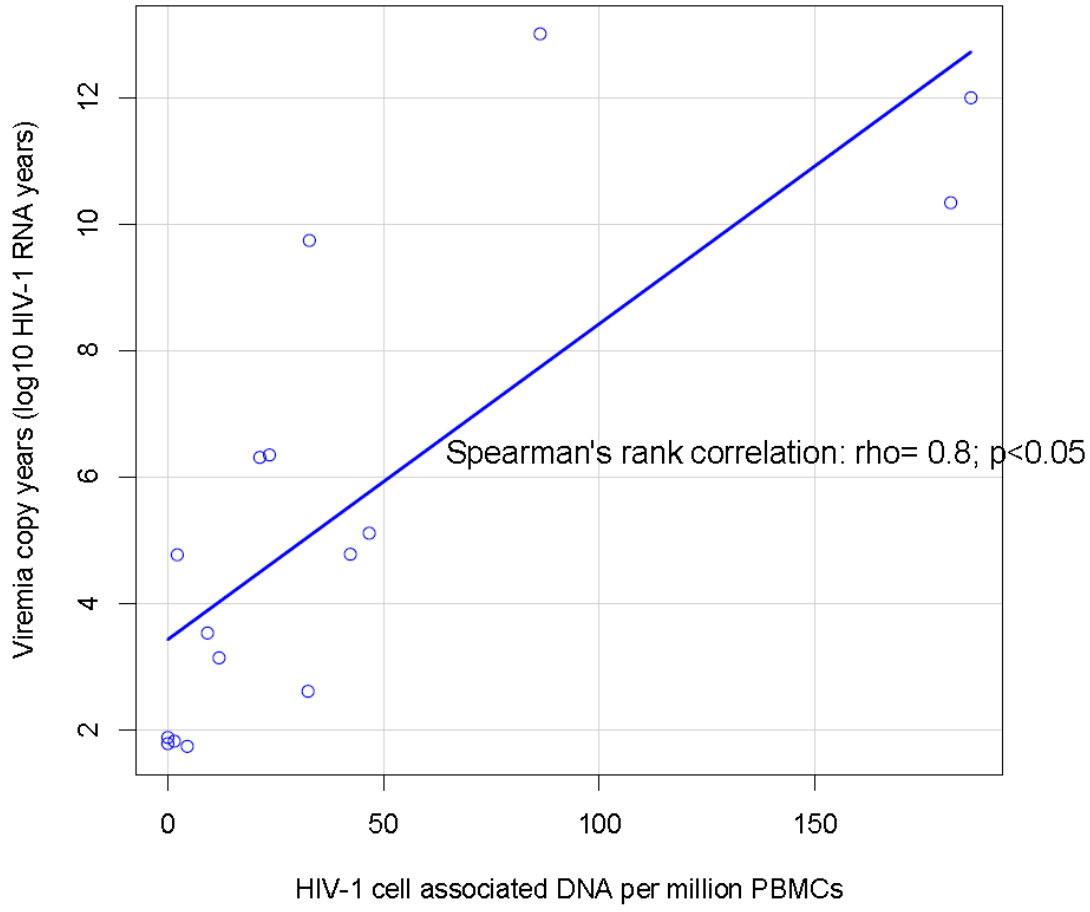

Figure 2.4: Correlation of Total HIV-1 DNA with cumulative viremia

2.8.2 Neighbour joining phylogenetic trees

The single genome sequences spanning a 1200bp region in HIV-1 *gag-pol* were generated for 10 of the children who had iCAD values above 10copies/10^6 PBMC and aligned to the ancestral subtype C reference sequence from the Los Alamos HIV database. All sequences that had evidence of G to A hypermutation when analysed in the 'Hypermut' program (www.hiv.lanl.gov) was excluded from phylogenetic analysis as these sequences are defective and unable to replicate.

Figure 2.5 below shows neighbour joining phylogenetic trees of each participant. Sequences were generated from two time points. The sample closest to therapy initiation was referred to as baseline. The second sample was from 6-9 years after ART initiation. Baseline sequences were derived from either plasma RNA or cell associated DNA depending on sample availability whereas sequences from 6-9 years on ART were derived from cell-associated DNA.

Participants were categorised as either being fully suppressed on ART or having had periods of partial viral suppression (longitudinal viral load graphs in Appendix A: Section 2.10). Eight participants had been fully suppressed since therapy initiation whereas two participants had earlier periods of delayed or poor suppression following ART initiation.

In the two partially suppressed participants, phylogenetic trees showed the clustering of sequences from long-term therapy on longer branches (blue clusters fig 2.5) indicating that these were distinct variants that had diversified from baseline populations. In patients who were fully suppressed however, sequences from the two different time points were randomly distributed in the tree with no particular clustering of sequences from either time point indicating a lack of diversification.

In all participants, there were sequences that were identical in the 1200bp region (indicated in purple bracket), in some cases this clustering was between viral RNA/DNA from baseline and DNA from long-term ART. This could be an indication of clonal expansion of latently infected cells during long-term ART.

Participants partially suppressed on ART:

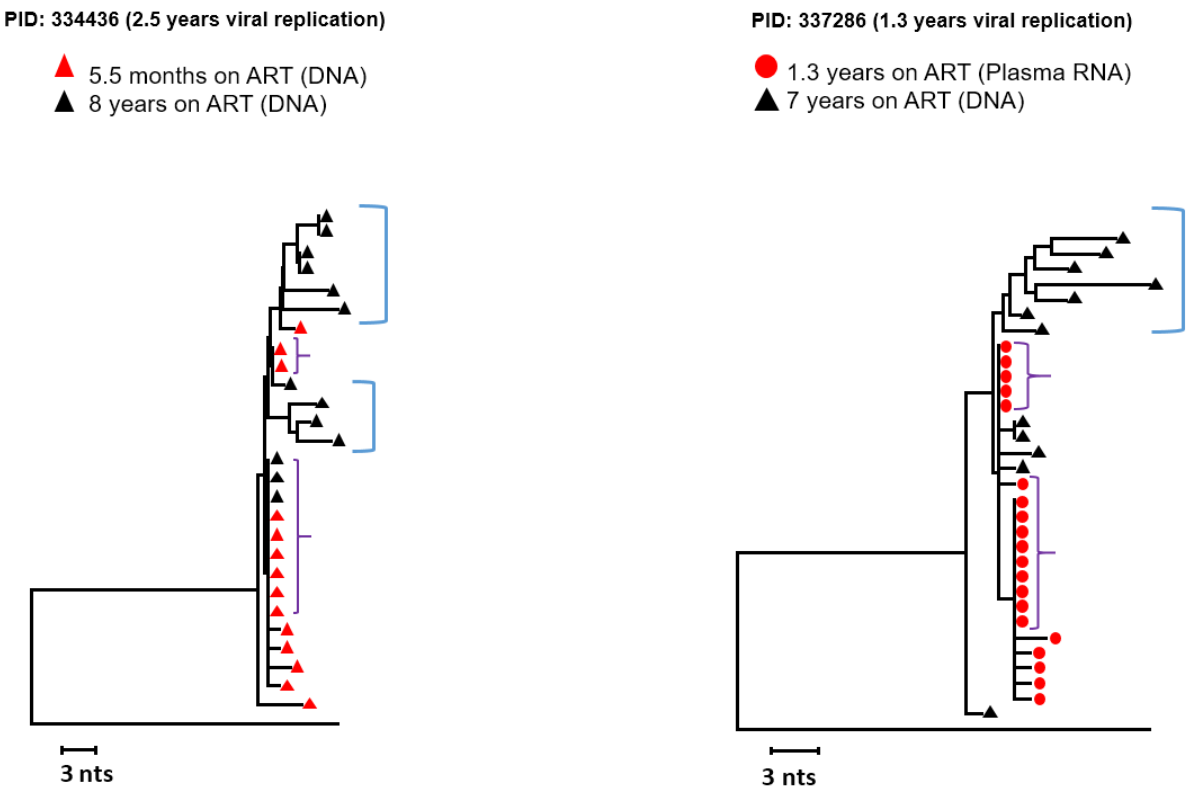

Participants fully suppressed on ART:

PID: 337916

● 14 days before ART (Plasma RNA)
▲ 8 years on ART (DNA)

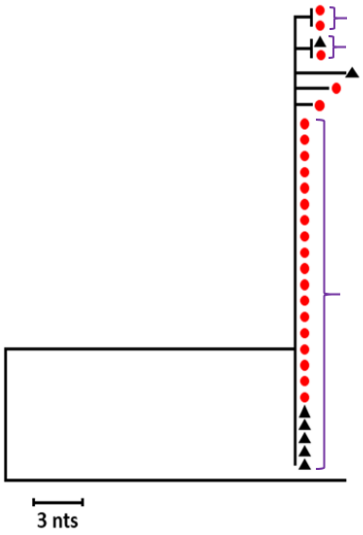

PID: 332406

▲ 9 months on ART (DNA)
▲ 8.5 years on ART (DNA)

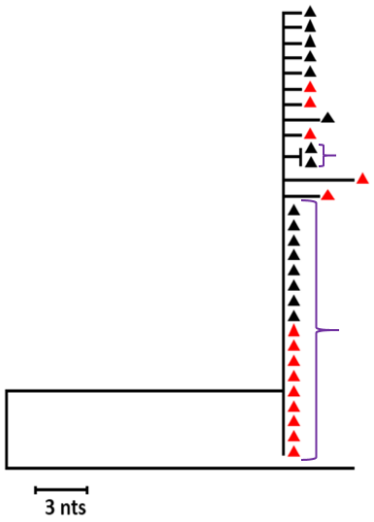

PID: 334696

▲ 8 months on ART (DNA)
▲ 8 years on ART (DNA)

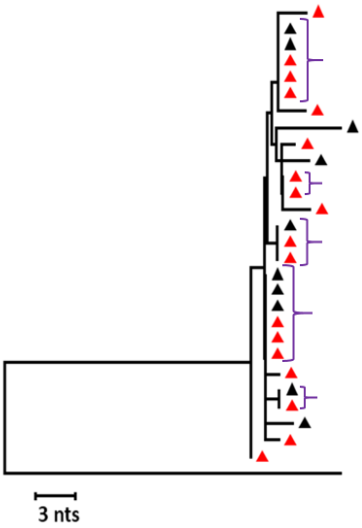

PID: 339266

▲ 5 months on ART (DNA)
▲ 7.5 years on ART (DNA)

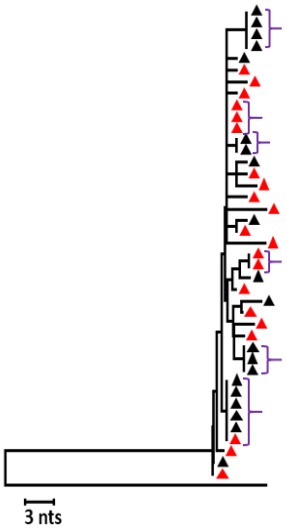

PID: 338206

▲ 5 months on ART (DNA)
▲ 7 years on ART (DNA)

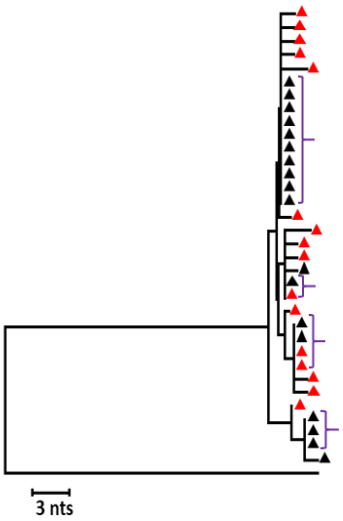

PID: 341862

▲ 2 years on ART (DNA)
▲ 6.75 years on ART (DNA)

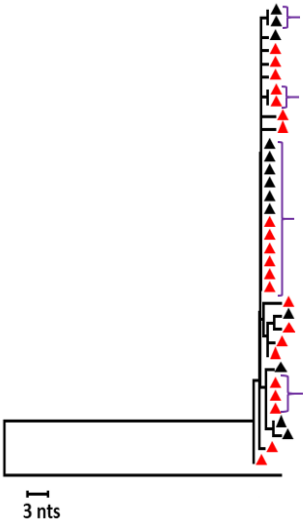

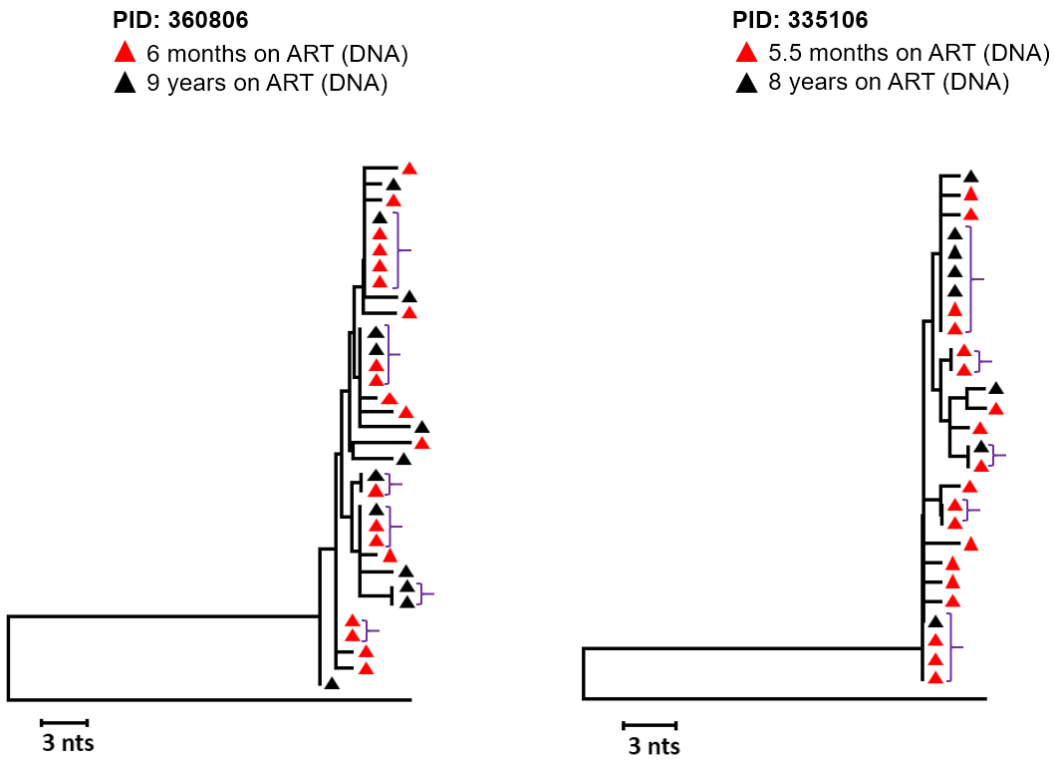

Figure 2.5: Neighbour joining phylogenetic trees of fully ART suppressed and partially ART suppressed children

2.8.3 Change in diversity between baseline and long-term ART by SGS

The sequences were used to analyse the diversity of viral populations by calculating the average pair-wise distance (APD) using the p-distance algorithm in MEGA6 at baseline and after 6-9 years on ART. The high cost of performing SGS and inadequate amount of sample limited the number of single genome sequences that could be generated for each participant. However, the likelihood of missing viral variants that were present in the circulatory but not sampled has been calculated elsewhere (Salazar-Gonzalez et al., 2008). Power calculations using probability theory estimated that the likelihood that a particular 'missed' variant comprises a fraction of the virus population is less than 14% when 20 single genome sequences are analysed (Salazar-Gonzalez et al., 2008). Therefore, sampling 10-20 sequences was sufficient to provide a reasonable estimate of population diversity as sequencing more than 20 but less than 100 genomes would not significantly decrease the standard error (personal communication: Mary Kearney, National Cancer Institute).

Either plasma RNA or cell associated DNA was used to assess the diversity at baseline. ART prevents new rounds of replication. Before an individual is suppressed on ART, viral replication ensures that circulating free viral variants in plasma match viruses infecting cells such that proviral diversity in cells reflects the circulating virus in plasma (Boritz et al., 2016; Gupta et al., 2013; Lorenzo-Redondo et al., 2016). It was thus appropriate to use either DNA or RNA as a baseline sample. Table 2.22 shows the percent diversity calculated as average

pair wise distance (APD) at baseline while Table 2.23 shows diversity after 6-9 years on ART for both the partially suppressed participants (red) and fully suppressed participants (blue).

Table 2.22: Average Pairwise Distance (APD) at baseline

PID	Age ART start (months)	Pre-ART Viral Load	Baseline Sample Type	Baseline iCAD	Months relative to ART initiation at sample	Number of single genome sequences	Average Pair-wise distance (APD)(%)
334436	11,1	696,000	PBMC	458,7	4	14	0,15
337286	17,1	654,000	Plasma	NA	-16	20	0,10
337916	1,9	>750,000	Plasma	NA	0	23	0,04
332406	2,8	>750,000	PBMC	2 342,1	9	14	0,11
334696	6,1	>750,000	PBMC	435,3	8	18	0,19
339266	9,2	635,000	PBMC	340,4	5	21	0,30
338206	10	>750,000	PBMC	65,1	5	16	0,25
341862	2,2	>750,000	PBMC	1 567,7	0	22	0,21
360806	2	>750,000	PBMC	28 084,2	6	20	0,24
335106	1,8	510,000	PBMC	63,4	6	19	0,21

Participants not suppressed on ART for duration of sampling

Participants fully suppressed on ART for duration of sampling

Table 2.23: Average Pairwise Distance (APD) at after 6-9 years on ART

PID	Age ART start (months)	Viral Load at sample	Sample Type	iCAD at sample	Months relative to ART initiation at sample	Number of single genome sequences	Average Pair-wise distance (APD)
334436	11,1	TND	PBMC	86,3	95	13	0,43
337286	17,1	TND	PBMC	32,8	82	12	0,57
337916	1,9	TND	PBMC	1,5	97	7	0,11
332406	2,8	TND	PBMC	23,6	105	16	0,09
334696	6,1	TND	PBMC	9,2	96	10	0,22
339266	9,2	LDL	PBMC	46,7	89	20	0,26
338206	10	TND	PBMC	21,3	99	18	0,18
341862	2,2	TND	PBMC	42,3	105	13	0,19
360806	2	TND	PBMC	186,2	110	13	0,33
335106	1,8	TND	PBMC	4,5	100	8	0,13

'TND': Target not detected' 'LDL': Lower than detection limit (indicating that target was detected but unquantifiable)

Participants not suppressed on ART for duration of sampling

Participants fully suppressed on ART for duration of sampling

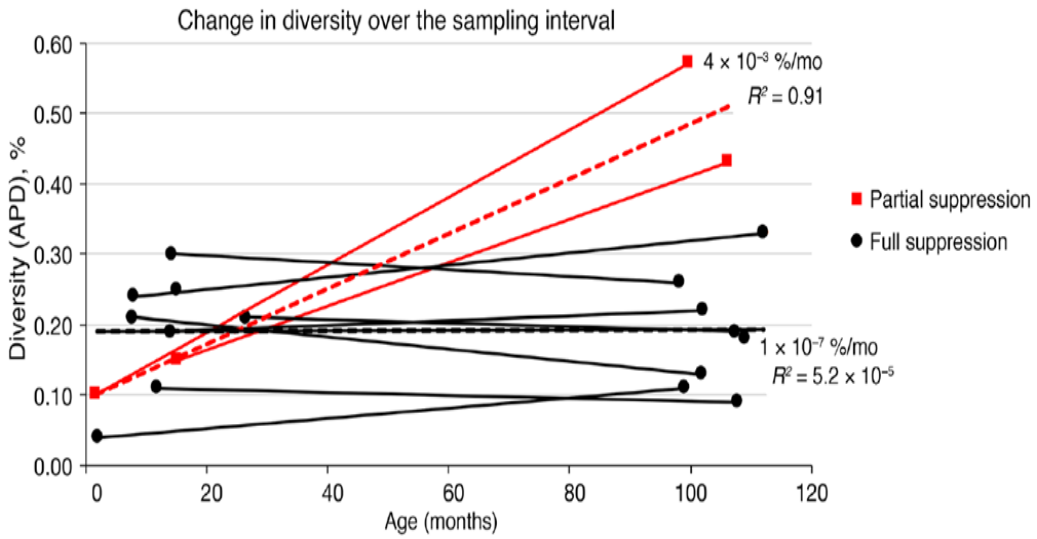

Figure 2.6: Change in diversity oversampling period

Figure 2.6 above illustrates the change in diversity between baseline and 6-7 years on ART for each participant. There was a significant change in diversity over time in the partially suppressed controls (coefficient of determination r = 0.91, p=0.05) whereas in those who were fully suppressed on ART, no significant change in diversity was observed between baseline and 6-9years on ART.

2.8.4 Further analysis for change in diversity

In addition to APD, two tests for change in diversity between baseline and long-term ART were performed on the sequences:

(i) A subdivision test for panmixia was used to determine the probability of shifts over time in viral population structure. A p value of less than 10^{-3} was set as the significance cut-off.

(ii) A maximum likelihood model to assess root to tip distance between sequences from baseline and 6-9 years on ART was performed. The root-to-tip slope measured the genetic distance from the majority sequence at baseline as well as the distance from the ancestral subtype C sequence respectively. The root-to-tip slope was calculated on the basis of the maximum likelihood (ML) trees with TreeStat, version 1.6.2, in the BEAST package. A significant root to tip distance was set at a p value of 10^{-3}.

Table 2.24 below compares APD, panmixia and root-to-tip slope for changes in diversity between baseline and long-term ART. A significant change in APD over time was determined using a 2-tailed, 1-sample t test,

where the assumed mean was the APD of the early time point and the sample distribution was the APD of the late time point, with variance estimation performed using 1,000 bootstrap replicates. For the two participants who were partially suppressed on ART, all three tests gave significant results for changes in diversity over time by APD, shifts in viral population structure by panmixia, the root to tip slope when rooted on consensus C and the majority baseline sequence. Participants on continuous ART suppression had no significant results when the three tests were applied.

Table 2.24: Phylogenetic tests for change in diversity over time

Participant group	PID	Sample time point	Months relative to ART initiation	HIV Diversity	Panmixia p-value	Root to Tip Slope (rooted on consensus C) (sub/site/months) ($x10^{-5}$)	p-value (rooted on consensus C)	Root to Tip Slope (rooted on baseline majority) (sub/site/months)($x10^{-5}$)	p-value (rooted on baseline majority)
Not suppressed on ART for duration of sampling	334436	Baseline (PBMCs) Long-term ART (PBMCs)	4 95	0.18% **0.42%**	**0.002**	3.91	**0.0008**	$3.91*10^{-5}$	**0.0008**
	337286	Baseline (plasma) Long-term ART (PBMCs)	-16 82	0.10% **0.57%**	**$<10^{-4}$**	2.3	**0.002**	$3.35*10^{-5}$	**$7*10^{-7}$**
Continuous Suppression on ART	337916	Baseline (plasma) Long-term ART (PBMCs)	0 97	0.04% 0.10%	0.3	2.8	0.3	$2.84*10^{-6}$	0.3
	332406	Baseline (PBMCs) Long-term ART (PBMCs)	9 105	0.11% 0.09%	0.5	-0.075	0.8	$-3.56*10^{-7}$	0.9
	334696	Baseline (PBMCs) Long-term ART (PBMCs)	8 96	0.19% 0.22%	0.8	0.29	0.7	$1.56*10^{-6}$	0.8
	339266	Baseline (PBMCs) Long-term ART (PBMCs)	5 89	0.29% 0.25%	0.06	0.021	1.0	$-1.11*10^{-6}$	0.7
	338206	Baseline (PBMCs) Long-term ART (PBMCs)	5 99	0.25% 0.18%	0.04	-0.55	0.3	$-2.48*10^{-6}$	0.4
	341862	Baseline (PBMCs) Long-term ART (PBMCs)	0 105	0.21% 0.19%	0.4	-0.13	0.8	$-2.73*10^{-6}$	0.7
	360806	Baseline (PBMCs) Long-term ART (PBMCs)	6 110	0.24% 0.33%	0.4	0.43	0.4	$6.28*10^{-6}$	0.1
	335106	Baseline (PBMCs) Long-term ART(PBMCs)	6 100	0.21% 0.17%	0.4	0.0062	1.0	$6.30*10^{-8}$	1.0

A p value of less than 10^{-3} was set as the significance cut-off for panmixia. Likewise, a significant root to tip distance was set at p value of 10^{-3}

2.8.5 iCAD and APD on long-term ART

Cell associated DNA and the average pairwise distance after 6-9 years on ART were positively associated.

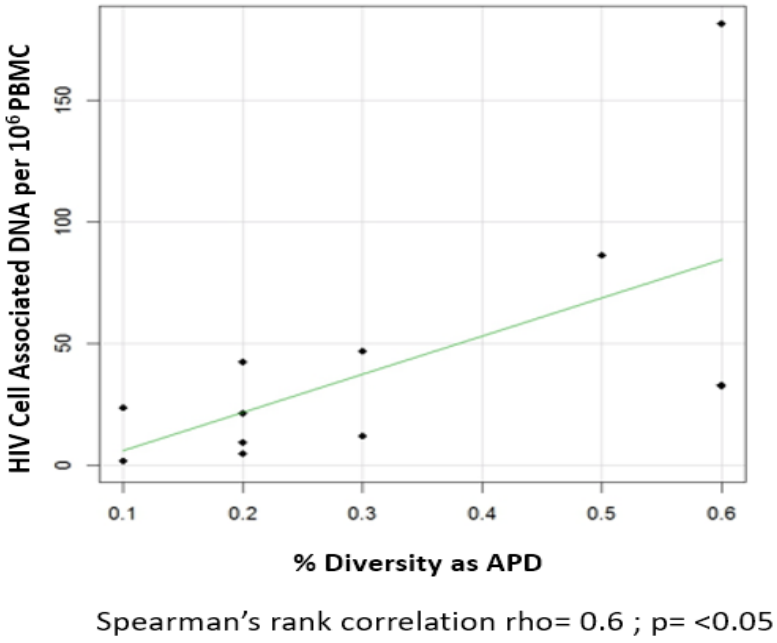

Figure 2.7: Spearman's rank correlation between iCAD and % Diversity

2.9 Discussion

2.9.1 HIV-1 cell associated DNA loads after 7-8 years on ART

After 7-8 years on ART, HIV-1 cell associated DNA loads (iCAD) in 16 children who initiated ART within the first 18 months of life were low. Although our iCAD values were in similar ranges as those found in children who were tested at 6 years on ART after initiating ART before 6 months of age (Ananworanich et al., 2014), we found no significant difference in proviral loads between children who initiated therapy before 3 months, between 3-8 months or within 9-18 months of age. It is likely that we did not detect a difference among the treatment age groups in our cohort because some children (i.e participants: 334436, 337266, 341862, 332406, 340116, 333466 (figure 2.1)) had periods after ART initiation where there was viral replication that may have replenished their proviral loads.

In contrast to our findings, a study in 20 well suppressed children from the post-CHER cohort found significantly lower cell-associated DNA and RNA loads in those who initiated ART within two months of birth compared to those who initiated later (Van Zyl et al., 2014). A similar study found that children who initiated ART within 3 months of age had CADs 6-fold lower than those who initiated after 3 months but within a year of life (Martínez-bonet et al., 2015). Luzuriaga et al compared children who initiated ART within the first year of life to those who initiated after 4 years and found significantly higher proviral loads, recoverable replication competent virus, T cell activation and slower proviral decay in the latter group (Luzuriaga et al., 2014). These findings have been mirrored by others (Foster et al., 2017) and along with ours highlight the long-term benefits of early initiation of ART in limiting the size of the reservoir. However, despite the benefit of early ART, the recent case of a Mississippi baby who initiated ART within 30 hours of life but later had viral rebound shows that early ART is unable to prevent the establishment of long-lived reservoirs (Luzuriaga et al., 2015; Persaud et al., 2013).

There was a significant positive association between cumulative viremia and the total HIV-1 DNA after 7-8 years on ART suggesting that the more viral replication over time, the larger the reservoir. This agrees with a recent study showing a positive correlation between RNA area under viral load curve in the first year of life and HIV DNA levels at one year (McManus et al., 2016). Studies by Persuad et al showing that time to first viral load suppression was strongly positively associated with infectious virus levels when using the gold standard viral outgrowth assay further support our findings (Persaud et al., 2014, 2012).

Due to limited sample availability, we were unable to perform further analysis using the gold-standard quantitative viral outgrowth assay (qVOA) that reactivates resting cells and quantifies the amount of infectious virus that grows out. A recent study attempted to detect infectious virus by qVOA in a cohort of early treated children and found no outgrowth showing that HIV-1 reservoirs are very limited in early-treated, long term suppressed children (Rainwater-Lovett et al., 2017). This suggests that we may have obtained similar VOA results in our cohort where proviral loads were low and, in some cases, undetectable. Total HIV-

1 DNA quantification provides a sensitive and feasible approach to estimate the reservoir in early treated children, where the expected reservoir size is small. Nevertheless, there is a need for more specific, but cost-effective assays that can distinguish between defective and intact proviral genomes. Such assays would be valuable to assess the effect of interventions that are aimed at eradicating or reducing the size of the latent reservoir especially for paediatric cohorts where sample availability is limited. One such assay using quantitative PCR that incorporates multiple probes to differentiate between intact, hypermutated and defective proviruses has recently been described (Bruner et al., 2019).

2.9.2 No evidence of viral evolution on suppressive ART

There have been conflicting views on whether ART completely halts ongoing cycles of viral replication that could replenish and maintain the reservoir in patients with clinically undetectable viral loads. Most of the children included in this study had low pre-treatment diversity, which increased our ability to detect any subsequent evolution. Our results show that when early treated children are fully suppressed on ART, there is no detectable evolution over time on ART suggesting that ART prevents ongoing viral replication.

Three phylogenetic tests to assess changes in viral population diversity, population divergence and maximum likelihood phylogenetics between baseline and 7-8 years on ART showed no evidence of viral evolution in 8 children that had been fully suppressed whereas in 2 children who were partially suppressed, all three tests showed significant evidence of viral evolution.

A recent study used the same methods to compare sequences from the plasma of adults before, during and after ART interruption (Kearney et al., 2014). The study found no significant difference between proviruses prior to ART and plasma virus that rebounded after ART interruption, suggesting that the reservoir is likely maintained by persistence and proliferation of cells that were infected before ART initiation. In another study, there was no divergence or evidence of evolution over time on ART in 12 children when replication competent viral sequences from an end point dilution culture assay were analysed (Persaud et al., 2007).

Our findings conflict with a recent report of ongoing viral evolution in lymphoid tissues of ART suppressed individuals (Lorenzo-Redondo et al., 2016). In that study, time-stamped Bayesian evolutionary analyses, which assumes that a genetic distance exists between sequences, was performed in the programme BEAST using a strict molecular clock and an evolutionary rate of 6.24×10^{-4} substitutions/site/month (Lorenzo-Redondo et al., 2016). Rose et al used a similar evolutionary rate in sequences from lymphoid tissues of ART treated and naïve patients and also found evidence of evolution when comparing across tissues of patients (Rose et al., 2016).

However, we have shown through further analysis published elsewhere (Kearney et al., 2017), that the use of time-stamped Bayesian phylogenetics with a strict molecular clock applied in the program BEAST can generate the appearance of HIV evolution, even in sets of identical sequences because it assumes that a genetic distance exists between sequences from different time points. It is therefore, not an accurate method

for addressing the question of ongoing HIV replication during ART. It is important to note that our study does not directly compare with the above mentioned as we sampled virus in the blood as opposed to the lymph nodes. However, it is widely accepted that over a period of 7-9 years, there would be migration of cells from the lymph nodes to the blood (Boritz et al., 2016; Lorenzo-Redondo et al., 2016).

Our findings agree with the notion that the low-level viremia that often persists below the detection limit of commercial assays in ART suppressed individuals (Maldarelli et al., 2007) is due to the occasional release of virus from cells infected before ART was initiated rather than ongoing cycles of viral replication due to suboptimal ART suppression. This is further supported by studies (Dinoso et al., 2009; Gandhi et al., 2012; McMahon et al., 2010; Rasmussen et al., 2018) showing that treatment intensification by the addition of a third drug did not reduce the low level viremia. Recent evidence further supports the notion that ongoing replication (evidenced by evolution) is not responsible for long-term reservoir persistence. A re-analysis of the Lorenzo-Redondo data does not support ongoing evolution (Kearney et al., 2017). Additionally, another group provided evidence that the observation of evolution could be an artefact of differential decay of proviruses rather than evolution (Rosenbloom et al., 2017). Recent evidence that dolutegravir intensification does not further suppress low level viremia (Rasmussen et al., 2018) further supports our findings.

The clustering of monotypic sequences in phylogenetic trees of all 10 participants is suggestive of clonal expansion. These clusters are similar to what was reported by Wagner et al where an increase in the proportion of monotypic sequences was observed in PBMC and sputum samples from early treated, long-term suppressed children (Wagner et al., 2013). Several studies have shown that clonal expansion and proliferation of latent cells can occur before and during ART (Maldarelli et al., 2014; Simonetti et al., 2016; Wagner et al., 2014) resulting in populations of cells with identical sites of integration in blood and tissue which are the source of infectious virus in plasma (Simonetti et al., 2016). Furthermore, clonal viral species have been shown contribute to rebound viremia when ART is interrupted (Kearney et al., 2016) and have been recovered from multiple viral outgrowth experiments providing strong evidence that clonal expansion is the major mechanism by which reservoirs are maintained on suppressive ART (Bui et al., 2017; Hosmane et al., 2017; Lorenzi et al., 2017). Samples from these 10 individuals in our study were further investigated for evidence of clonal expansion in chapter 3 of this project.

Lastly, we found a significant positive association between HIV-1 cell- associated DNA loads after 7-8 years on ART and proviral diversity (calculated as average pairwise distance) at the same time point suggesting that the higher the cell-associated DNA load, the more diverse the viral populations are.

2.9.3 Strengths and limitations of the study:

We were able to adapt a sensitive quantitative PCR assay to detect total HIV-1 DNA loads in long-term subtype C infected children. Furthermore, most of the children included in this study had low pre-treatment diversity, which increased our ability to detect any subsequent evolution.

A limitation of the study was that we were only able to quantify HIV-1 cell-associated DNA in peripheral blood and this may not be reflective of cell-associated DNA loads in other anatomical sites where HIV reservoirs persist (Boritz et al., 2016). We also could not show that there is no compartmentalized viral evolution in lymphoid tissues. Additionally, it is well known that a large proportion of HIV-1 cell-associated DNA is defective (Bruner et al., 2016) and quantitative PCR assays that detect cellular biomarkers of latent HIV overestimate the amount of infectious virus that can be re-activated in cell culture by 300-fold (Eriksson et al., 2013). Due to limited sample availability, we were unable to perform further analysis using the gold-standard viral outgrowth assay (VOA) that reactivates resting cells and quantifies the amount of infectious virus that grows out. Also, because we sequenced a section of the HIV genome, we could not determine whether the single genome sequences represented defective or genetically intact variants. Lastly, in the neighbour joining phylogenetic trees, we detected monotypic clusters that could have been indications of expanded clones in proviral DNA but could not link the sequences to integration sites to prove clonality.

2.9.4 Conclusion:

Our work shows that early initiation of ART halts ongoing cycles of replication and limits the establishment of long-lived reservoirs that persist overtime. In light of these findings, efforts should be focused on developing strategies to eliminate latently infected cells that were present before therapy was initiated rather than the development of better ART regimens.

2.10 Appendix A: Supplementary figures

Longitudinal Viral load graphs:

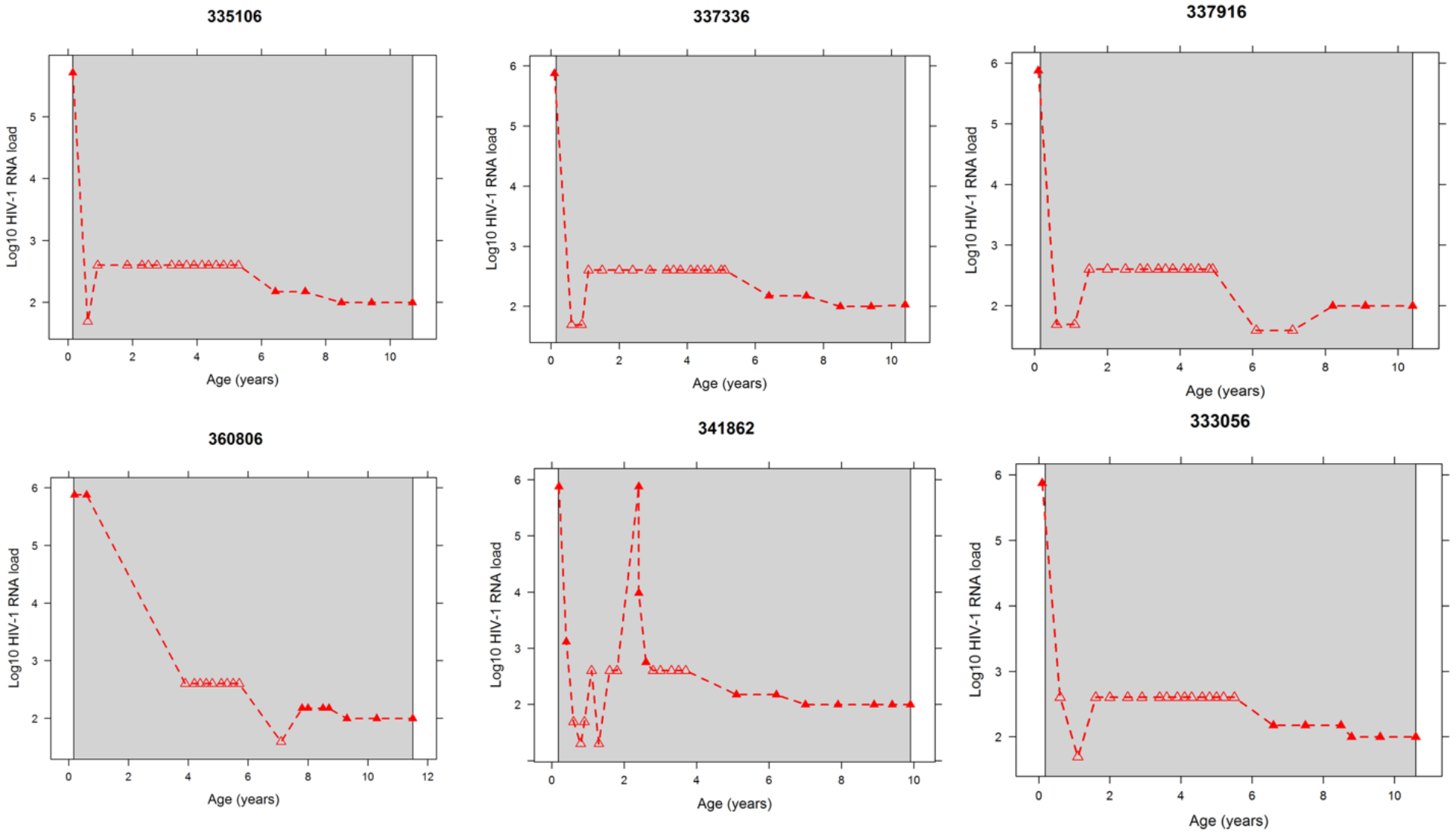

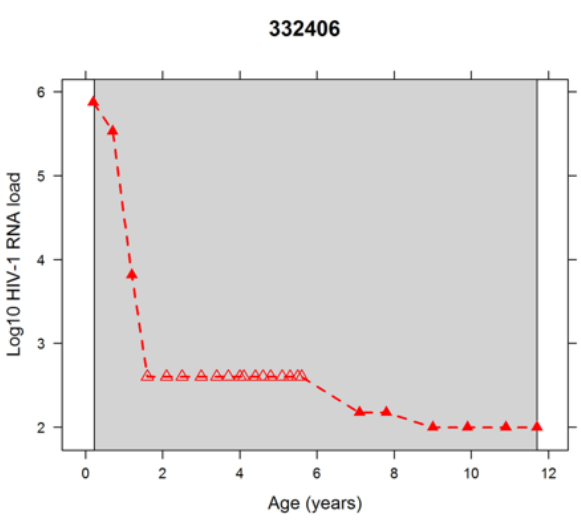

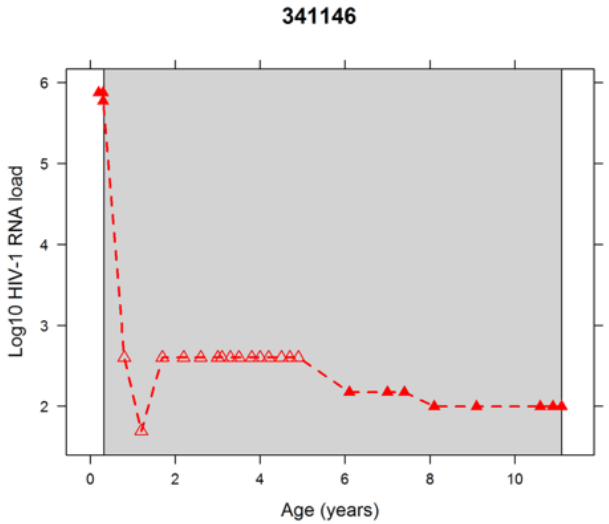

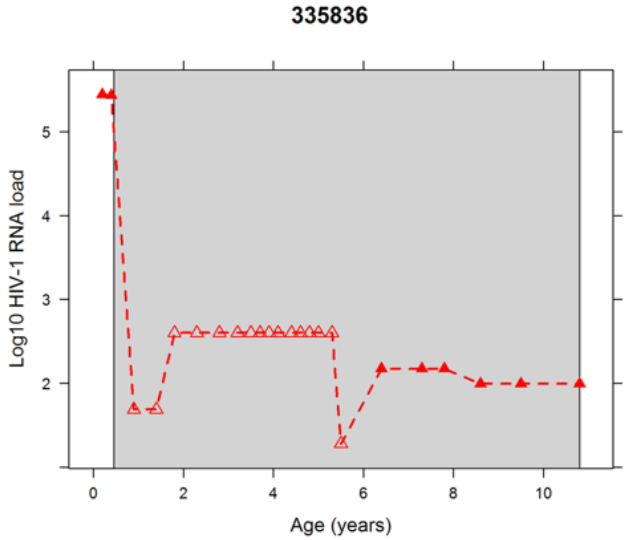

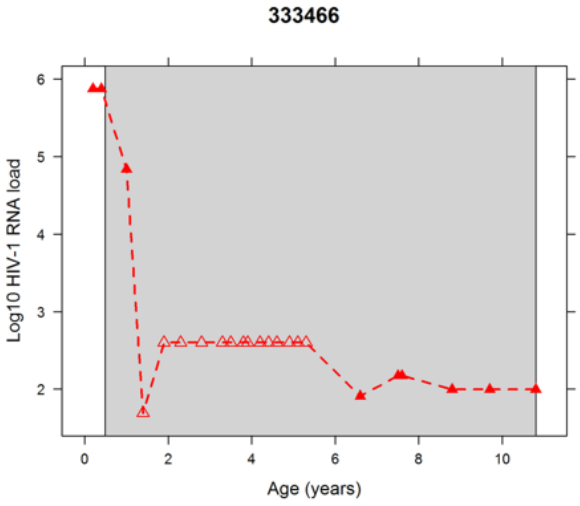

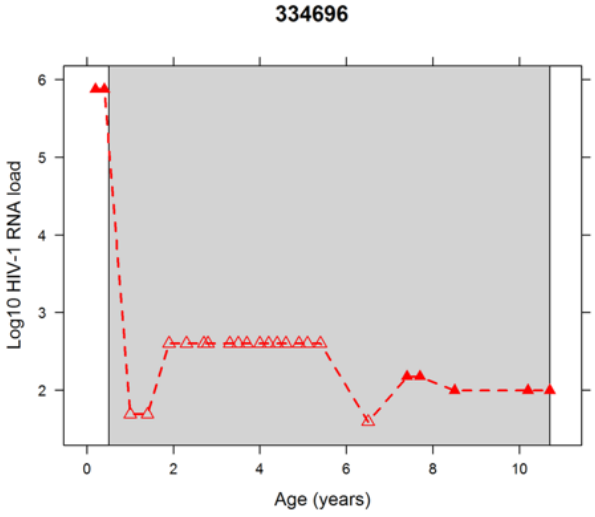

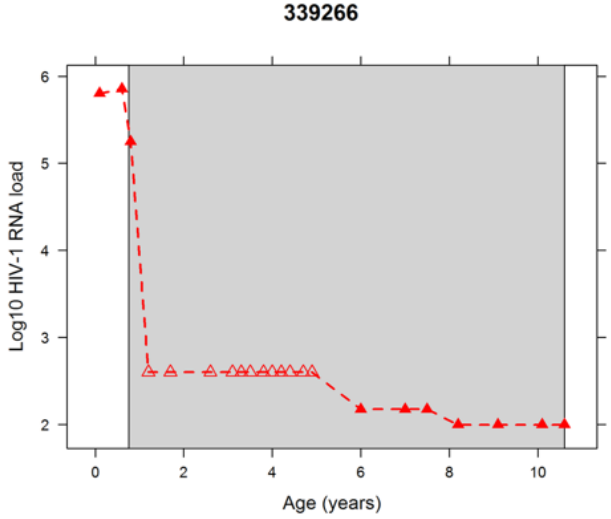

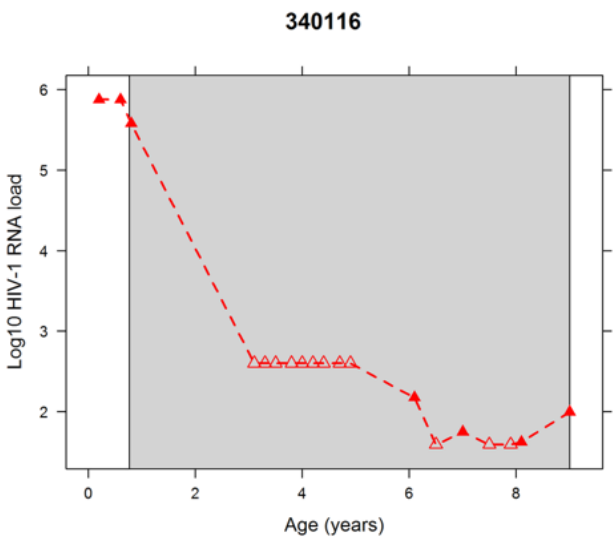

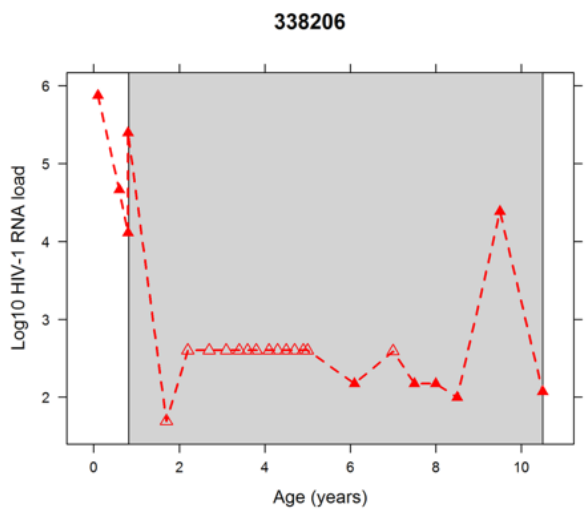

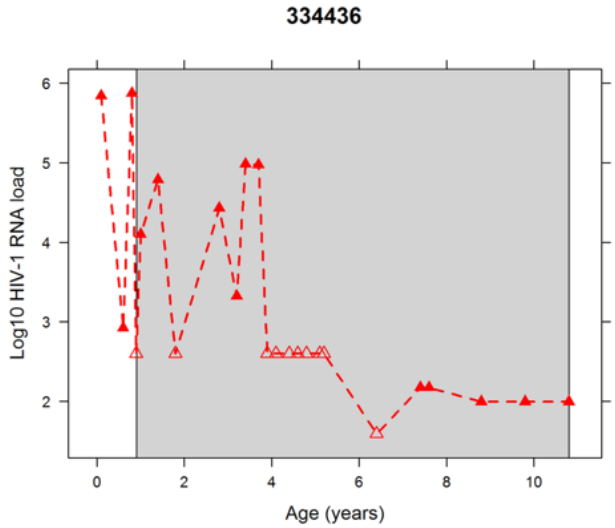

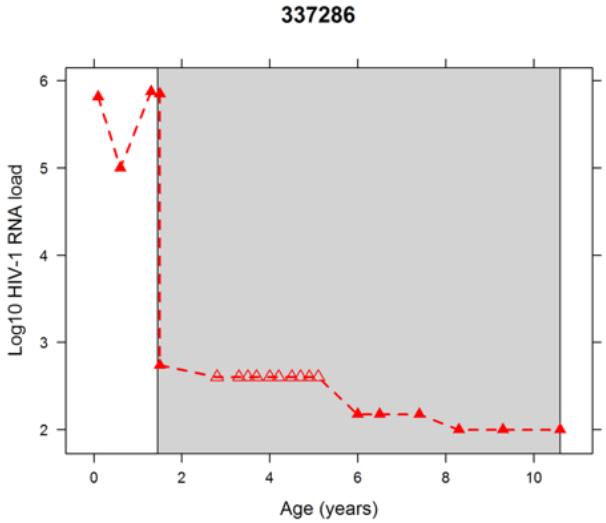

2.11 Published Article

The Journal of Clinical Investigation RESEARCH ARTICLE

No evidence of HIV replication in children on antiretroviral therapy

Gert U. Van Zyl,[1] Mary Grace Katusiime,[1] Ann Wiegand,[2] William R. McManus,[2] Michael J. Bale,[2] Elias K. Halvas,[3] Brian Luke,[4] Valerie F. Boltz,[2] Jonathan Spindler,[2] Barbara Laughton,[5] Susan Engelbrecht,[1] John M. Coffin,[6] Mark F. Cotton,[5] Wei Shao,[4] John W. Mellors,[3] and Mary F. Kearney[2]

[1]Division of Medical Virology, Stellenbosch University and National Health Laboratory Service (NHLS) Tygerberg, Cape Town, South Africa. [2]HIV Dynamics and Replication Program, National Cancer Institute (NCI), Frederick, Maryland, USA. [3]Department of Medicine, University of Pittsburgh, Pittsburgh, Pennsylvania, USA. [4]Advanced Biomedical Computing Center, Leidos Biomedical Research Inc. and Frederick National Laboratories for Cancer Research, Frederick, Maryland, USA. [5]Department Pediatrics and Child Health, Tygerberg Children's Hospital and Family Clinical Research Unit, Stellenbosch University, Cape Town, South Africa. [6]Department of Molecular Biology and Microbiology, Tufts University, Boston, Massachusetts, USA.

It remains controversial whether current antiretroviral therapy (ART) fully suppresses the cycles of HIV replication and viral evolution in vivo. If replication persists in sanctuary sites such as the lymph nodes, a high priority should be placed on improving ART regimes to target these sites. To investigate the question of ongoing viral replication on current ART regimens, we analyzed HIV populations in longitudinal samples from 10 HIV-1–infected children who initiated ART when viral diversity was low. Eight children started ART at less than ten months of age and showed suppression of plasma viremia for seven to nine years. Two children had uncontrolled viremia for fifteen and thirty months, respectively, before viremia suppression, and served as positive controls for HIV replication and evolution. These latter 2 children showed clear evidence of virus evolution, whereas multiple methods of analysis bore no evidence of virus evolution in any of the 8 children with viremia suppression on ART. Phylogenetic trees simulated with the recently reported evolutionary rate of HIV-1 on ART of 6×10^{-4} substitutions/site/month bore no resemblance to the observed data. Taken together, these data refute the concept that ongoing HIV replication is common with ART and is the major barrier to curing HIV-1 infection.

The full article is available online at: https://www.jci.org/articles/view/94582

Chapter 3

3.1 Introduction

Neighbour joining phylogenetic analysis of the single genome sequences obtained in chapter 2 revealed the clustering of monotypic sequences from baseline and 6-9 years on-ART in 10 participants (fig 2.5). This clustering could be indicative of clonal expansion of latently infected cells or represent the homogenous viral populations from pre-therapy that were archived and persisted on long-term ART. To further investigate whether expanded clones were present in all participants at these time points, integration site analysis (ISA) was performed. The integration site assay is a method used to determine the exact location in the infected cell's genome where an HIV provirus has integrated.

3.2 Study Aim II

To investigate the role that clonal expansion plays in the persistence HIV in early-treated, long term suppressed children from the CHER cohort.

3.3 Objectives

- Conduct Integration Site Analysis (ISA) on samples from prior to ART initiation to determine whether clonal expansion of latently infected cells occurs before ART is initiated in early treated children
- Conduct ISA on post-ART samples to determine whether the clones from pre-ART are detectable and more expanded after long periods of ART suppression.
- Describe genomic regions of HIV integration

3.4 Study population and Inclusion criteria

The participants included in this sub-study were the same as those studied in chapter 2. Each participant needed to have an available baseline PBMC sample as well as an additional PBMC sample from periods of long-term suppression on ART. The baseline and on-ART sample time points differed with each participant. Baseline samples ranged from 0 months before to 5 months after ART was initiated. On-ART samples ranged 6 to 9 years on ART. To ensure detection of persisting infected cells rather than short lived cells, participants also had to have undetectable viral loads for the most recent 36 months of the on-ART sample. Twelve participants were identified with these criteria shown in table 3.1 below. iCAD and APD values were not available for the baseline time-points as there was insufficient sample available to perform those tests.

Table 3.1: Participant characteristics

PID	Gender	Age ART start (months)	Time to viral load suppression (years)	Longitudinal Viral Load	Time relative to ART start at sample (years)	APD at time of sample (%)	iCAD at time of sample (per 10^6 cells)
337286	Male	17.7	1.37	Suppressed	0	-	-
					6.87	0.6	32.8
337916	Male	1.9	0.46	Suppressed	-0.03	-	-
					8.06	0.1	1.5
332406	Male	2.7	1.38	Suppressed	0	-	-
					8.76	0.1	23.6
334696	Male	6.1	0.47	Suppressed	0	-	-
					8.04	0.8	9.2
339266	Female	9.0	0.44	Suppressed	0	-	-
					7.45	0.3	46.7
338206	Male	9.9	0.92	Suppressed	-0.44	-	-
					8.24	0.2	21.3
341862	Female	2.2	0.44	One episode of viremia at 2yrs on ART	0	-	-
					6.77	0.3	42.3
360806	Female	2.0	3.76	1 viremic episode 6 months after ART	-0.23	-	-
					9.13	0.3	186.2
335106	Female	1.8	0.46	Suppressed	-0.08	-	-
					8.35	0.2	4.5
340116	Female	9.3	2.29	Suppressed	-0.57	-	-
					7.35	0.6	181.5
335836	Male	5.1	0.93	Suppressed	-0.27	-	-
					8.6	0.3	11.9

3.5 Methods

3.5.1 Isolation and purification of CD4$^+$ T cells

To enrich the ISA sample for cells that contained proviral DNA, total CD4+ T cells were isolated and purified from cryopreserved PBMC by positive selection using the EasySep cell separation technology (Stem Cell technologies; VA Canada). CD4+ T cell isolations were from the 6-9 year on-ART samples as the children were older and larger blood volume collection was feasible and allowable(Stellenbosch University and HEALTH RESEARCH ETHICS COMMITTEE, 2015).

Cells were thawed, pelleted and re-suspended in EasySep buffer to a concentration of 50 x10^6 cells/ml. The EasySep total CD4+ T-cell enrichment cocktail was added to the cells followed by the addition of magnetic particles. The mixture was then incubated on the easy 50 magnet for 10 minutes at room temperature. The CD4+ T-cell enriched cell suspension was taken, pelleted and re-suspended in PBS before sample extraction.

3.5.2 Extraction of total gDNA

Due to limited sample available from the pre-therapy time-point, gDNA was extracted from PBMC. Extractions from CD4$^+$ T cells and PBMC were performed using Guanidinium Isothiocynate and precipitated in Isopropanol as previously described (Hong et al., 2016). DNA extracts were stored at -80^{o}C until use.

3.5.3 PCR reactions to amplify U3 and U5 regions

The ISA assay uses primers targeting U3 and U5 regions on the terminal ends of the HIV genome and linker specific primers that are complementary to a linker ligated to the ends of fragments. To improve the sensitivity of the assay, patient specific primers were designed. This required sequencing of the LTRs of each participant. First, patient U3 and U5 LTR sequences were amplified using nested PCRs, followed by Sanger sequencing of the PCR products. The following optimised PCR reactions (Tables 3.2-3.11) were used to generate a 311bp amplicon from the U3 region and a 766bp amplicon from the U5 region for each participant (Fig 3.1 and 3.2). These amplicons contained the ISA primer binding site. PCR was conducted using GoTaq G2 Hot Start Polymerase (Promega, WI, USA) on an ABI Veriti thermal cycler (Applied Biosystems, CA, USA).

Table 3.2: Primers to amplify U3 region

Primer description	Primer name	Sequence (5' to 3')	HXB2 binding Position
Forward outer	U3-FO	CACATACCTAGAAGAATAAGACAGGGCTT	8748-8776

Forward Inner	U3-FI	ACATGGGTGGCAAGTGGTCAAAA	8795-8817
Reverse Inner	U3-RI	GGTCTAACCAGAGAGACCCAGTACAGG	9557-9531
Reverse Outer	U3-RO	GCACTCAAGGCAAGCTTTATTGAGGCTTA	9604-9632

Table 3.3: PCR master-mix for pre-nested U3 amplification

Reagent	**Stock concentration**	**Final concentration**	**Volume (µL)/Rxn**
Molecular Grade Water	NA	NA	19.25
GoTaq Buffer	5X	1X	10
dNTPs	40mM total	0.8mM total	1
Forward Primer	10µM	0.5µM	2.5
Reverse Primer	10µM	0.5µM	2.5
$MgCl_2$	25mM	2mM	4
GoTaq Enzyme	5U/µL	3.75U	0.75
DNA	30ng/µL	300ng	10
Total			50

Table 3.4: Cycling conditions for U3 pre-nested reaction

	Cycles	**Temperature**	**Time**
Initial Denaturation	1X	94°C	2min
Denaturation	35X	94°C	1min
Annealing		62°C	1min
Extension		72°C	30sec
Final extension	1X	72°C	7min
Hold		4°C	∞

Table 3.5: PCR master-mix for nested U3 amplification

Reagent	Stock concentration	Final concentration	Volume (µL)/Rxn
Molecular Grade Water	NA	NA	28.25
GoTaq Buffer	5X	1X	10
dNTPs	40mM total	0.8mM total	1
Forward Primer	10µM	0.5µM	2.5
Reverse Primer	10µM	0.5µM	2.5
$MgCl_2$	25mM	2mM	4
GoTaq Enzyme	5U/µL	3.75U	0.75
DNA	30ng/µL	300ng	1
Total			50

Table 3.6: Cycling conditions for U3 nested reaction

	Cycles	Temperature	Time
Initial Denaturation	1X	94°C	2min
Denaturation	35X	94°C	1min
Annealing		60°C	1min
Extension		72°C	30sec
Final extension	1X	72°C	20min
Hold		4°C	∞

Figure 3.1: U3 Amplicons 311bp. L= 1kb DNA ladder; NC= No Template Control; S1 – S12 = patients

Table 3.7: Primers to amplify U5 region

Primer description	Primer name	Sequence (5' to 3')	HXB2 binding Position
Forward outer	U5-FO	GAACCCACTGCTTAAGCCTCAAT	507-529
Forward Inner	U5-FI	TAAGCCTCAATAAAGCTTGCCTTGAGTGC	519-547
Reverse Inner	U5-RI	TCTAATTTTCCGCCTCTTAATATTGACGCIIIIICACCCAT	790-830
Reverse Outer	U5-RO	GGCCTGGTGTACCATTTGCCCTTG	1204-1227

Table 3.8: PCR master-mix for pre-nested U5 amplification

Reagent	Stock concentration	Final concentration	Volume (µL)/Rxn
Molecular Grade Water	NA	NA	19.25
GoTaq Buffer	5X	1X	10
dNTPs	40mM total	0.8mM total	1
Forward Primer	10µM	0.5µM	2.5

Reverse Primer	10µM	0.5µM	2.5
$MgCl_2$	25mM	2mM	4
GoTaq Enzyme	5U/µL	3.75U	0.75
DNA	30ng/µL	300ng	10
Total			50

Table 3.9: Cycling conditions for U5 pre-nested reaction

	Cycles	**Temperature**	**Time**
Initial Denaturation	1X	94°C	2min
Denaturation	35X	94°C	1min
Annealing		60°C	1min
Extension		72°C	30sec
Final extension	1X	72°C	7min
Hold		4°C	∞

Table 3.10: PCR master-mix for nested U5 amplification

Reagent	**Stock concentration**	**Final concentration**	**Volume (µL)/Rxn**
Molecular Grade Water	NA	NA	28.25
GoTaq Buffer	5X	1X	10
dNTPs	40mM total	0.8mM total	1
Forward Primer	10µM	0.5µM	2.5
Reverse Primer	10µM	0.5µM	2.5
$MgCl_2$	25mM	2mM	4
GoTaq Enzyme	5U/µL	3.75U	0.75
DNA	30ng/µL	300ng	1
Total			50

Table 3.11: Cycling conditions for U5 nested reaction

	Cycles	Temperature	Time
Initial Denaturation	1X	94°C	2min
Denaturation	35X	94°C	1min
Annealing		63°C	1min
Extension		72°C	30sec
Final extension	1X	72°C	20min
Hold		4°C	∞

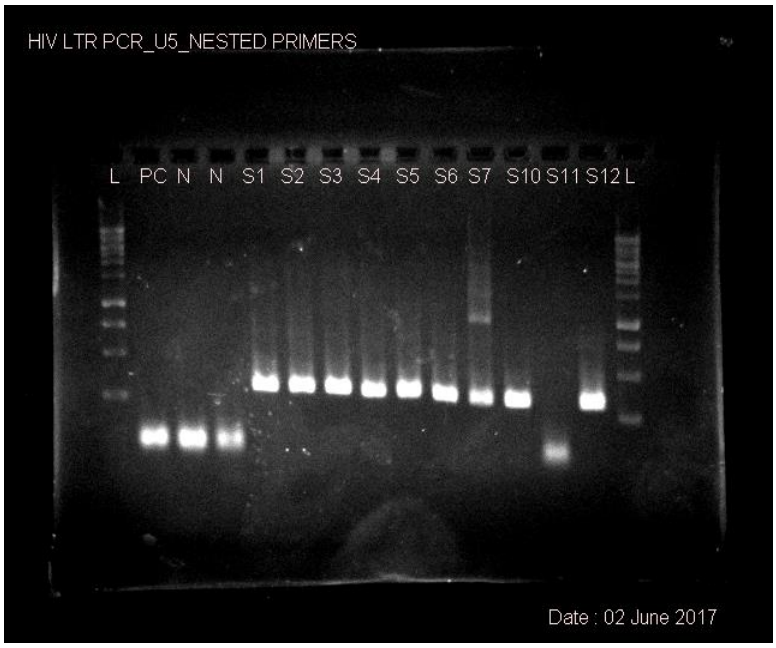

Figure 3.2: U5 amplicons 766bp. L=1kb DNA ladder; N= No Template Control; S1-S12=patients

3.5.4 Cloning of U3 and U5 amplicons

Initial attempts to directly sequence the U3 and U5 amplicons using the second round primers produced poor quality sequences. In order to obtain good quality sequences, each amplicon was cloned into the PTZ57R/T vector using the Instaclone PCR cloning kit (Thermofisher Scientific, MA, USA). The final extension for U3 and U5 nested PCRs was 20 minutes to allow for the addition of 3' dA overhangs. The amplicons were then purified using the MinElute PCR clean up Kit (Qiagen, Hilden, Germany) according to manufacturer's instructions. All the purified PCR products were quantified and diluted to the recommended quantity required for the ligation reaction. The ligation mix was incubated as shown in table 3.12 below:

Table 3.12: U3 and U5 Ligation reaction

	Cycles	Temperature	Time
Incubation	1X	25°C	60min
	1X	25°C	60min
	8X	4°C	60min
		4°C	60min
	1X	75°C	5min
	1X	4°C	∞

The ligation product was transformed into 'Mix &Go' chemically competent E.Coli cells (Zymo Research, CA, USA) according to manufacturer's instructions. The transformation mixture was then spread onto pre-warmed LB agar plates containing Ampicillin, IPTG and Xgal and incubated for 12-15 hours at 37°C. Three individual colonies per agar plate were picked and added to pre-warmed culture flaks containing LB broth and Ampicillin. The flasks were incubated at 37°C while shaking at 200-250 rpm for 12-16 hours. The bacterial cultures were harvested by centrifugation at 8000rpm for 2 minutes at room temperature. The supernatant was discarded, and the plasmids purified using the GeneJet Plasmid Miniprep Kit (Thermofisher Scientific, MA, USA).

3.5.5 Sequencing U3 and U5 plasmids

For each patient, U3 and U5 plasmid preps were quantified and diluted such that 150-300ng was added into the sequencing reaction. The insert was sequenced using M13 forward and reverse primers. The sequencing reaction is shown in table 3.13 and 3.14 below:

Table 3.13: Sequencing reaction for U3 and U5 plasmids

Reagent	Concentration	1X rxn
Nuclease free H_2O	-	4ul
Primers	5uM	1ul
Reaction Mix	1X	1ul
EDTA buffer	5X	3ul

Table 3.14: Sequence cycling conditions

	Cycles	Temperature	Time
Denaturation	25X	96°C	0.10sec
Annealing		50°C	0.05sec
Elongation		60°C	4min
Hold		4°C	∞

3.5.6 Integration Site analysis

The ISA assay (Fig 3.3) has been previously described (Maldarelli et al., 2014), and was conducted by our collaborators at the HIV Dynamics and Replication Program (NCI, MD, USA). During the assay, DNA from 1.25 million cells was randomly sheared to give fragment sizes of 300bp-500bp using the Covaris Adaptive Acoustics (Covaris, MA, USA). The sheared fragments were then end-repaired using the End-it DNA repair kit (Epicentre, Wi, USA). A single dA was added to the 3' ends of the fragments using a dA tailing kit (NEB, MA, USA). This allowed for ligation of a partially double stranded linker that contained a 3' dT overhang. Amplification using primers specific for HIV *LTR* and a primer complementary to the single stranded portion of the linker was performed to select for integration sites. This was followed by a nested PCR using HIV *LTR* and linker specific primers. During the second round PCR, Illumina sequencing adapters and bar codes were introduced into the sample. This was followed Illumina paired end next generation sequencing (Illumina, CA, USA) to generate sequence reads that contained the host cell-virus junctions. The sequences were mapped to human genome hg19. Considering the size of the human genome, sequence reads with identical HIV-1-human genome junctions were considered to represent a particular integration event. Therefore, the identification of a particular HIV-1 human junction with sequence reads that show multiple different genome break points (due to random shearing) represented clonal expansion of a particular HIV infected cell (as each cell only harbours a diploid genome copy and the assay recovers approximately 10% of integration sites in a sample). For each participant, we attempted to obtain at least 100 integration sites from the baseline and on-therapy time points to ensure that proper comparisons could be drawn between the two time points. All integration site data was entered into the Retrovirus Integration Database (https://rid.ncifcrf.gov/).

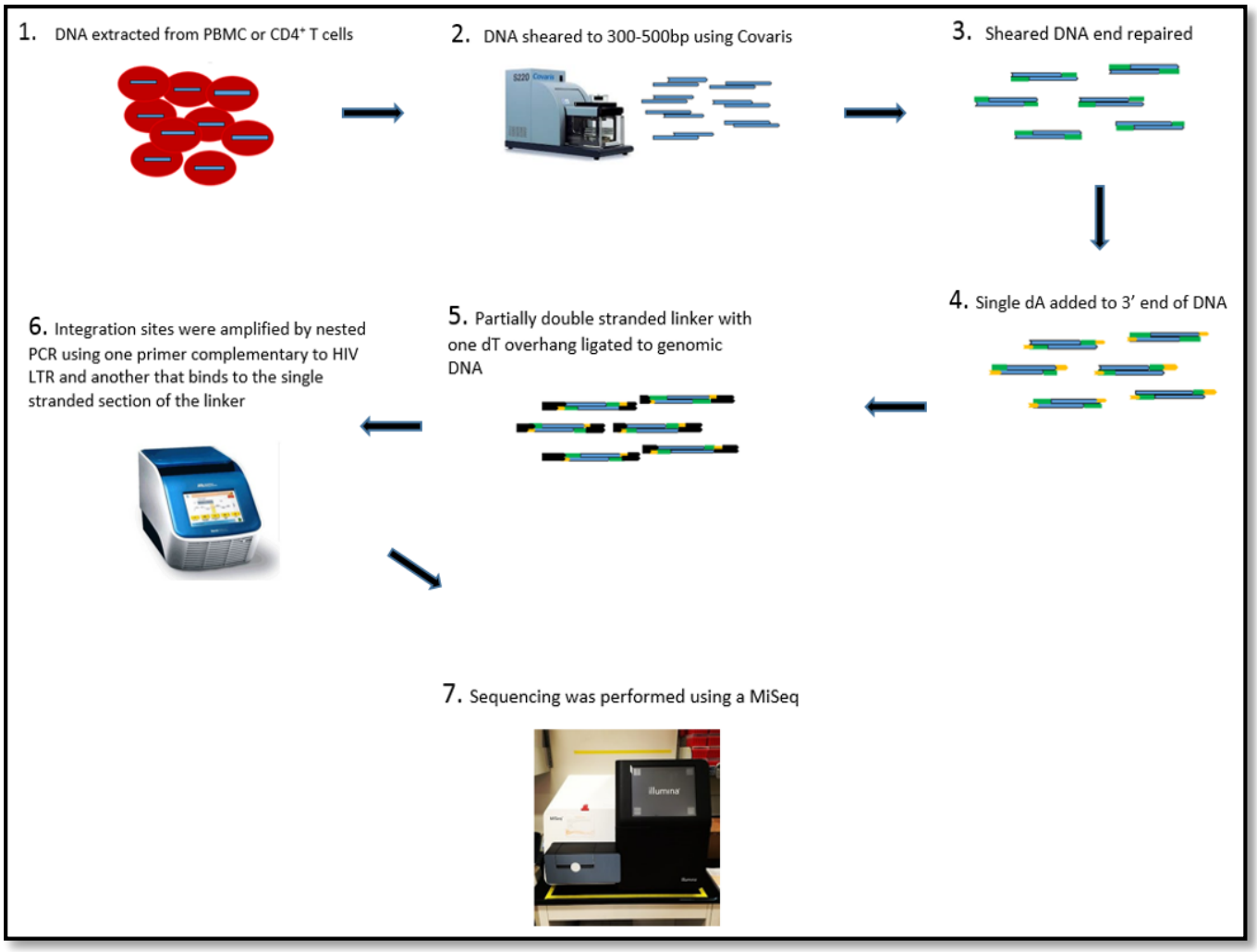

Figure 3.3: Integration Site Analysis schematic

3.6 Results

3.6.1 Integration site analysis (ISA) at baseline and after 6-9 years ART

For each of the 11 participants, ISA was performed on a sample from close to ART initiation (baseline) and another sample after 6-9 years on therapy. For each integration site (IS), data included the following variables that described the proviral integration into the host cell: a) the specific chromosome, b) gene name (when not in an intergenic region), c) the exact base pair location and d) the orientation of the provirus (+/-) relative to the gene (when not in intergenic regions). An integration event (IE) was defined as the historic infection and integration of a provirus into a specific site in the host cell's genome and considering the size of the human genome each unique IS in the human genome uniquely identifies a single IE. Therefore, when ISA recovered multiple cases of the same IE it indicated cellular proliferation.

To ensure adequate sampling, we aimed to obtain at least 100 IS at both time points for each participant. For the 6-9 year on-ART time point where participants were suppressed, a clone was defined as two or more identical integration sites. At baseline, participants were not yet viral load suppressed by ART. As there was active viral replication at this time point, it was possible that clonally expanding cells could represent short living subsets (such as effector CD4 T-helper cells). Clones at baseline were therefore defined as three or more identical integration sites.

Tables 3.15 and 3.16 below show: the number of integration sites obtained, number of clonal populations, proportion of integration sites in clones, and the size of the most expanded clone from baseline and 6-9 years on ART respectively. The proportion of integration sites that formed part of clones was calculated in two ways:

Method A: $$\frac{Number\ of\ Clones}{Total\ number\ of\ unique\ Integration\ Events\ (IE)}$$

Method B: $$\frac{Number\ of\ integration\ sites\ belonging\ to\ clones}{Total\ number\ of\ Integration\ Sites\ (IS)\ recovered}$$

In method A, the number of clones was divided by the number of unique integration events, this gives an idea of the number of infection events that resulted in detectable clonal expansion.

In method B, the number of times each clone was recovered was added together and then divided by the total number of integration sites recovered, this gives an indication of the fraction of the total population that consists of expanded clones.

Table 3.15: ISA at Baseline

CHER PID	Age ART Start (months)	Months relative to ART start at sample[#]	Number of Integration sites (IS) detected	Number of clones detected	Proportion IS in clones (Method A)	Proportion IS in clones (Method B)	Size of the largest clone (Gene name)
337286	17.7	0	438	14	0.03	0.09	7 (MAPKAPK2)
337916	1.9	-0.5	772	26	0.04	0.1	11 (PFKFB3)
332406	2.7	0	407	7	0.02	0.04	4 (PKN1)
334696	6.1	0	291	-	-	-	-
339266	9.0	-4.7	194	-	-	-	-
338206	9.9	-5.3	197	5	0.03	0.09	8 (NUP50)
341862	2.2	0	472	-	-	-	-
360806	2.0	+5.8	249	-	-	-	-
335106	1.8	0	279	-	-	-	-
340116	9.3	-19	148	5	0.04	0.08	4 (PDE4B)
335836	5.1	+2.3	703	6	0.01	0.02	3 (RXRA)

#: (+) = Months after ART start

(-) = Months before ART start

Table 3.16: ISA after 6-9 years on ART

CHER PID	CAD	Age ART start (months)	Years on ART at sample	Number of Integration sites (IS) detected	Number of clones detected	Proportion IS in clones (Method A)	Proportion IS in clones (Method B)	Size of the largest clone (Gene name)
337286	32.8	17.7	6.87	100	2	0.02	0.10	8 (STAT5B)
337916	1.5	1.9	8.06	124	14	0.13	0.26	4 (PHKB)
332406	23.6/--	2.7	7.92/8.76	256	21	0.11	0.31	14 (ROCK1)
334696	9.2	6.1	8.04	77	3	0.05	0.20	7 (MYB)
339266	46.7	9.0	7.45	110	16	0.23	0.52	12 (GPC1)
338206	21.3	9.9	8.24	85	6	0.12	0.48	18 (SRSF10)
341862	42.3	2.2	6.77	116	10	0.10	0.21	4 (GPATCH8)
360806	186.2	2.0	9.13	125	5	0.04	0.09	3 (ZNRF2)
335106	4.5	1.8	8.35	110	3	0.03	0.18	16 (RUNX2)
340116	181.5	9.3	7.35	149	5	0.04	0.12	6 (PPM1D)
335836	11.9	5.1	8.6	431	30	0.08	0.20	7 (C10orf76/ QRICH1)

A median of 310 integration sites per participant (range:148-808) from baseline and 128 from 6-9 years on ART (range: 94-454) were obtained. There were more integration sites obtained at baseline than the 6-9 year on ART time point due to the expected higher proviral load at baseline. Of note, infected cell clones were detected in 6 participants from baseline (including two participants who initiated ART at <3 months of age) and in all 11 participants at the 6-9 years on ART time point, reflective of the monotypic clusters observed from the neighbour joining trees of the 10 participants in Aim 1 (Fig 2.5). At baseline, the number of clonal populations ranged from 5 to 26 while the size of the largest clone ranged from 3 to 11 proviruses in a clone. At 6-9 years on ART, the number of clonal populations ranged from 2 to 30 clonal populations and the size of the largest clone ranged from 3 to 18 proviruses in a clone.

3.6.2 Increase in proportion of integration sites in clones over time on ART

Fishers exact tests were performed for individual participants to compare proportions of integration sites in clones (method B) between the baseline and 6-9 year ART sample. As shown in table 3.17 below, there was a significant increase in the proportion of IS in 9 of the 11 participants. Figure 3.4 further illustrates this by plotting the proportion of integration sites in clones against years treated.

Table 3.17: Fishers exact test on proportion of IS in clones between baseline and 6-9 years on ART

CHER PID	Months relative to ART start at Baseline sample	Proportion IS in clones (Method B) at Baseline	Years on ART at 6-9 year sample	Proportion IS in clones (Method B) at 6-9 years on ART	Fishers exact P value
337286	0	0.09	6.87	0.10	0.049
337916	-0.5	0.1	8.06	0.26	<0.0001
332406	0	0.04	7.92/8.76	0.31	<0.0001
334696	0	0	8.04	0.20	<0.0001
339266	-4.7	0	7.45	0.52	<0.0001
338206	-5.3	0.09	8.24	0.48	<0.0001
341862	0	0	6.77	0.21	<0.0001
360806	+5.8	0	9.13	0.09	<0.0001
335106	0	0	8.35	0.18	<0.0001
340116	-19	0.08	7.35	0.12	0.003
335836	+2.3	0.02	8.6	0.20	<0.0001

Using data from all 11 participants, a paired t-test was conducted on baseline and 6-9 years ART clone proportions (using method B) to assess whether there was an overall significant change in the proportion of integration sites in clones over time on ART. Results showed a highly significant change in proportion of IS in clones over time on ART [$t = 4.4$; $p<0.005$; CI (0.14 – 0.41)].

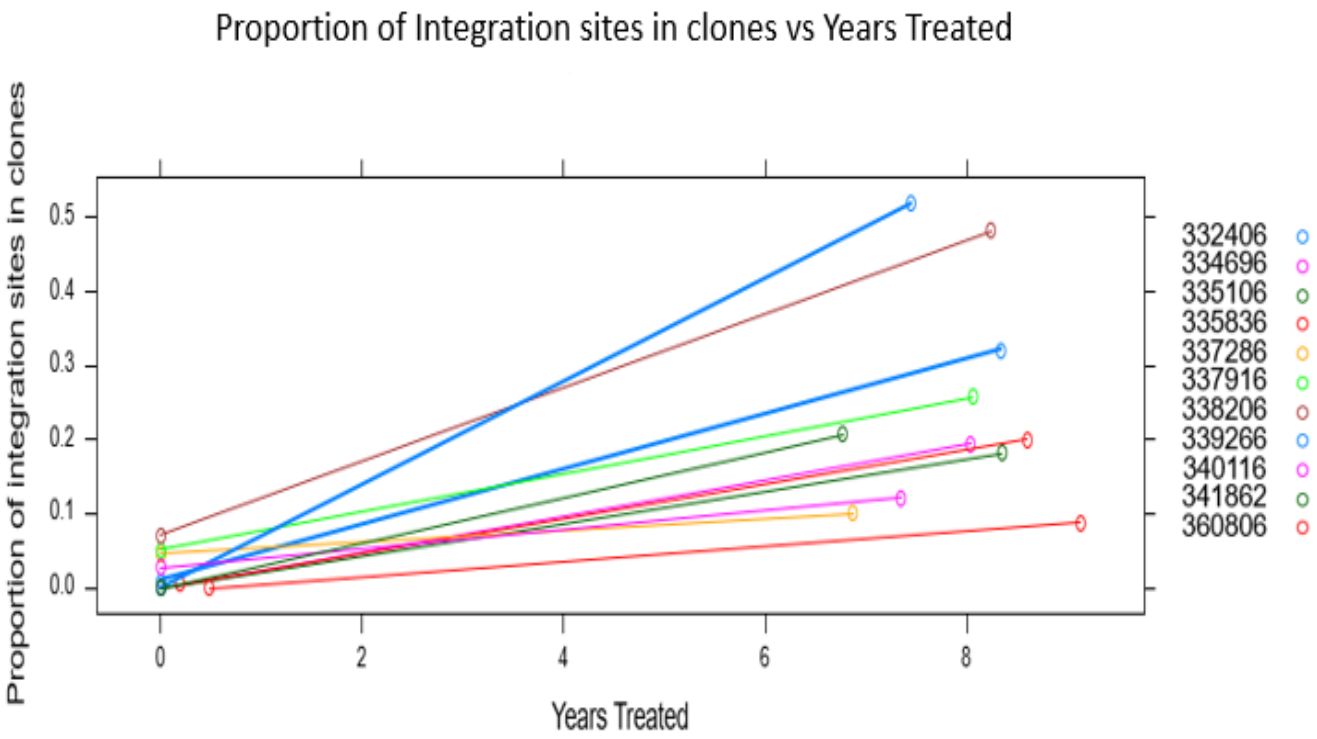

Figure 3.4: Proportion of integration sites in clones at baseline and after 6-9 years on ART

3.6.3 Longitudinal detection of integration sites

A distinct integration site (IS) was described as having the same: chromosome, gene name, bp position in the gene and provirus orientation. As shown in table 3.18 below, the same integration sites were detected at baseline and after 6-9 years on ART in 4 participants (337286, 332406, 338206, and 335836). In participant 332406, one integration site at baseline was detected 3 times after 8.76 years on ART suggesting the long term persistence and expansion of an infected cell clone.

Table 3.18: Longitudinal detection of integration events

CHER PID	Chromosome	Gene name	Bp position in gene	Provirus orientation relative to gene	Duration between baseline and On-ART samples (years)	Frequency of particular IS at Baseline (*total number unique IE at baseline)*	Frequency of particular IS on long-term ART *(total number unique IE on long-term ART)*
337286	chr6	BACH2	90726507	(-)	6.87	1 *(414)*	1 *(92)*
	chr17	STAT5B	40408920	(-)		1 *(414)*	1 *(92)*
337916	-	-	-	-	-	-	-
332406	chr16	ZCH74	11870250	(+)	8.76	1 *(398)*	3 *(196)*
334696	-	-	-	-	-	-	-
339266	-	-	-	-	-	-	-
338206	chr22	NUP50	45578851	(-)	8.24	8 *(184)*	1 *(50)*
	chr20	RNF24	3932944	(+)		2 *(184)*	1 *(50)*
341862	-	-	-	-	-	-	-
360806	-	-	-	-	-	-	-
335106	-	-	-	-	-	-	-
340116	-	-	-	-	-	-	-
335836	chr3	ACAP2	195084598	(+)	8.6	1 *(696)*	1 (375)
	chr16	RBBP6	24562603	(+)		1 *(696)*	1 *(375)*

3.6.4 Integrations into genes of interest

Several studies have suggested that the long-term persistence of expanded clones is associated with integrations into human genes responsible for cell growth, survival and regulation of cellular proliferation (Cohn et al., 2015; Ikeda et al., 2007; Maldarelli et al., 2014; Wagner et al., 2014). In this study, distinct integrations into four such genes: BACH2, STAT5B, MKL1 and MKL2 genes were observed in 9 of the 11 participants at baseline (table 3.19) and 8 of the 11 participants after 6-9 years on ART (table 3.20).

In participant 337286, there were 13 distinct integrations into BACH2 at baseline (table 3.19). Interestingly, this participant also had its largest clone consisting of 8 proviruses in the STAT5B gene (table 3.16). This was also the only participant were there was longitudinal detection of the same integration events between baseline and 6.85 years on ART in both BACH2 and STAT5B (table 3.18).

Further analysis is ongoing to compare the fraction of integration sites in genes to an ex-vivo infected PBMC library to investigate whether integrations into genes of interest is selective or random. Those findings will be compiled in a separate publication.

Table 3.19: Integrations into genes of Interest at baseline

CHER PID	Age ART Start	Months relative to ART start at sample[#]	Number of Integration sites (IS) detected	Distinct integrations into Genes of interest
337286	17.7	0	438	BACH2 (13) MKL1 (1) MKL2 (1) STAT5B (4)
337916	1.9	-0.5	772	MKL1 (1) STAT5B (3)
332406	2.7	0	407	BACH2 (1) MKL2 (1) STAT5B (1)
334696	6.1	0	291	MKL1 (2)
339266	9.0	-4.7	194	BACH2 (1) MKL2 (1)
338206	9.9	-5.3	197	-
341862	2.2	0	472	MKL1 (1) STAT5B (3)
360806	2.0	+5.8	249	-
335106	1.8	0	279	BACH2 (1) STAT5B (1)
340116	9.3	-19	148	MKL1 (1)
335836	5.1	+2.3	703	BACH2 (1) STAT5B (1)

Table 3.20: Integrations into genes of Interest after 6-9 years on ART

CHER PID	iCAD	Age ART start (months)	Years on ART at sample	Number of Integration sites (IS) detected	Distinct integrations into Genes of interest
337286	32.8	17.7	6.87	100	BACH2 (4) STAT5B (6)
337916	1.5	1.9	8.06	124	STAT5B (2)
332406	23.6/--	2.7	7.92/8.76	256	BACH2 (7) MKL1 (3) MKL2 (1) STAT5B (8)
334696	9.2	6.1	8.04	77	--
339266	46.7	9.0	7.45	110	--
338206	21.3	9.9	8.24	85	STAT5B (5)
341862	42.3	2.2	6.77	116	MKL2 (1)
360806	186.2	2.0	9.13	125	MKL1 (1) STAT5B (2)
335106	4.5	1.8	8.35	110	--
340116	181.5	9.3	7.35	153	BACH2 (2) MKL2 (2) STAT5B (7)
335836	11.9	5.1	8.6	431	STAT5B (4)

3.7 Discussion

3.7.1 Expanded clones in early treated children

This is the first study to show that infected cells begin clonally expanding before ART is initiated in early treated children. These clones persist and increase significantly in proportion over several years on ART. In some participants, there were multiple integrations into genes responsible for cell growth and survival. The detection of expanded clones using ISA mirrored the monotypic sequences observed by CAD-SGS in chapter 2.

The detection of clones in the pre-therapy samples of children who were treated as early as two months of age shows that the latent reservoir begins to expand even before early therapy. A similar observation has been reported (Maldarelli et al., 2014) where in one adult, the same integration site was detected at pre-therapy and after long-term ART. Likewise, another group (Haworth et al., 2018) recently characterized clonal expansion during acute untreated HIV-1 infection in a humanized mice model and found evidence of clonal expansion associated with integration in genes involved in signalling pathways, which may alter transcription, translation or cell cycle regulation. Although a large proportion of infected cells are defective (Bruner et al., 2016; Ho et al., 2013), it has been shown that highly expanded infected cell clones can contain intact proviruses and result in viremia (Simonetti et al., 2016). The recent case of a child, who despite initiating ART within hours of birth (Luzuriaga et al., 2015), eventually rebounded after treatment interruption shows that long-lived cells are infected very early. The potential for these early infected cells to persist through proliferation poses a major barrier to cure. Altogether, these observations suggest that ART has no effect on the proliferation and expansion of infected cells but instead prevents new rounds of infection and allows shorter-lived infected cell subsets to die (Coffin and Swanstrom, 2013; Hellerstein et al., 2003) making it easier to detect expanded clones. We did not however, detect clones in the pre-therapy samples of all our participants. It is likely that clones were present but not detected. The ISA method is relatively insensitive as it detects a small fraction of infected cells and therefore only the most expanded clones. This, coupled with the large HIV-1 infected cell population at pre-therapy, sampling restricted to PBMCs, as well as the presence of shorter lived infected cell subsets during unsuppressed replication (that then decay at different rates over time on ART) could have made it difficult to detect clones in all participants at the pre-therapy time point (Coffin and Swanstrom, 2013; Hellerstein et al., 2003).

We observed the persistence of clones over several years on ART and an increase in the proportion of integration sites that formed part of clones. Wagner et al showed that in 6 paediatric patients during a median of 10 years on ART, monotypic DNA sequences detected with single genome sequencing increased in proportion (Wagner et al., 2013). Furthermore, using an alternative assay for integration sites, the Integration Site Loop Amplification Assay (ISLA) in 3 individuals over 10 years on ART, there was an increase in sequences that formed part of clones (Wagner et al., 2014). Several other studies have since reported that

after several years on ART, 40-60% of integrations are in clonally expanded cells (Cohn et al., 2015; Kim and Siliciano, 2016; Maldarelli et al., 2014; Pinzone et al., 2018; Simonetti et al., 2016).

The increase in proportion of persisting cells in clones could in part be due to the high cell turnover and clearance of protein expressing cells during unsuppressed infection leading to the loss of shorter lived cell subsets over time on ART (Coffin and Swanstrom, 2013). However, there is evidence of ongoing proliferation and expansion of infected cells during ART. Latently infected cells can proliferate in response to antigen stimulation of T cell receptors (Douek et al., 2002) which often leads to reactivation of the latently infected cell. The residual clonal viremia detected in participants on long-term suppressive ART provides evidence for antigen driven clonal expansions that result in proviral reactivation and release of virions into the blood (Bailey et al., 2006; Kearney et al., 2016; Simonetti et al., 2016; Tobin et al., 2005).

On the other hand, it has been shown that HIV integrates into memory subsets that can undergo homeostatic proliferation in response to cytokine stimulation (Chomont et al., 2010). It is possible for this to occur without reactivation of the provirus and subsequent immune clearance (Bosque et al., 2011; Chomont et al., 2010; Wang et al., 2018). It has recently been reported in an individual where 50% of the reservoir was composed of an intact clone, that only a small proportion of that expanded clone was expressing virus during long term ART. Likewise, latently infected cells containing intact provirus can proliferate in vivo in response to mitogens without producing virus (Hosmane et al., 2017). Ultimately, it is likely that both antigen-driven and homeostatic proliferations play a role in maintaining the reservoir. This notion is supported by recent work showing that some intact clones remain detectable (due to homeostatic proliferation) while others appear and disappear (due to antigen induced proliferation) over several years on ART (Wang et al., 2018).

The ongoing clonal expansion of intact proviruses during suppressive ART poses a challenge for cure. Currently, 'functional cure' interventions aim to reduce the number of infected cells using either therapeutic vaccines or agents that reactivate latent cells followed by elimination of reactivated cells by immune effectors (Douek, 2018; Margolis et al., 2016; Mylvaganam et al., 2016; Rasmussen and Lewin, 2016). However, if therapy is interrupted, there is a chance that the few remaining infected cells could expand. This is likely to have occurred in the two 'Boston patients' where there was rebound viremia within 6 months of ART interruption following the elimination of 99% of their infected cells (Henrich et al., 2014). This highlights the need for approaches that specifically target clonal expansion of infected cells.

Several studies have suggested that the long-term persistence of expanded clones is associated with integrations into human genes responsible for cell growth, survival and regulation of cellular proliferation (Cesana et al., 2017; Cohn et al., 2015; Ikeda et al., 2007; Maldarelli et al., 2014; Wagner et al., 2014). Wagner et al looked at 534 proviruses from 3 individuals and found a significant proportion integrated into genes associated with cancer, regulation of cell proliferation and survival (Wagner et al., 2014). We detected in multiple participants, distinct integrations into four such genes: BACH2, STAT5B, MKL1 and MKL2. However, the fact that clones wax and wane (Wang et al., 2018) challenges the idea that integrations into certain genes

results in a steady increase in proportion of proviruses in clones. It is likely that antigen driven and homeostatic proliferation rather than integration into growth genes drives the long-term persistence of expanded clones. In our study, further analysis is ongoing to compare the fraction of integration sites in genes to an ex-vivo infected PBMC library and investigate whether integrations into these genes of interest is selective or random. Those findings will be compiled in a separate publication.

Although total HIV DNA levels remain relatively constant with a very slow rate of decay after 4 years on suppressive ART (Besson et al., 2014), the composition of the reservoir (intact vs defective) is dynamic and mostly shaped by selective pressures of the immune system. In our work, we were unable to link integration sites with intactness of the provirus and could not determine what proportion of expanded clones were replication competent. However, we know that majority of proviral DNA is defective (Bruner et al., 2016; Ho et al., 2013). Despite this, Bui et al recently showed that a large proportion of the replication competent reservoir is clonal (Bui et al., 2017). During suppressive ART, a proportion of intact clones continue transcribing and expressing protein (Kearney et al., 2016; Simonetti et al., 2016; Wiegand et al., 2017) while the other fraction of these cell survive because they don't release antigen (Boritz et al., 2016). As a result, intact proviruses in clones that express proteins are selected against and decline overtime on ART (Pinzone et al., 2018). The recent report of a post treatment controller with an intact clone but suppressed virus shows that cytotoxic T lymphocytes (CTLs) control the expression of intact clones in such individuals (Veenhuis et al., 2018).

Severely defective proviruses that are unable to express proteins are enriched over time on ART (Imamichi et al., 2014). On the other hand, recent studies have shown that some defective clones are expressed and induce CTL responses that shape the proviral landscape during suppressive therapy (Pinzone et al., 2018; Pollack et al., 2017). These defective clones are able to recruit transcription factors to their LTRs (Lusic et al., 2003), express HIV-1 RNA transcripts at similar levels as those without defects (Barton et al., 2016; Wiegand et al., 2017) and induce a CTL response (Imamichi et al., 2016). Therefore, both CTL selection pressure and clonal expansion shape the proviral landscape overtime on therapy.

The ISA method used in our study is high throughput and informative for describing host genomic regions of integration and the proportion of proviruses in clones. However, ISA is relatively insensitive and only detects the most expanded clones in the blood sample at a given time. Previous studies have shown that expanded clones are widely distributed throughout various anatomic sites (Simonetti et al., 2016; Wagner et al., 2013). The clones detected in our participants are therefore only a conservative picture of the extent of clonal expansion throughout the body. In addition, the ISA assay provides a very short terminal U5 or U3 proviral sequences and can therefore not inform about the intactness of clones.

In this study, there was a correlation between the ISA results from study Aim 2 and SGS results from study Aim 1, participants with detectable monotypic sequences by SGS had detectable clones by ISA. However, in our cohort of early treated children with low background diversity, monotypic sequences detected by SGS

could also have been a result of evolutionary bottlenecks caused by rapid burst of replication without enough time for evolution. We show that ISA is able to identify expanded clones even when the background diversity is low.

An alternative to ISA is the integration site loop mediated assay (ISLA) which uses loop mediated PCR to sequence a 2.8kb fragment that includes part of the provirus and the integration site and therefore allows some matching of integration sites with partial proviral sequences (Wagner et al., 2014). However, the assay is cumbersome as it has to be performed at limiting dilution and has relatively low yield when preceded only by linear (unidirectional primer) amplification of provirus-human-genome junctions. Yield may be increased by whole genome amplification prior to linear amplification of junctions, but this increases costs.

In order to detect the proportion of intact proviruses that form part of clones, several studies have used an approach that combines variations of the quantitative outgrowth assay (qVOA) to reactivate latent cells followed by single genome sequencing (Bui et al., 2017; Hosmane et al., 2017; Lorenzi et al., 2017). This approach, however, is time consuming, laborious and requires large volumes of blood that are not feasible for studies in younger paediatric cohorts where sample availability is limited. There is therefore a need for more efficient methods that can detect rare clones and link integration sites to full length viral genomes to ascertain intactness.

3.7.2 Strengths and Limitations of the study

This is the first study to investigate clonal expansion in 11 early treated, long-term suppressed children. Although we detected clones in all 11 children after long-term ART, the ISA assay was unable to link integration sites to proviral sequences in order to determine intactness. We sampled only a fraction of infected cells that were circulating in the sample, and this may therefore not be fully representative of expanded clone populations in other anatomical sights throughout the body. Nonetheless, the fact that clones are detectable despite limited sampling of the total infected cell population highlights the significant extend to which clones persist and expand over long-term ART in early treated children.

3.7.3 Conclusion

We were able to show that infected cells begin clonally expanding before ART is initiated in children who start therapy as early as two months of age. These clonal populations persist and increase in proportion over several years on ART and are possibly the main mechanism driving persistence of the latent reservoir. It is likely that both antigen-driven and homeostatic proliferations play a role in inducing these expansion. The potential for these early infected cells to persist through proliferation poses a major barrier to cure. To understand the full extent to which clonal expansion maintains the replication competent reservoir, there is a need for more efficient methods that can detect rare clones and link integration sites to full length viral genomes to ascertain intactness.

Chapter 4

4.1 Introduction

Studies have shown that HIV-1 DNA decays rapidly in individuals who initiate ART during acute infection, with long-lived infected cell populations that constitute the latent reservoir emerging after 4 years on suppressive ART (Besson et al., 2014; Buzon et al., 2014a). More recently, studies describing the composition of these long-lived infected cell populations in adults starting ART during acute infection have shown that the majority of proviral DNA is defective due to the error prone RT enzyme and hypermutations caused by APOBEC 3G, a host restrictive factor (Bruner et al., 2016; Hiener et al., 2017). Only 2-5% of proviruses have been shown to be genetically intact by full-length sequencing (Bruner et al., 2016; Hiener et al., 2017). There is limited data on the proviral landscape in early treated, long-term suppressed children, particularly in Sub-Saharan Africa where HIV-1 subtype C predominates. In an observational paediatric from the United states of America, no intact full-length proviral sequences were detected out of 162 near full length sequences (Rainwater-Lovett et al., 2017). Investigating the sequence-intact reservoir could provide insight on the mechanisms by which intact proviruses persist and is informative for ongoing cure efforts.

4.2 Study Aim III

To screen HIV-1 proviral DNA in 9 early treated, long-term suppressed children from the post-CHER cohort by near full length proviral amplification and sequencing (NFL-PAS) in order to describe the distribution of intact vs defective proviruses.

4.3 Objectives

- Amplify 8.8kb near full length single genome proviral amplicons in 9 participants from the post-CHER cohort who initiated ART at variable time points.
- Screen 8.8kb amplicons by sequencing 1.5kbs within the *gag-pol* region to identify sequences with stop codons in the *gag-pol* gene that would render them defective.
- Perform barcoded Illumina MiSeq next generation sequencing on samples that have no stop codons in the 1.5kb *gag-pol* amplicon
- Construct consensus sequences from MiSeq sequence reads demultiplexed by sample barcode to determine whether there are further defects (deletions, insertions or hypermutations) elsewhere in the viral genome that would render the proviruses defective
- Further asses viral intactness by amplifying and sequencing the packaging signal (*psi*) and major splice donor site (*MSD*), from the pre-nested (PCR-1) wells of samples that appear intact by MiSeq

4.4 Study Population and Inclusion criteria

The study cohort consisted of 9 children who started ART at variable ages ranging from 1.7 to 11.1 months. These participants were selected on the basis of having a total HIV-1 DNA iCAD above 40 copies/10^6 PBMC. Some participants had undergone therapy interruption as per the CHER trial whereas others had no treatment interruption since ART was initiated. At the time of testing, participants had been on ART for a period ranging from 6 -9 years. Table 4.1 below is a summary of participants' clinical characteristics.

Table 4.1: Clinical characteristics of study participants

PID	Gender	Age ART start (months)	CHER study Arm	Treatment History	ART Regimen	Nadir CD4%	Time to first viral load suppression (years)	Time on ART at sample (years)	CD4% at sample	CAD at sample (copies/10^6 PBMC)
333676	Female	1.7	Arm 2	Interrupted after 9 months on ART; reinitiated after 3.6 years; viremic until after re-initiation	AZT/3TC/LPV/r	19.7	0.58	8.57	36	55.5
360806	Female	2.0	Arm 2	Continuous therapy; Delayed suppression for first 6 months on ART, good suppression thereafter	AZT/3TC/LPV/r Single drug switch to AZT/3TC/EFV after 7.7 years on ART	12.9	3.76	9.13	29	186.2
341622	Female	2.16	Arm 2	Interrupted after 9.9 months on ART; reinitiated after 13 months; viremic until after re-initiation	AZT/3TC/LPV/r	24.2	0.76	6.9	43.65	81.9
341862	Female	2.20	Arm 3	Continuous therapy; Detectable viral load after 2.2 years on ART, supressed 5 months later and good suppression thereafter	AZT/3TC/LPV/r	19.2	0.63	6.96	36	42.3
333716	Female	2.3	Arm 3	Interrupted after 2 years on ART; blip 4months after interruption; reinitiated 4 months after interruption; viremic until after re-initiation	AZT/3TC/KLT	25.9	0.46	8.55	37	129.6
339606	Male	8.5	Arm 1	Continuous therapy	AZT/3TC/LPV/r	17.1	1.34	7.93	48	247.6
340116	Female	9.23	Arm 1	Continuous therapy	AZT/3TC/LPV/r	28.4	2.3	7.31	54	181.5
339266	Female	9.32	Arm 1	Continuous therapy	AZT/3TC/LPV/r	28.2	1.2	8.2	50	46.7
334436	Female	11.1	Arm 1	Poorly suppressed for first 2.5 years on ART	AZT/3TC/LPV/r	28	0.92	8.83	47	86.3

AZT – zidovudine, 3TC – lamivudine, LPV-r: Lopinavir-ritonavir, EFV - efavirenz

4.5 Methods

4.5.1 Validation of the Near Full Length Proviral Amplification and Sequencing (NFL-PAS) protocol for HIV-1 Subtype C

The NFL-PAS protocol was developed by our collaborators in Prof. John Mellors' lab at the University of Pittsburgh and was designed for HIV-1 subtype B. To implement the assay in our lab, validation experiments were conducted to establish the sensitivity and the influence of background human genomic DNA in generating the 8.8kb near full length amplicons. Optimisation was conducted using the HIV-1 LAV infected 8E5 T cell line that contains one integrated copy of HIV per cell. The cell line was obtained through the NIH AIDS Reagent Program, Division of AIDS, NIAID, NIH: from Dr. Thomas Folks.

4.5.1.1 Quantification and serial dilution of 8E5 cells

Total DNA was extracted from $1x10^6$ 8E5 cells as previously described (Kearney et al., 2009, 2008; Palmer et al., 2005). The extracted DNA was diluted 1:10 and quantified on the Qubit spectrophotometer using the Qubit dsDNA BR Assay kit (Thermo Fisher Scientific; MA; USA). The Qubit reading for this sample was 11,4ng/µL. Taking the DNA concentration and the length of the DNA template ($3.3x10^9$ bp of human genome per cell) into account, this corresponded to $3.3x10^3$ copies/µL. An online copy number calculator (http://cels.uri.edu/gsc/cndna.html) was used to determine this. Thereafter, 10-fold serial dilutions were performed ranging from 320 copies/µL; 32 copies/µL; and 3.2 copies/µL.

4.5.1.2 Background spike experiments

DNA from 8E5 cells was spiked into varying amounts of HIV negative DNA to mimic patient samples where there is a low HIV-1 cell-associated DNA load in a high background of cellular genomic DNA. The aim of these experiments was to determine whether there would be inhibition when amplifying samples with low total HIV-1 DNA or whether there would be non-specific priming in human genome resulting in non-specific amplification due to the high concentration of background human genomic DNA. HIV negative DNA was extracted from 1.25 $x10^6$ cells and serially diluted 2-fold over 5 dilution concentrations ranging from 50 000 to 1 563 cells per PCR reaction. Each dilution was spiked with 60 copies of 8E5 cells. For each of the 5 dilutions, PCR was performed in replicates of 6 as shown in figure 4.1 below. PCR amplicons were stained with EZ vison blue light DNA dye (AMRESCO; PA; USA) and viewed under ultraviolet (UV) light. Amplicons were run on a 1% sodium borate (SB) agarose gel. Results showed that proviral HIV was amplified in various amounts of background genomic DNA with no inhibition or non-specific priming (fig 4.2).

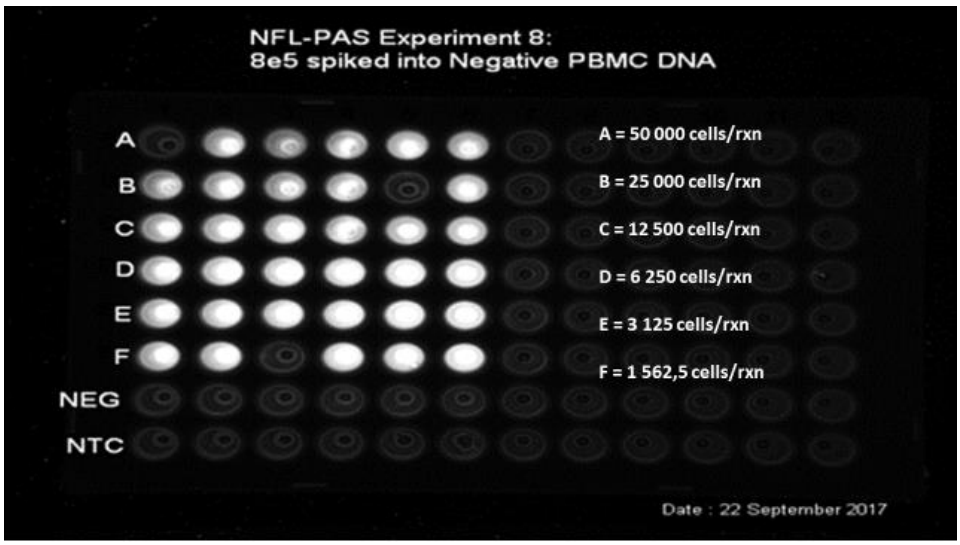

Figure 4.1: 96 well PCR plate with 8E5 spiked into negative PBMC DNA. NEG=Negative Control; NTC= No Template Control; A-F = 8E5 dilutions.

Figure 4.2: 1% SB agarose gel of products from the 'Background spike' experiment. A-F = 8E5 dilutions as shown in figure 4.1.

4.5.1.3 Sensitivity of NFL-PAS

This experiment aimed to determine the lowest 8E5 copy number that gives an NFL product when spiked into a background of DNA from HIV negative cells. To do this, 8E5 cells were serially diluted 2-fold ranging from 60 copies/reaction to 1.9 copies/reaction. Each dilution was spiked into a background of DNA from 1.25 $x10^6$ HIV negative cells which equated to the expected amount of DNA that would be extracted from patient samples. This was then loaded into PCR reactions of 12 replicates for each dilution and viewed on an agarose gel (fig 4.3 and 4.4).

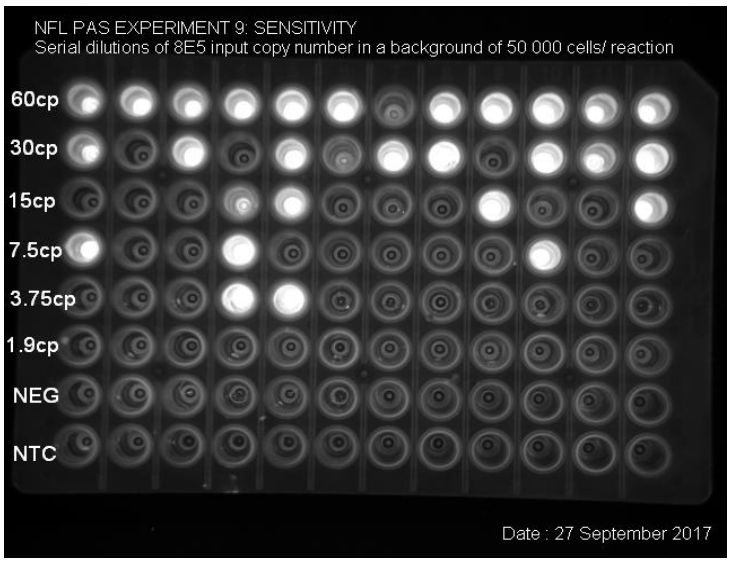

Figure 4.3: 96 well PCR plate with serial dilutions of 8E5 spiked into a background of DNA from 50,000 HIV negative PBMC. NEG= Negative Control; NTC= No Template Control.

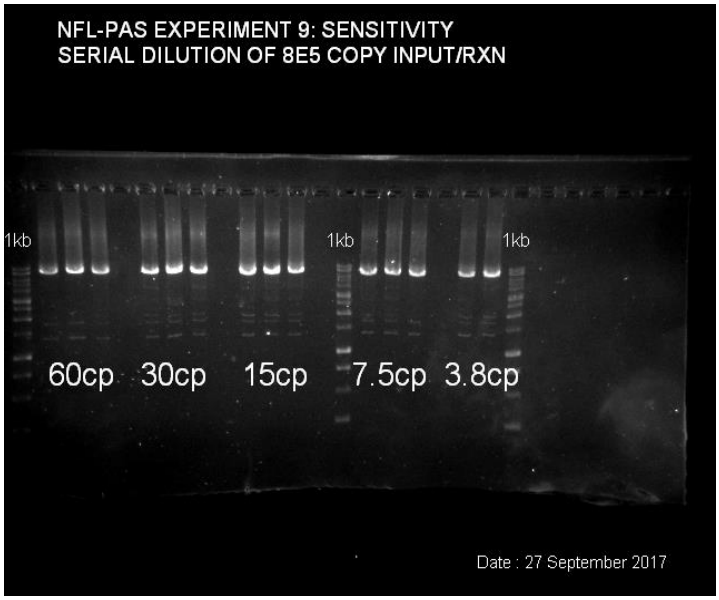

Figure 4.4: 1% SB agarose gel of products from the 'Sensitivity' experiment

As shown in figure 4.4 above, the dilution at which 30% of the replicates amplified was 7.5 copies/reaction. Considering that some margin of error is to be expected with Qubit quantification and taking into account a recent study (Busby et al., 2017) that reports a loss of integrated HIV copies in 8E5 cells with subsequent passages (we did not know the passage number of the aliquot we received), it is likely that there were fewer than 7.5copies HIV-1 DNA/reaction at that dilution. Altogether, the assay appeared to have high sensitivity.

4.5.2 Extraction and NFL-PAS on participant samples

Genomic DNA was extracted from $1.25x10^6$ PBMC as previously described but modified to exclude sonification in order to preserve the integrity longer fragments (Hong et al., 2016). Single genome PCR followed. Genomes were amplified with a nested PCR using Ranger mix (Bioline; OH; USA) and previously described primers (Li et al., 2010; Salminen et al., 1995; Wang et al., 2005). Reaction conditions and primers are listed in tables 4.2, 4.3, 4.4 and 4.5 below. Single genome amplification was achieved as follows: first, the target dilution was determined using a 'screening plate' which was generated by performing 3-fold serial dilutions on the extracted DNA (fig 4.5). Each dilution had 20 replicate PCR reactions. According to Poisson statistics, the dilution at which only 30% of the replicates had PCR amplification was chosen as the target dilution at which it is likely that a single template was amplified. To obtain a sufficient number of single genome sequences, DNA at the target dilution was spread across an 'expansion plate' of 96 wells (fig 4.6). For each NFL-PAS plate, two reactions with 8E5 as the template were used as a positive control. Two no-template controls (NTC) were also included on each plate. PCR reactions on the 96 well plates were stained with EZ vison blue light DNA dye (AMRESCO; PA; USA) and viewed under UV light. All fluorescing wells were run on a 1% SB buffer agarose gel to assess the size. If the provirus had no internal deletions, a fragment of 8.8kb was expected after nested PCR. Samples that were 8.8kb were selected for further analysis while shorter fragments were considered as having large internal deletions.

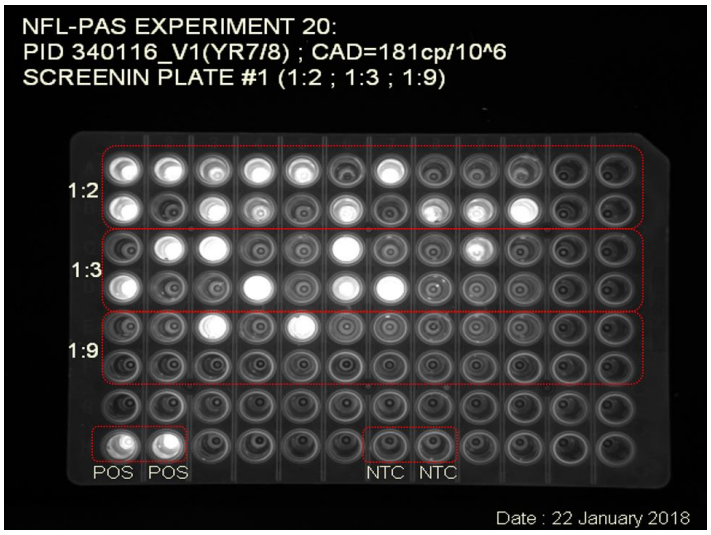

Figure 4.5: Screening plate for participant 340116. POS= Positive Control; NTC= No Template control.

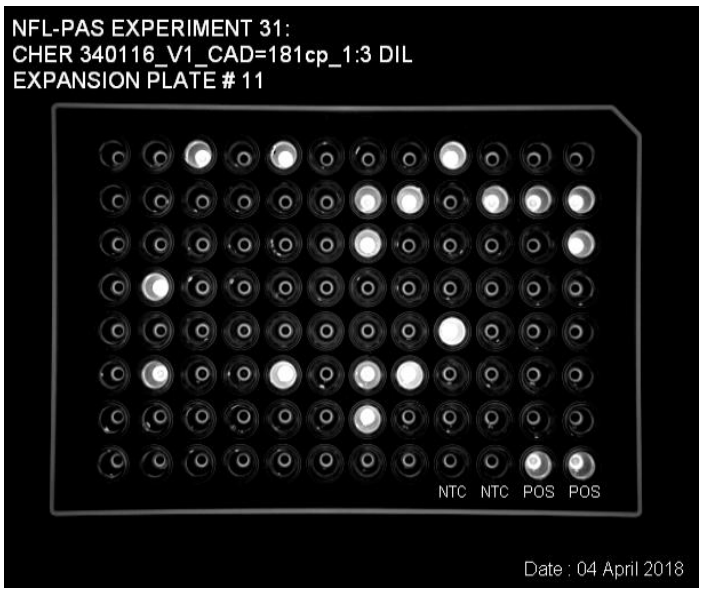

Figure 4.6: Expansion plate for participant 340116 at target dilution of 1:3. POS= Positive Control; NTC= No Template Control.

Table 4.2: NFL-PAS primers

Primer description	Primer name	Sequence (5' to 3')	HXB2 binding Position
Forward Outer primer	Li_Outer F	AAATCTCTAGCAGTGGCGCCCGAACAG	623 – 649
Reverse Outer primer	Li_Outer R	TGAGGGATCTCTAGTTACCAGAGTC	9662 – 9686
Forward Inner primer	Li_Inner F	GCGGAGGCTAGAAGGAGAGAGATGG	769 – 793
Reverse Inner primer	Li_Inner R	GCACTCAAGGCAAGCTTTATTGAGGCTTA	9604 – 9632

Table 4.3: NFL-PAS master mix

Reagent	Stock concentration	Final concentration	Volume (µL)/Rxn
Ranger Mix	2x	1x	5
Forward Primer	10µM	400nm	0.4µl
Reverse Primer	10µM	400nm	0,4µl
Molecular grade H_2O	NA	NA	2,2µl

DNA	NA	NA	2µl
Total			10µl

Table 4.4: NFL-PAS Pre-nested PCR cycling conditions

Temperature	Time	Number of cycles
95 °C	2 min	1X
98 °C	10 s	}
61 °C	10 min	30X
72 °C	10 min	1X
4 °C	∞	

PCR products were diluted by adding 80µl of cold 5mM tris, thereafter 2µl of the pre-nested product was loaded into the nested PCR mastermix.

Table 4.5: NFL-PAS Nested PCR cycling conditions

Temperature	Time	Number of cycles
95 °C	2 min	1X
98 °C	10 s	}
65.5 °C	10 min	30X
72 °C	10 min	1X
4 °C	∞	

4.5.3 Selection of 8.8kb fragments for MiSeq

For all 8.8kb amplicons, a 1.5kb region spanning *gag P6, Protease* and the first 900nt of *Reverse Transcriptase* (p6-PR-RT; nt 1893 - 3408, HXB2 positions (Korber et al., 1998)) was sequenced. Sequences were aligned using ClustalW (http://www.ebi.ac.uk/Tools/msa/ clustalw2/) and those that were not true single genome products (i.e two or more templates) were excluded. This allowed the identification of sequences with stop codons in this region that would render them defective. All sequences that passed these two criteria where selected as candidates for next generation sequencing by Illumina MiSeq (Illumina; CA; USA). These samples were gel extracted from a 1% SB agarose gel using the NucleoTrap Gel Extraction Kit (Macherey-Nagel; Germany) according to manufacturer's instructions.

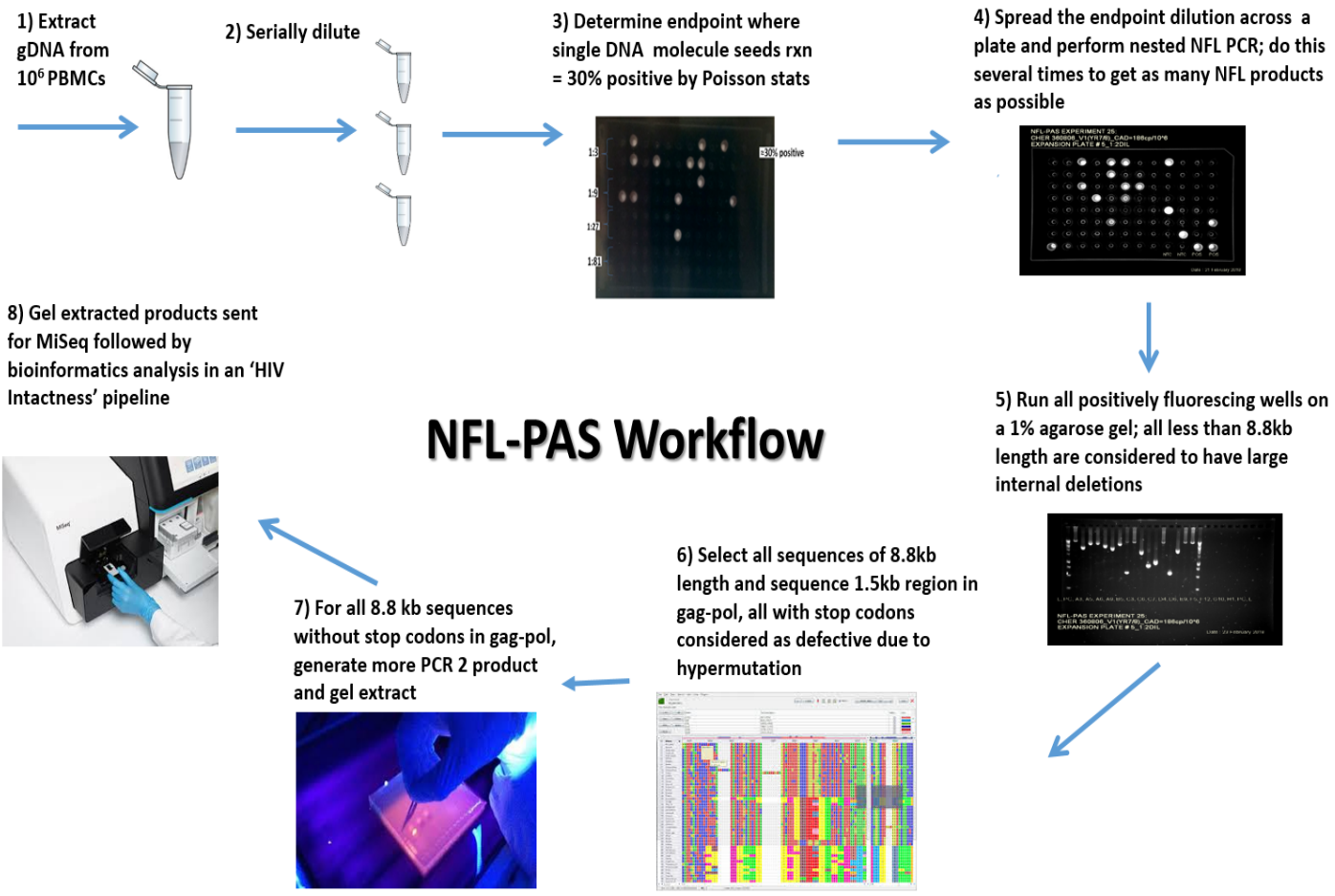

Figure 4.7: NFL-PAS workflow

4.5.4 MiSeq library preparation

MiSeq library preparation and sequencing was performed at the Institute for Microbial Biotechnology and Metagenomics (IMBM) at the University of Western Cape. The Illumina Nextera DNA library prep kit (Illumina; CA; USA) was used. In a single reaction, DNA was enzymatically fragmented, and adapters added to the template. The DNA was then purified and amplified by a PCR that indexed the samples by adding different primer pairs to individual samples. The 300 cycle V2 MiSeq Reagent kit (Illumina; CA; USA) was used to sequence the library.

4.5.5 Bioinformatic analysis of MiSeq data

After sequencing, all reads with the same index were assembled to form a consensus sequence. The sequences were then subjected to checks for viral intactness in an 'Intactness pipeline' developed by a collaborator Dr. Imogen Wright. Sequences were first checked for correct size (i.e 8.8kb). Next, sequences that appeared to be mixed templates were detected and eliminated from further analysis. The remaining sequences were then translated to allow further analysis of the 9 viral open reading frames (ORFs). A sequence was determined to be intact if within these ORFs, there were no: stop codons, frameshift mutations, or hypermutations that could preclude viral infectivity.

4.5.6 Amplification and sequencing of the HIV Packaging Signal and Major Splice Donor site

The NFL-PAS protocol has the benefit of using primers that bind in conserved regions of the HIV genome. However, the 8.8kb NFL-PAS product (fig 4.8) excluded the first 793 nucleotides (gag-leader region) of the viral genome (*p17- 3'LTR*; nt 794 - 9857, HXB2 positions (Korber et al., 1998)) that encode the viral packaging signal (*psi*) and major splice donor site (*MSD*) (*gag pr55*; nt 634 – 789, HXB2 positions (Korber et al., 1998)) which play essential roles in viral replication. In the literature, Ho et al found deletions in this region in 6% of sequences (8-98bp deletions); Bruner et al, in 5% (15-97bp deletions) and Hiener et al, in 11% of sequences (Bruner et al., 2016; Hiener et al., 2017; Ho et al., 2013). Deletions, mutations, or deleterious stop codons in these regions destroy viral infectivity (Ho et al., 2013). Eighteen of the NFL-PAS products that were sent for MiSeq appeared to be intact after analysis in the bioinformatic pipeline. To determine whether the *psi*, and *MSD* were intact in the 18 samples, a forward primer was designed to bind upstream of the NFL product (*gag Pr55*; nt 642, HXB2 position (Korber et al., 1998)). For each limiting dilution that yielded an 8.8kb intact sequence, pre-nested PCR product was added to a nested PCR, using the newly designed forward primer and the pre-nested reverse primer (fig 4.9) to generate an amplification product that included the *gag*-leader region. The generated product was 9044bp in length (*Gag Pr55 – 3'LTR*; nt 642 – 9686, HXB2 position (Korber et al., 1998)) .

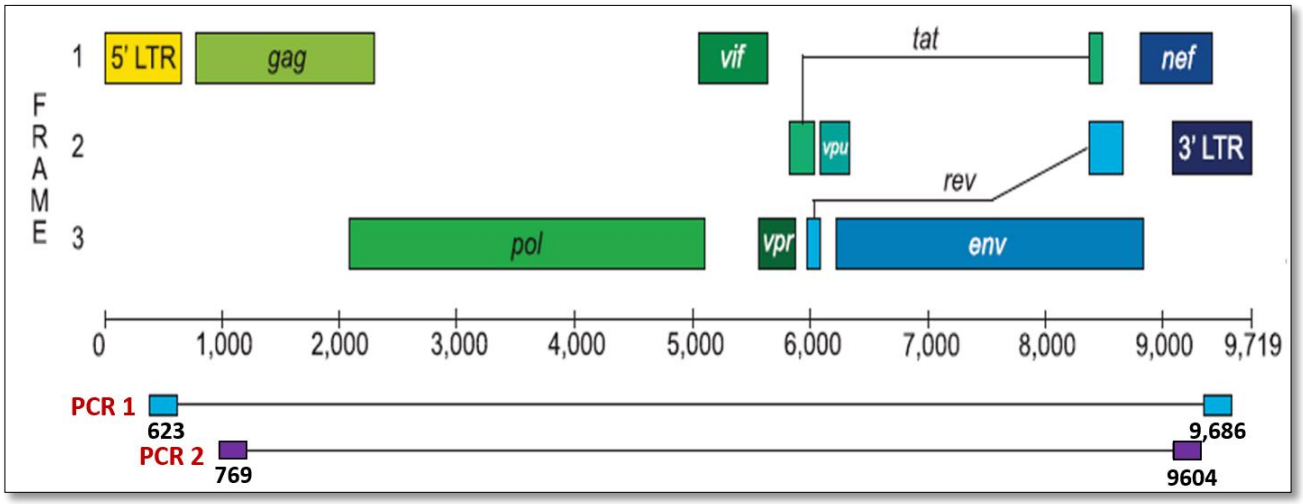

Figure 4.8: NFL-PAS PCR 1 and PCR2 primer binding sights; product length 8,835kb

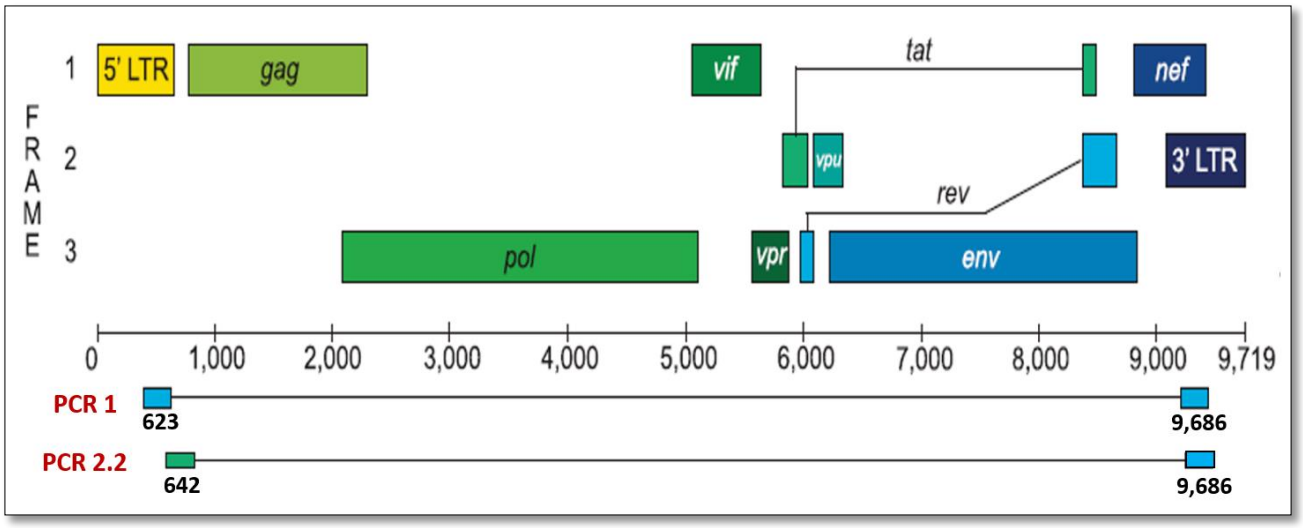

Figure 4.9: Nested PCR to obtain psi & MSD; A forward primer that bound internal to the PCR 1 product was used with the PCR1 reverse primer to generate a product of 9044bp

Table 4.6 – 4.8 below show primers and PCR conditions that were used to generate the NFL product containing *psi* and *MSD* regions:

Table 4.6: psi & MSD PCR primers

Primer description	Primer name	Sequence (5' to 3')	HXB2 binding Position
Forward primer	NFL_alt_in_FW	CCGAACAGGGACBHGAAAGCGAA	642 – 664
Reverse primer	Li_Outer R	TGAGGGATCTCTAGTTACCAGAGTC	9662 – 9686

Table 4.7: psi & MSD mastermix

Reagent	Stock concentration	Final concentration	Volume (µL)/Rxn
Ranger Mix	2x	1x	12.5µl
Forward Primer	10µM	400nm	1µl
Reverse Primer	10µM	400nm	1µl
Molecular grade H_2O	NA	NA	8.5µl
DNA	NA	NA	2µl
Total	NA	NA	25µl

Table 4.8: psi & MSD PCR cycling conditions

Temperature	Time	Number of cycles
94 °C	2 min	1X
94 °C	30 s	}
44 °C	30 s	30X
72 °C	7 min	1X
4 °C	∞	

The 9044bp fragment was gel extracted from a 0.8% TAE buffer using the NucleoTrap gel extraction kit (Macherey-Nagel; Germany). A 1 kb region containing the psi, MSD and PBS was Sanger sequenced. The 1kb length ensured enough overlap with the region that was previously sequenced by Miseq and confirmed that the same variant was sequenced. In table 4.9 below are the sequencing primers:

Table 4.9: psi and MSD sanger sequencing primers

Primer description	Primer name	Sequence (5' to 3')	HXB2 binding Position
Forward primer	NFL_alt_in_FW	CCGAACAGGGACBHGAAAGCGAA	642 – 664
Forward primer	Li_Inner F	GCGGAGGCTAGAAGGAGAGAGATGG	769 – 793
Reverse primer	gag-P17	TGACGCTCTCGCACCCATCT	788 - 807

4.6 Results

4.6.1 Obtaining intact proviral genomes

Figure 4.10 below illustrates the process by which genetically intact sequences were obtained from 9 children after 6-9 years on ART. A total of 738 single-genome amplicons were obtained by NFL-PAS. Of these, 538 had large internal deletions. Of the remaining 200 amplicons, a 1.5kb region of *gag-pol* was amplified and sequenced. One hundred and sixty-six were shown to be hypermutated, characterized by stop codons. Following bio-informatic analysis, 10 NFL-PAS amplicons appeared to be intact, 9 were hypermutated and 15 had small internal deletions. To determine whether *psi*, and *MSD* were intact in the 10 samples, the viral packaging signal and major splice donor site were amplified and sequenced. Of these, 3 sequences were characterized by mutations in the psi and/or MSD region. Finally, 7 sequences were shown to be genetically intact.

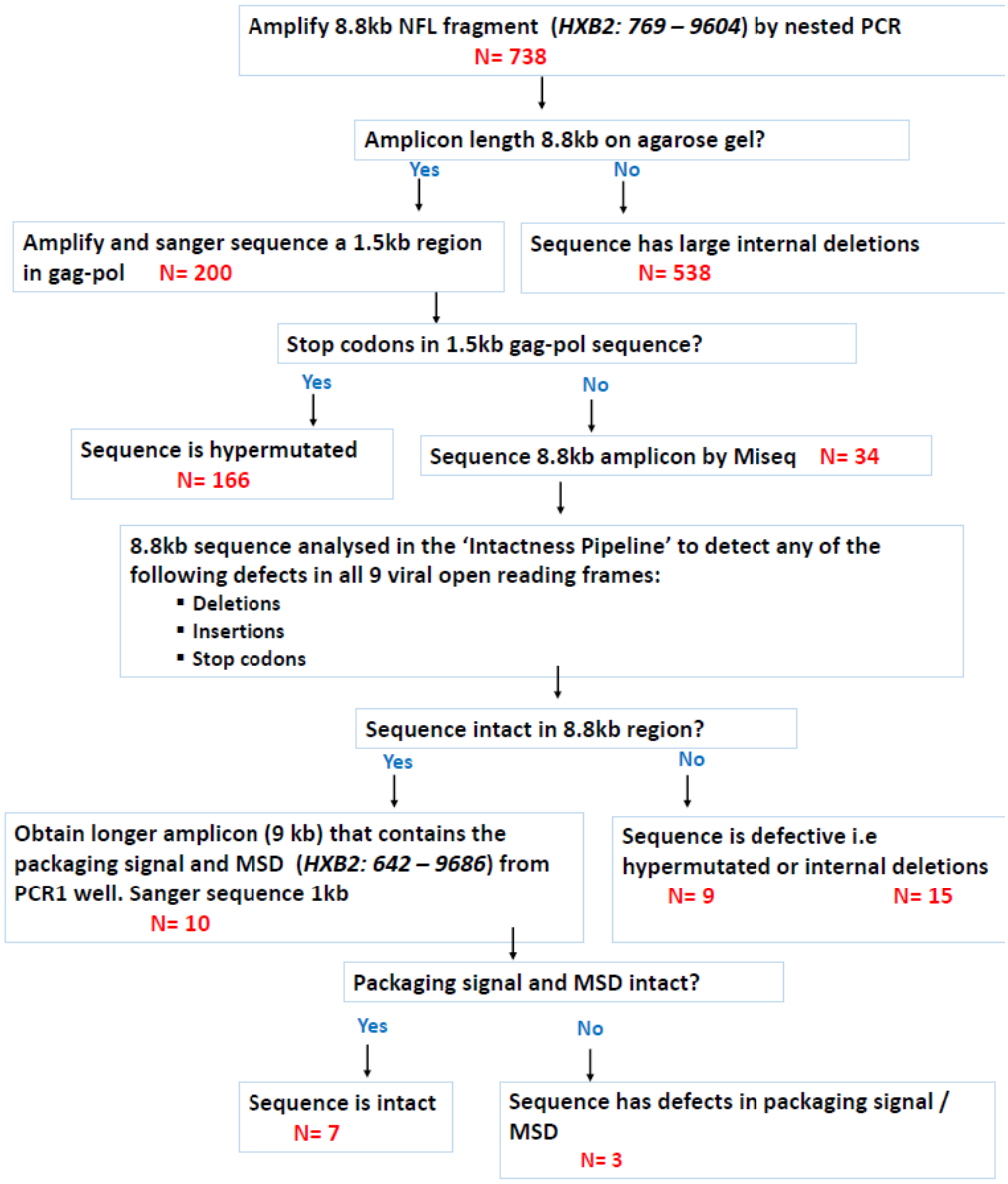

Figure 4.10: Schematic for obtaining intact proviruses by NPL-PAS

4.6.2 NFL-PAS participants

Table 4.10 below shows characteristics of the 9 participants that formed the NFL-PAS cohort. The median age of ART initiation was 2.3 months (range: 1.7 – 11.1). Three participants had periods when ART was interrupted as part of the CHER trial. Periods of interruption ranged from 4 months to 3.6 years. One participant was poorly suppressed for the first 2.5 years on ART probably due to poor adherence. The remaining 4 participants had never been interrupted and were fully suppressed on ART. At the time of testing, participants had been on ART for a median of 8.2 years (range: 6.9 – 9.1). The median iCAD at time of testing was 86.3 copies/10^6 (range: 42.3 – 247.6).

Table 4.10: Patient characteristics and NFL sequences

PID	Gender	Age ART start (months)	Duration of ART at sample (years)	HIV CAD (copies/10^6 PBMC)	Sequences with internal deletions	Sequences with hyper-mutations and stop codons	Sequences with packaging signal/MSD defects	Intact Sequences	Total number of single genomes	Total number of cells assayed
333676	F	1.7	8.6	55.5	4	1	0	0	5	$2.6x10^6$
360806	F	2.0	9.13	186.2	68	19	0	0	88	$9.2x10^6$
341622	M	2.16	6.9	81.9	30	4	0	0	34	$2.6x10^6$
341862	F	2.2	6.96	42.3	89	101	0	0	190	$6.1x10^6$
333716	F	2.3	8.55	129.6	18	3	0	0	21	$3.9x10^6$
339606	M	8.5	7.93	247.6	27	9	1	2	39	$3.9x10^6$
340116	F	9.23	7.31	181.5	207	23	2	1	233	$9.6x10^6$
339266	F	9.32	8.2	46.7	56	15	0	4	75	$6.6x10^6$
334436	F	11.1	8.82	86.3	54	0	0	0	54	$1.8x10^6$
Total	NA	Median= 2.3	Median = 8.2	Median = 86.3	553	175	3	7	738	$46.3x10^6$

4.6.3 Distribution of sequences by participant:

Figure 4.11 below illustrates the distribution of single genome PCR products in each of the 9 participants.

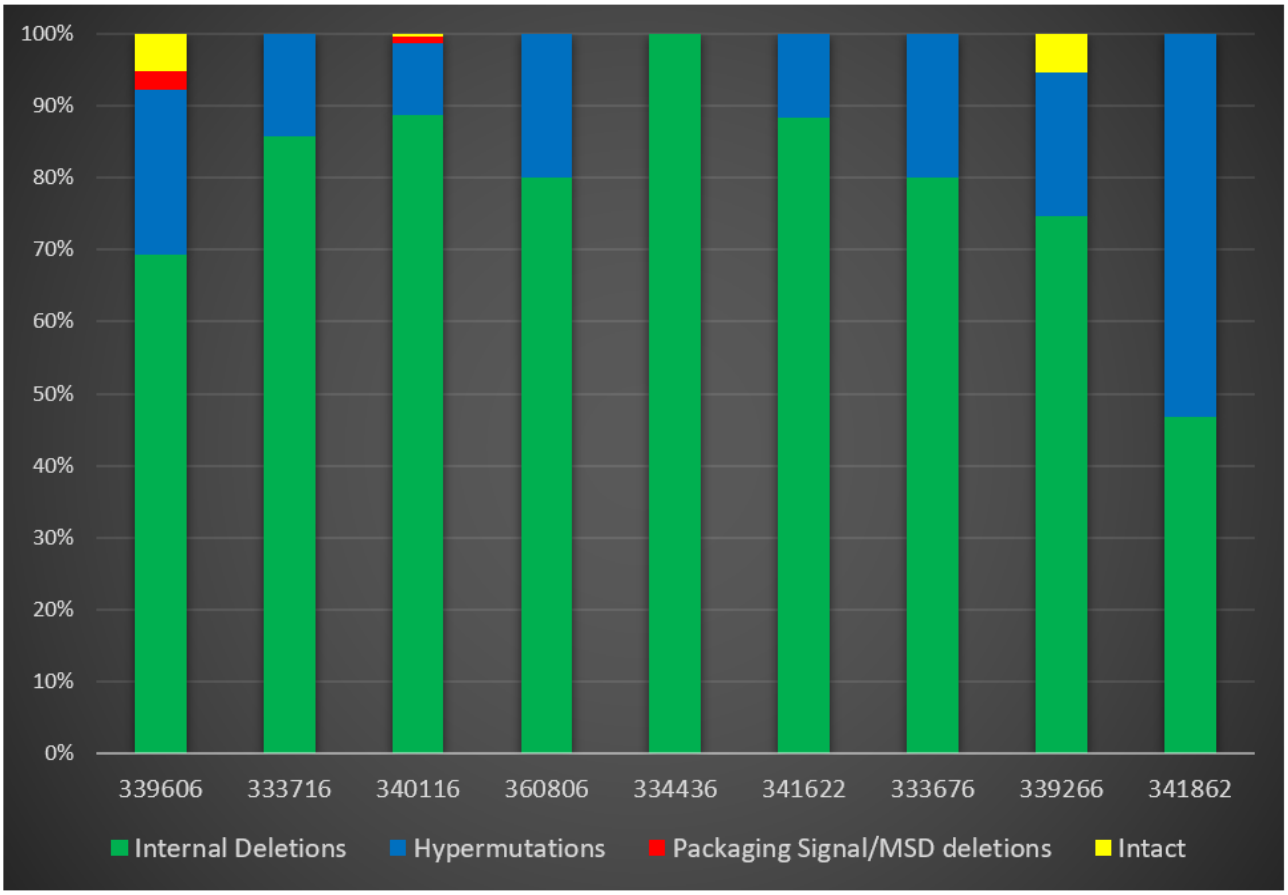

Figure 4.11*:* Distribution of sequences per participant

4.6.4 Overall distribution of intact and defective sequences

Figure 4.12 below illustrates the distribution of the 738 amplicons from all 9 participants, 72.9% had large internal deletions and 23.7% had hypermutations that rendered them defective. As the packaging signal/MSD mutations (gag-leader) were only assessed in 10 cases that were provisionally intact, this proportion (1%) and the proportion of sequences with small internal deletions (1.4%) were adjusted using the expected rate as found in those that had a gag-leader sequence. Only 0.9 % were genetically intact. When compared to data from adults who initiated ART in acute infection (Hiener et al., 2017) using Fisher's exact tests, the proportion of intact sequences and psi/MSD deletions were significantly lower ($p<0.05$).

In figure 4.13, the proportion of intact and defective sequences were compared between the 5 participants who were fully suppressed and 4 who were partially suppressed on ART. The distribution of intact vs defective in the fully suppressed participants appeared similar to what was observed in total sequences from all participants.

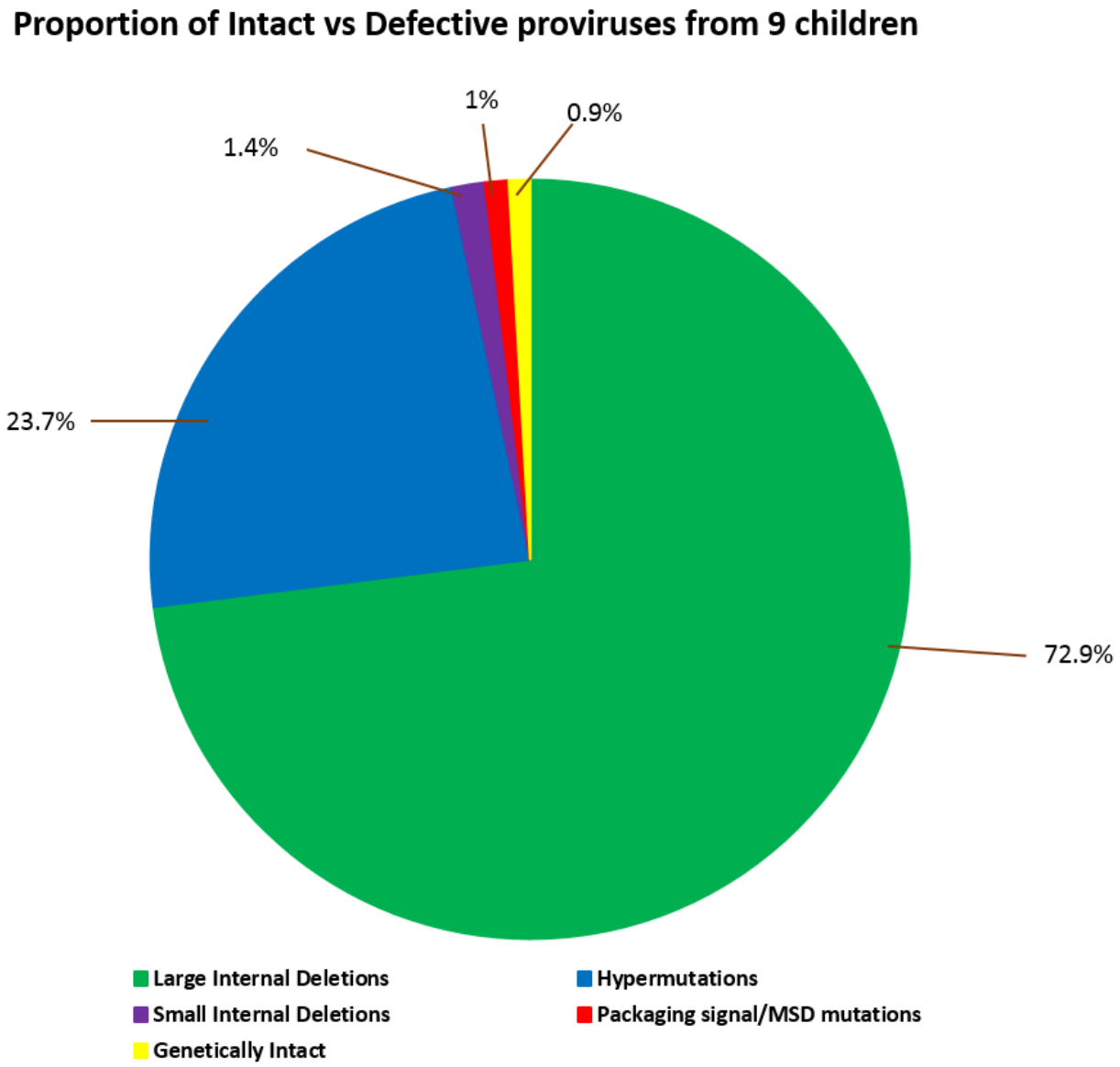

Figure 4.12: Distribution of Amplicons in the 9 participants

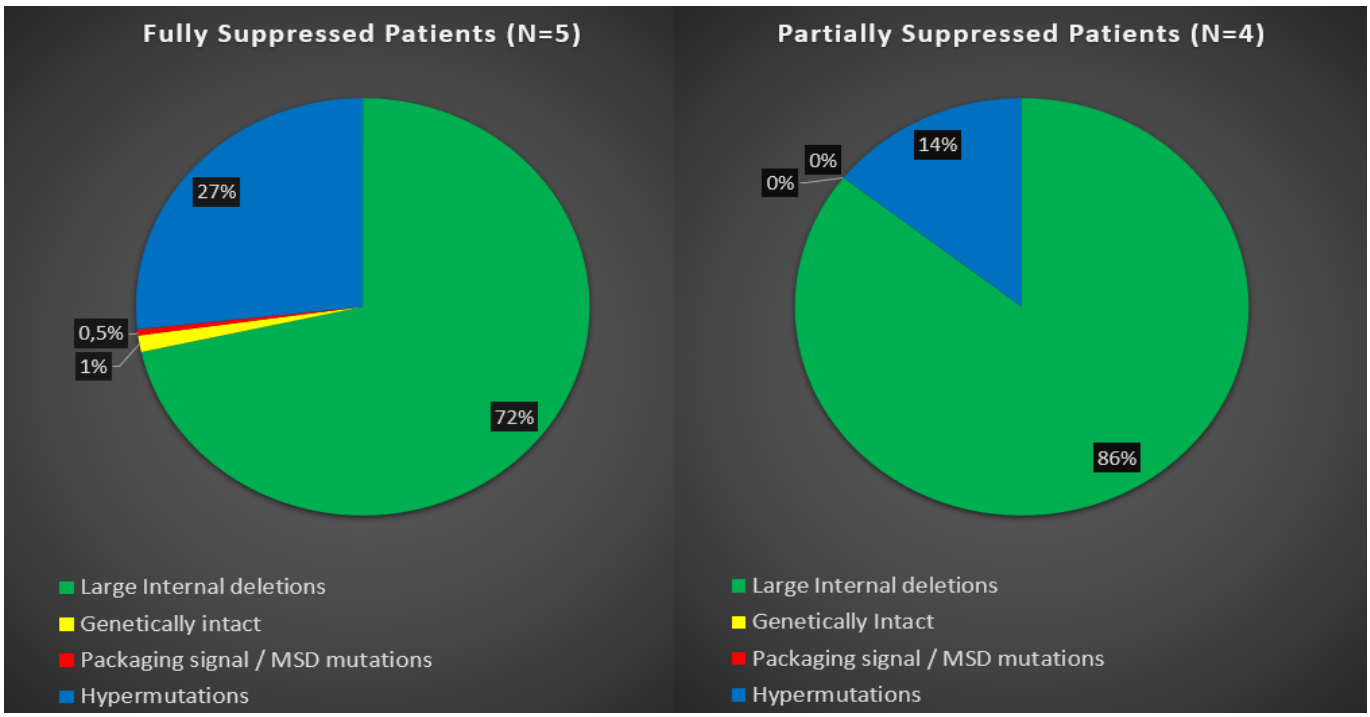

Figure 4.13: Distribution of amplicons in fully suppressed vs partially suppressed participants

4.6.5 Evidence of clonally expanded intact sequences

Participants 340116, 360806 and 339266 had intact NFL sequences and had *gag-pol* single genome sequence data from Aim 1. For each of these participants, an alignment was made of intact NFL sequences and *gag-pol* sequences from Aim 1 to assess whether the intact NFL sequences would form part of a monotypic cluster with *gag-pol* sequences, indicating the probability of an expanded clone.

In participant 339266, two sets of intact NFL sequences were identical in the 9kb region. When these sequences were assembled in a neighbour-joining phylogenetic tree (fig 4.14 below) with 1.2kb *gag-pol* sequences from pre-therapy plasma RNA, PBMC DNA from 1.2 years on ART and cell associated DNA sequences from 8 years on ART, two of the intact NFL sequences formed part of a monotypic cluster (blue bracket) with a *gag-pol* DNA sequence from 1.2 years on ART, suggesting the persistence of a possible intact clone that was present soon after ART was initiated. Intact sequences from participant 360806 and 339266 were not identical in the 1.2kb *gag-pol* region.

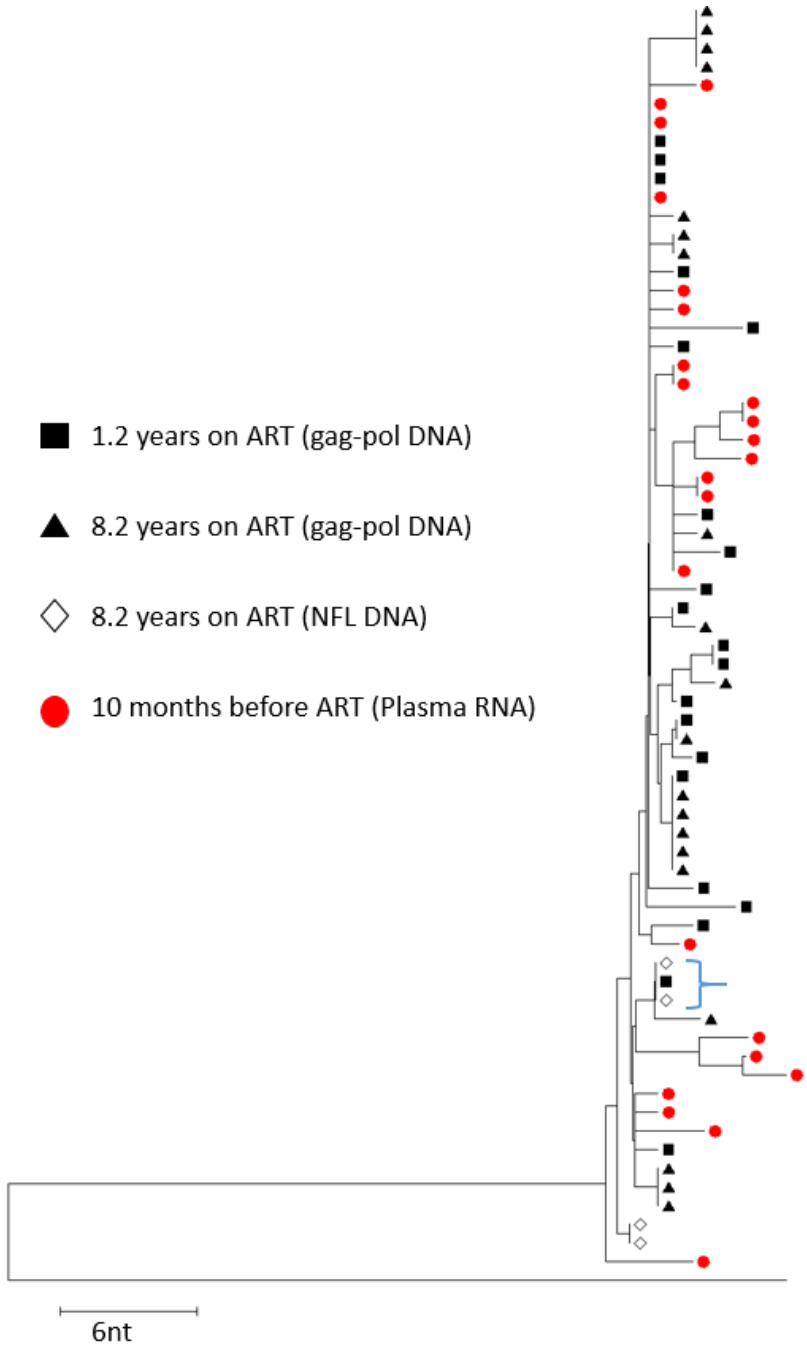

Figure 4.14: Neighbour joining phylogenetic tree for participant 339266

4.7 Discussion

4.7.1 Intact HIV proviruses can be detected in early treated children after long-term ART

To our knowledge, this is the first study to show that after 6-9 years on suppressive ART, genetically intact HIV-1 proviral sequences are detectable by near full-length sequencing in children who initiate ART within the first year of life. Our aim was to investigate proviral intactness and we classified sequences as genetically intact when we found none of the known defects on sequencing. Nevertheless, this does not prove replication competence, which would require identifying the integration sites, amplifying full-length HIV from the host, cloning and transfection with production of infectious virus and should be done in future studies.

In one participant, we observed two sets of identical, intact near full-length sequences. When aligned with *gag-pol* sequences from 1.2 years after ART initiation, two of the intact sequences formed a monotypic cluster, suggesting the persistence of an intact expanded clone. Our findings show that early ART does not prevent the establishment of long-lived reservoirs. Although rare in early treated children, these reservoirs can be detected after several years on ART and are probably, just as in adults (Bui et al., 2017; Hosmane et al., 2017; Lorenzi et al., 2017; Simonetti et al., 2016), maintained by clonal expansion/proliferation of cells infected before ART initiation.

A recent study found no intact HIV proviral sequences out of 164 near full length sequences derived from viral outgrowth culture wells in 11 early treated, long-term suppressed children who initiated ART before 6 months (Rainwater-Lovett et al., 2017). We generated 738 single-genome amplicons and found 7 (0.9%) to be intact. Whereas in the previous study, proviruses were sequenced from non-induced viral outgrowth wells, we performed NFL-PAS directly on DNA from PMBC samples. On the other hand, the different findings between the two cohorts could be due to differences in age of ART initiation. In our study we detected intact sequences from children who initiated ART after 8 months of age and thus likely had a larger proportion of intact sequences while in the previous study, all participants initiated ART within 4 months of age and had no detectable intact sequences. Furthermore, the difference in viral genotypes between the two cohorts could have played a role. In our setting, HIV-1 subtype C predominates whereas the previous cohort was of subtype B infection which supports the need for representation of paediatric cohorts across different geographical regions as differences in viral genotypes and host factors may affect HIV persistence in children.

We found that the majority (99%) of HIV-1 proviruses in our cohort were defective either due to large internal deletions or stop codons that led to hypermutation similar to what has been reported in both children and adults (Bruner et al., 2016; Hiener et al., 2017; Ho et al., 2013; Rainwater-Lovett et al., 2017). The large internal deletions are a result of template switching of the *reverse transcriptase* enzyme between the two viral RNA copies during reverse transcription (Golden et al., 2014; Temin, 1993; Zhuang et al., 2002). *Reverse transcriptase* also lacks proof reading activity which leads to errors that increase the accumulation of stop codons (Battula and Loeb, 1977). Furthermore, the host cell's cytidine deaminases APOBEC3F and APOBEC3G

induce G to A hypermutations during the minus strand cDNA synthesis step of reverse transcription which render proviruses defective (Bishop et al., 2004; Harris et al., 2003; Mangeat et al., 2003). The proportion of intact proviruses in our cohort (1%) was similar to the 2% (Bruner et al., 2016) and 5% (Hiener et al., 2017) reported in adults who initiated during acute infection but distinct from the 12% reported in adults who initiated ART during chronic infection (Ho et al., 2013). It is not known if the children in our study were infected intra-uterine or perinatally. However, the three children who had intact proviruses started ART after 8 months of age, based on clinical or CD4 criteria. Nevertheless, the proportion of intact proviruses were more similar to acutely treated adults than adults who initiated ART in chronic infection.

In one child, we detected two identical intact sequences from 8 years on ART which formed a monotypic cluster with a sequence from 14.4 months after ART initiation. This suggests that clonal expansion of intact proviruses could be the mechanism that maintains the replication competent reservoir in these children. Similar identical sequences have been observed in adults treated during acute infection (Hiener et al., 2017). Furthermore, it has been shown that genetically intact clonal proviral sequences are replication competent in viral outgrowth assays (Bui et al., 2017; Hosmane et al., 2017; Lorenzi et al., 2017; Simonetti et al., 2016). These findings complicate the prospect of eradicating reservoirs in these children as latently infected cells can become activated and proliferate without viral antigen expression, and therefore remain hidden to the immune system or immune-based therapies (Bosque et al., 2011; Chomont et al., 2010; Hosmane et al., 2017; Wang et al., 2018).

Our cohort consisted of 5 children who were fully suppressed on ART and 4 children who either had periods of ART interruption or were poorly suppressed for a brief period. All 7 intact sequences obtained in this study were from three children who were fully suppressed on ART, but who started ART after 8 months of life, whereas the children without detectable intact proviruses, started ART before 2.3 months, but had subsequent periods of poor suppression or therapy interruption. More sequences were obtained from the suppressed children than the interrupted thus intact proviruses in ART interrupted children could have been missed due to insufficient sampling. However, a recent study (Clarridge et al., 2018) showed that the proportion of intact vs defective proviruses remained the same before and after brief ART interruptions of about three months. In our study, some patients were interrupted for up to 3 years yet did not have recoverable intact proviruses. These findings corroborate previous studies showing that the largest proportion of the long-surviving reservoir is established before therapy initiation (Ananworanich et al., 2015; Archin et al., 2012; Buzon et al., 2014) with limited replenishment during periods of therapy failure (Miller et al., 2000) or interruption (Clarridge et al., 2018; Strongin et al., 2018). Early treatment initiation may therefore be the most important for reducing the reservoir size, whereas short monitored periods of interruption, necessary to assess the effect of curative interventions, may not have long-term effects on reservoirs (Clarridge et al., 2018).

The fact that intact proviruses were not detected in some participants does not mean they are not present. During the CHER trial, all interrupted children, except one, eventually had rebound viremia regardless of how early ART was initiated proving that infectious virus was present (Cotton et al., 2013). The one participant that showed post therapy control or remission, initiated ART at 2 months, interrupted after 40 weeks and has maintained viral suppression for 8.5 years (Violari et al., 2019). This child was not included in our study, as this child was recruited at another site. It is not known if intact proviruses are present or whether control is due to unique immune responses. Another French child from the ANRS EPF-CO10 paediatric cohort received ART from birth, interrupted after 5 years and has maintained viral suppression for over 11 years (Frange et al., 2016). The mechanisms of long term viral remission after early infant ART are unknown and warrant further investigation to understand possible host immune factors that could play a role. In contrast, infectious virus could be recovered from viral outgrowth assays, on samples from children who started ART at a median age of 8.1 weeks for up to 2 years of age(Persaud et al., 2012). In children who start earlier, infectious virus is often not recoverable (Bitnun et al., 2014; Luzuriaga et al., 2014), or DNA undetectable (Bitnun et al., 2014), suggesting a smaller reservoir size, but this does not constitute cure. Mathematical models (Hill et al., 2014) and studies in adult cohorts (Steingrover et al., 2008; Williams et al., 2014) suggest that a very small reservoir may be associated with delayed rebound. In the case of the Mississippi baby who initiated therapy within 30 hours of birth, virus rebounded 27 months after therapy cessation (Luzuriaga et al., 2015; Persaud et al., 2013). In contrast, another infant who received immediate antiretroviral therapy, continued for 4 years, rebounded within 7 days of therapy interruption (Butler et al., 2015). This shows that the reservoir is seeded very early during infection and persists over long periods on ART despite being undetectable by culture and molecular methods.

Although the quantitative viral outgrowth assay (qVOA) is considered a gold- standard for detecting replication competent viruses, not all intact proviruses are reactivated in cell culture and it has recently been reported that qVOA underestimates reservoir size by 25-fold in patients treated during acute infection and 27-fold in chronic phase treated patients because not all genetically intact proviruses are sufficiently reactivated in-vitro and may require multiple rounds of stimulation (Bruner et al., 2016). Therefore, molecular assays such as the one used in this study provide a more sensitive estimate of the reservoir and are even more appropriate for paediatric studies where sample availability is often limited. There is however, a need for more efficient methods that can generate near-full-length amplicons and differentiate between intact and defective proviruses. A recent study (Bruner et al., 2019) highlights one such approach where a quantitative PCR assay utilises multiple probes (based on the known distribution of defects in long-term treated patients) to detect full-length proviruses and simultaneously differentiate between intact, hypermutated and defective variants. On the other hand, host and viral factors may influence the proviral landscape. Whereas cells with hypermutated proviruses that produce peptides through alternative splicing can be recognised and killed by cytotoxic T lymphocytes (CTLs), cells that do not produce HIV-1 antigen may preferentially survive after long term therapy (Pollack et al., 2017). It is therefore not clear if this real time

PCR assay would be equally valid in populations that differ by HIV-1 genotype, patient age, duration of treatment or having started therapy during acute or chronic HIV infection.

4.7.2 Strengths and Limitations of the study

To our knowledge, this is the first study to detect potentially intact HIV-1 proviruses in early treated-long term suppressed children through near full length single genome sequencing. The detection of identical intact sequences provides evidence for possible clonal expansion as the mechanism of persistence of the reservoir in these children. Through extensive sampling, were able to generate 738 amplicons from 9 participants. Our study adds to the limited data available on early treated children especially those with subtype C infection.

The near full length sequencing approach did not amplify the entire HIV genome due to the lack of conserved primer binding sites in the LTR gene. There could have been primer binding mismatches that led to missed detection of some variants in these patients. Furthermore, we did not perform viral outgrowth experiments to prove that the intact proviruses were infectious because sample availability was limited and the assay requires large sample volumes for optimal sensitivity. Our study cohort consisted of only 9 participants where there was sufficient sample and a high enough proviral load and thus our findings may not be fully representative of reservoirs in long-term suppressed subtype C infected children. In addition, the NFL-PAS assay is cumbersome and would not be feasible in children with ultra-low proviral loads such as very early treated infants (Veldsman et al., 2018). Lastly, we did not sequence integration sites of the identical proviruses detected in this study to prove that these are expanded clones rather than homogenous variants that persisted from the time of infection.

4.7.3 Conclusion

Although rare, intact proviruses are detectable in early treated, subtype C infected children after 6-9 years. As is seen in adults, these proviruses are probably maintained by clonal expansion/proliferation of cells infected before ART initiation. We did not observe intact proviruses in interrupted children, this is likely due to the fact that they initiated ART earlier than the uninterrupted children. Future work could include linking intact proviral sequences to CD4 T cell clones and to plasma virus that rebounds after therapy cessation or due to latency reversing agents. There is also a need for more efficient sequencing of long proviruses, possibly involving third generation sequencing platforms (Parikh et al., 2017).

4.8 Appendix B: Supplementary figures

Longitudinal Viral load graphs:

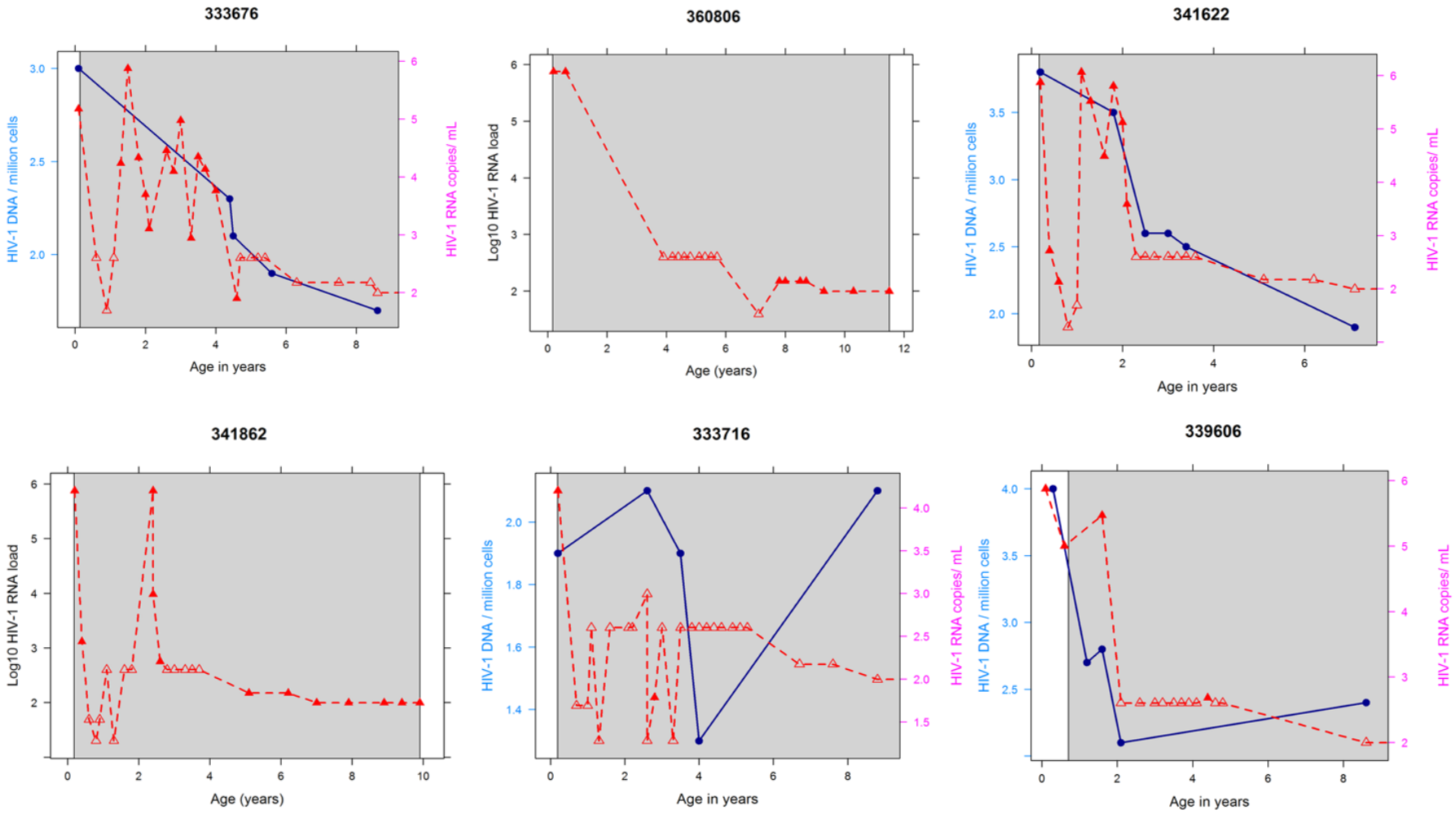

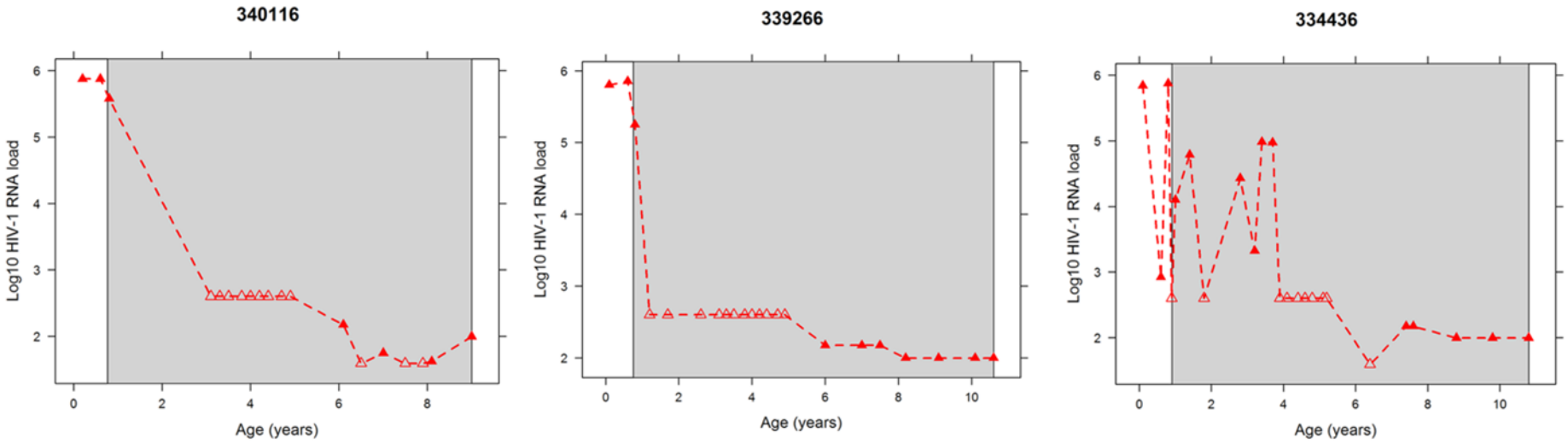

Chapter 5

5.1 Conclusion

Long-lived cells that harbour dormant forms of infectious HIV are known as latent reservoirs and currently the major barrier to cure despite optimal ART suppression (Brooks et al., 2001; Siliciano and Greene, 2011). Reservoir establishment occurs early after infection and is facilitated by various host and viral factors (Baldauf et al., 2012; Blazkova et al., 2009; Brooks et al., 2001; Chun et al., 1998; Lenasi et al., 2008; Wang et al., 2015; Ylisastigui et al., 2004). The CHER randomised trial showed that early ART lead to increased survival and long term benefits in HIV infected South African infants (Cotton et al., 2013; Payne et al., 2015; Van Zyl et al., 2014). Other studies have since shown that perinatally HIV infected children who initiate ART soon after infection have limited reservoirs with increased decay rates (Ananworanich et al., 2014; Luzuriaga et al., 2014; Persaud et al., 2012; Veldsman et al., 2018). Furthermore, early treated children have a lower proportion of central memory CD4 T cells, better CD4 T cell function and lower immune activation states, factors that would make them good candidates for cure interventions (Adland et al., 2018; De Rossi et al., 2002; Klein et al., 2013; Lynch et al., 2011). There is therefore a need to characterize the latent reservoir in this population and describe the mechanisms by which it persists during long-term ART in order to inform cure strategies. This study was aimed at characterising latent reservoirs in a subset of the post-CHER cohort who have been maintained on long-term suppressive ART.

In chapter two we investigated the size of the persisting reservoir by quantifying cell associated DNA (CAD) as a biomarker in 16 post-CHER children. To do this, a previously described highly sensitive CAD assay was adapted for HIV-1 subtype C (Hong et al., 2016). Its implementation involved the preparation of a real-time PCR standard and optimization of real-time PCR conditions on the Bio-Rad CFX 96 platform. This was followed by quantification of CAD in patient PBMC samples after 6-9 years on ART. Participants were divided into three categories based on the age at which at which ART was initiated (0-3 months / 3-8 months and 9-18 months). We found overall that the CAD loads were low (ranging from 0 copies/10^6 PMBC to 186.2 copies/10^6 with a median CAD value of 22.45 copies/10^6) in the 16 participants who initiated ART within the first 18 months of life. However, where others have found lower CADs in children who start ART earlier than 2-3 months (Martínez-bonet et al., 2015; Van Zyl et al., 2014), we did not see a significant difference in the three treatment categories in our study. This could have been due to some of the earlier treated patients having had periods of poor ART suppression where viral replication likely replenished the reservoir.

We found that the amount of viral replication over time on therapy (calculated as ‘area under log viral load curve’) was significantly associated with CAD levels, further showing that unsuppressed viral replication leads to increased reservoir size and highlighting the importance of early and good adherence to ART in perinatally infected children. However, qPCR approaches detect both intact and defective proviruses and thus over-

estimate the reservoir by over 300-fold (Eriksson et al., 2013; Ho et al., 2013). Due to limited sample availability, we were unable to assess reservoir size using the gold-standard viral outgrowth assay.

We also investigated whether there is genetic evolution in the reservoir over time in long term ART suppressed children. Our findings allowed us to contribute to an ongoing debate in the field on whether the reservoir is maintained by ongoing viral replication in tissues sanctuaries where ART penetration is sub-optimal and resulting in the low level viremia typically seen in well treated patients. The fact that the children were early treated provided a low background genetic diversity which would be ideal to detect any evidence of viral evolution over time. We selected eight children who had been fully suppressed on ART since initiation and two children who had earlier periods of poor suppression; this allowed us to draw comparisons. We performed single genome sequencing in each participant and compared sequences from two time points, one close to ART initiation and another after 6-9 years on ART. We then utilised 3 sensitive tests for evolution i.e (i) average pairwise distance (APD) to determine intra-patient population diversity, (ii) panmixia to look for probability of shifts in viral population structure and (iii) maximum likelihood (ML) root-to-tip distances to detect emergence of new viral populations. With all three tests, no significant change in intra patient diversity, shifts in viral population structure or emergence of new viral populations were detected in the eight fully suppressed children whereas significant changes were observed in the two partially suppressed children. We were thus able to show that in well-suppressed children, ART prevents cycles of ongoing replication that could replenish the reservoir. Our findings are supported by a recent study in adults where similar methods were used to show no significant difference in viral populations before and after ART interruption (Kearney et al., 2014). Furthermore, it has been shown that treatment intensification with an addition of a third drug has no effect on low level viremia (Dinoso et al., 2009; Gandhi et al., 2012; McMahon et al., 2010; Rasmussen et al., 2018). These findings once again highlight the benefits of early, fully suppressive ART in preventing the development of phylogenetically diverse reservoirs that would further complicate cure efforts. The detection of identical single genome sequences on neighbour-joining phylogenetic trees of each participant pointed to clonal expansion rather than ongoing viral replication as the possible means by which the reservoir persists despite effective ART. This was further investigated in chapter 3.

It has been established in the field, that latently infected cells have the capacity to clonally expand and maintain the reservoir over time on ART (Simonetti et al., 2016). There has also been recent evidence that intact proviruses are present in clonally expanded cells (Einkauf et al., 2019).The monotypic sequences we detected in chapter 2 were likely evidence of expanded clones. However, since most children were treated early and long-term suppressed, we could not exclude the possibility that identical sequences were a result of homogenous viral populations that persisted from the pre-therapy era. We performed integration site analysis (ISA) to detect expanded clones in samples close to ART initiation and after 6-9 years on therapy. Because HIV infected cells in our participants were rare in a high background of negative cells, we sequenced patient specific U3 and U5 LTR regions for each of the 12 participants to increase the specificity of the ISA

assay. ISA involved the random fragmentation of cellular DNA, ligation of a linker and then amplification using linker specific primers followed by Miseq Illumina sequencing.

ISA detected clones in pre-ART samples of 6 participants who started as early as 2 months of age showing that the latent reservoir begins to expand even before ART is initiated. The recent case of an infant who was treated within hours of birth but eventually had viral rebound after ART interruption further illustrates the early infection of long-lived cells and possible rapid clonal expansions soon after (Luzuriaga et al., 2015; Persaud et al., 2013). We also found an increase in the proportion of integration sites that formed part of clones across the two time points possibly a combination of the decay of shorter lived cells (Ananworanich et al., 2016; Besson et al., 2014) and expansions turned on by antigenic or homeostatic stimuli (Chomont et al., 2010; Wang et al., 2018). Although ISA is high throughput, it is a relatively insensitive assay that detects the most expanded clones in a sample and likely gives a conservative estimate of clonal expansions. Additionally, it has been shown that clones wax and wane over time on ART (Wang et al., 2018). We therefore could not rule out that single integrations were part of clonal populations not detected by the assay.

We were limited in our ability to link integration sites with proviral intactness as the ISA assay provides only a few bases of the proviral genome sequence. We therefore could not show the extent to which clonal expansions maintain the replication competent reservoir. This highlights the need for more efficient methods that can detect rare clones and link integration sites to full length viral genomes to ascertain intactness. It has however been shown elsewhere, that the majority of replication competent proviruses are part of clonal populations (Bui et al., 2017) and a recent mathematical model further estimates that after 1 year on ART, more than 99% of infected cells are part of clonal populations (Reeves et al., 2018).

A recent study in adults who initiated ART during acute infection showed that 98% of proviruses are defective due to stop codons, hypermutations and large internal deletions that arise during reverse transcription (Bruner et al., 2016). In another study, no intact proviruses were detected out of 164 sequences from a cohort of early treated children (Rainwater-Lovett et al., 2017). Chapter 4 of this study aimed to describe the proviral landscape in children from the post-CHER cohort using near full length single genome sequencing (NFL-PAS). Following assay validation, we generated 738 near full length sequences from 9 children and found that intact proviruses were detectable in children who initiated ART after 2.3 months of age and similar to acutely treated adults, 99% were defective. We also detected identical intact sequences in one participant and although we did not obtain integration sites, it is likely that these were part of an expanded clone that persisted over long-term ART. The participants who initiated ART before 2.3 months, had later periods of ART interruption yet no detectable intact proviruses after long-term ART, supporting that the largest proportion of the reservoir is established before ART is initiated (Ananworanich et al., 2015; Buzon et al., 2014a) and short analytical treatment interruptions may not significantly affect reservoir size (Clarridge et al., 2018). Our findings show that intact proviruses in early treated children are rare and point to a need for sensitive

methods that can quantitatively differentiate between intact and defective proviruses similar to what has recently been described (Bruner et al., 2019).

Altogether, this study showed that early therapy and long-term suppression in children leads to limited reservoir size and genetic diversity, factors that are favourable for cure interventions. In well-suppressed individuals, the reservoir appears not to be maintained by ongoing viral replication but rather clonal expansion that begins even before therapy is initiated. Furthermore, although a large proportion of proviral DNA in long-term suppressed children is defective, genetically intact variants are detectable in some patients and most likely form part of expanded clones. Clonal expansion appears to be the main mechanism that drives persistence of the latent reservoir in early treated, long-term suppressed children. This suggests the need for novel approaches that target HIV reservoirs by reducing proliferation of cells that harbour intact and replication competent proviruses in order to reduce the reservoir size. It has yet to be seen whether such approaches could result in SIV/HIV reservoir reduction in pre-clinical studies when used in isolation or combined with other interventions before this can be considered for clinical studies.

Chapter 6

6.1 Bibliography

Achaz, G., Palmer, S., Kearney, M., Maldarelli, F., Mellors, J.W., Coffin, J.M., Wakeley, J., 2004. A robust measure of HIV-1 population turnover within chronically infected individuals. Mol. Biol. Evol. 21, 1902–1912.

Adland, E., Mori, L., Laker, L., Csala, A., Muenchhoff, M., Swordy, A., Mori, M., Matthews, P., Tudor-Williams, G., Jooste, P., Goulder, P., 2018. Recovery of effective HIV-specific CD4 + T-cell activity following antiretroviral therapy in paediatric infection requires sustained suppression of viraemia. Aids 32, 1413–1422.

Agwu, A.L., Fairlie, L., 2013. Review article Antiretroviral treatment , management challenges and outcomes in perinatally HIV-infected adolescents. J. Int. AIDS 16, 1–13.

Ananworanich, J., Chomont, N., Eller, L.A., Kroon, E., Tovanabutra, S., Bose, M., Nau, M., Fletcher, J.L.K., Tipsuk, S., Vandergeeten, C., O'Connell, R.J., Pinyakorn, S., Michael, N., Phanuphak, N., Robb, M.L., 2016. HIV DNA Set Point is Rapidly Established in Acute HIV Infection and Dramatically Reduced by Early ART. EBioMedicine 11, 68–72.

Ananworanich, J., Dube, K., Chomont, N., 2015. How does the timing of antiretroviral therapy initiation in acute infection affect HIV reservoirs? Curr. Opin. Hiv Aids 10, 18–28.

Ananworanich, J., Puthanakit, T., Suntarattiwong, P., Chokephaibulkit, K., Kerr, S.J., 2014. Reduced markers of HIV persistence and restricted HIV-specific immune responses after early antiretroviral therapy in children. AIDS 28, 1015–1020.

Anderson, J.A., Archin, N.M., Ince, W., Parker, D., Wiegand, A., Coffin, J.M., Kuruc, J., Eron, J., Swanstrom, R., Margolis, D.M., 2011. Clonal sequences recovered from plasma from patients with residual HIV-1 viremia and on intensified antiretroviral therapy are identical to replicating viral RNAs recovered from circulating resting CD4+ T cells. J. Virol. 85, 5220–3.

Archin, N., Vaidya, N.K., Kuruc, J.D., Liberty, A.L., Wiegand, A., Kearney, M.F., Cohen, M.S., Coffin, J.M., Bosch, R.J., Gay, C.L., Eron, J.J., Margolis, D.M., Perelson, A.S., 2012. Immediate antiviral therapy appears to restrict resting CD4+ cell HIV-1 infection without accelerating the decay of latent infection. Proc. Natl. Acad. Sci. U. S. A. 109, 9523–8.

Archin, N.M., Kirchherr, J.L., Sung, J.A.M., Clutton, G., Sholtis, K., Xu, Y., Allard, B., Stuelke, E., Kashuba, A.D., Kuruc, J.D., Eron, J., Gay, C.L., Goonetilleke, N., Margolis, D.M., 2017. Interval dosing with the HDAC inhibitor vorinostat effectively reverses HIV latency. J. Clin. Invest. 127, 3126–3135.

Archin, N.M., Liberty, A.L., Kashuba, A.D., Choudhary, S.K., Kuruc, J.D., Crooks, A.M., 2012. Administration of vorinostat disrupts HIV-1 latency in patients on antiretroviral therapy. Nature 487, 482–485.

Bailey, J.R., Sedaghat, A.R., Kieffer, T., Brennan, T., Lee, P.K., Wind-Rotolo, M., Haggerty, C.M., Kamireddi, A.R., Liu, Y., Lee, J., Persaud, D., Gallant, J.E., Cofrancesco, J., Quinn, T.C., Wilke, C.O., Ray, S.C., Siliciano, J.D., Nettles, R.E., Siliciano, R.F., 2006. Residual human immunodeficiency virus type 1 viremia in some patients on antiretroviral therapy is dominated by a small number of invariant clones rarely found in circulating CD4+ T cells. J. Virol. 80, 6441–57.

Baldauf, H.-M., Pan, X., Erikson, E., Schmidt, S., Daddacha, W., Burggraf, M., Schenkova, K., Ambiel, I., Wabnitz, G., Gramber, T., Panitz, S., Flory, E., Landau, N., Sertel, S., Rutsch, F., Lasitschka, F., Kim, B., Konig, R., Fackler, O., Keppler, O., 2012. SAMHD1 restricts HIV-1 infection in resting CD4+ T cells. Nat. Med. 18, 1–18.

Bangsberg, D.R., Moss, A.R., Deeks, S.G., 2004. Paradoxes of adherence and drug resistance to HIV antiretroviral therapy. J. Antimicrob. Chemother. 53, 696–699.

Barouch, D.H., Whitney, J.B., Moldt, B., Klein, F., Oliveira, T.Y., Lui, J., Stephenson, K., Chang, H.-W., Shekhar, K., Gupta, S., Nkolola, J., Seaman, M.S., Smith, K., Borducchi, E.N., Cabral, C., Smith, J.Y., Blackmore, S., Sanisetty, S., Perry, J., Beck, M., Lewis, M.G., Rinaldi, W., Chakraborty, A., 2013. Therapeutic Efficacy of Potent Neutralizing HIV-1-Specific Monoclonal Antibodies in SHIV-Infected Rhesus Monkeys. Nature 503, 224–228.

Barré-Sinoussi, F., Ross, A.L., Delfraissy, J.F., 2013. Past, present and future: 30 years of HIV research. Nat. Rev. Microbiol. 11, 877–883.

Barton, K., Hiener, B., Winckelmann, A., Rasmussen, T.A., Shao, W., Byth, K., Lanfear, R., Solomon, A., Mcmahon, J., Harrington, S., Buzon, M., Lichterfeld, M., Denton, P.W., Olesen, R., Østergaard, L., Tolstrup, M., Lewin, S.R., Søgaard, O.S., Palmer, S., 2016. Broad activation of latent HIV-1 in vivo. Nat. Commun. 7, 1–8.

Battula, N., Loeb, L.A., 1977. On the Fidelity of DNA Replication. J. Biol. Chem. 3605–3610.

Baxter, A.E., Niessl, J., Fromentin, R., Richard, J., Porichis, F., Charlebois, R., Massanella, M., Brassard, N., Alsahafi, N., Delgado, G.G., Routy, J.P., Walker, B.D., Finzi, A., Chomont, N., Kaufmann, D.E., 2016. Single-Cell Characterization of Viral Translation-Competent Reservoirs in HIV-Infected Individuals. Cell Host Microbe 20, 368–380.

Baxter, A.E., Russell, R.A., Duncan, C.J.A., Moore, M.D., Willberg, C.B., Pablos, J.L., Finzi, A., Kaufmann, D.E., Ochsenbauer, C., Kappes, J.C., Groot, F., Sattentau, Q.J., 2014. Macrophage infection via selective capture of HIV-1-infected CD4+T cells. Cell Host Microbe 16, 711–721.

Bebenek, K., Abbotts, J., Roberts, J.D., Wilson, S.H., Kunkel, T.A., 1989. Specificity and mechanism of error-prone replication by human immunodeficiency virus-1 reverse transcriptase. J. Biol. Chem. 264, 16948–16956.

Besson, G.J., Lalama, C.M., Bosch, R.J., Gandhi, R.T., Bedison, M.A., Aga, E., Riddler, S.A., Mcmahon, D.K., Hong, F., Mellors, J.W., 2014. HIV-1 DNA Decay Dynamics in Blood During More Than a Decade of Suppressive Antiretroviral Therapy. Clin. Infect. Dis. 59, 1312–1321.

Bikaako-Kajura, W., Luyirika, E., Purcell, D.W., Downing, J., Kaharuza, F., Mermin, J., Malamba, S., Bunnell, R., 2006. Disclosure of HIV Status and Adherence to Daily Drug Regimens Among HIV-infected Children in Uganda. AIDS Behav. 10, S85–S93.

Bishop, K.N., Holmes, R.K., Sheehy, A.M., Davidson, N.O., Cho, S.-J., Malim, M.H., 2004. Cytidine Deamination of Retroviral DNA by Diverse APOBEC Proteins. Curr. Biol. 14, 1392–1396.

Bitnun, A., Samson, L., Chun, T.W., Kakkar, F., Brophy, J., Murray, D., Justement, S., Soudeyns, H., Ostrowski, M., Mujib, S., Harrigan, P.R., Kim, J., Sandstrom, P., Read, S.E., 2014. Early initiation of combination antiretroviral therapy in HIV-1 Infected newborns can achieve sustained virologic suppression with low frequency of CD4+T cells carrying HIV in peripheral blood. Clin. Infect. Dis. 59, 1012–1019.

Blankson, J.N., Finzi, D., Pierson, T.C., Sabundayo, B.P., Chadwick, K., Margolick, J.B., Quinn, T.C., Siliciano, R.F., 2000. Biphasic Decay of Latently Infected CD4 + T Cells in Acute Human Immunodeficiency Virus Type 1 Infection. J. Infect. Dis. 182, 1636–1642.

Blazkova, J., Trejbalova, K., Gondois-Rey, F., Halfon, P., Philibert, P., Guiguen, A., Verdin, E., Olive, D., Van Lint, C., Hejnar, J., Hirsch, I., 2009. CpG methylation controls reactivation of HIV from latency. PLoS Pathog. 5, e1000554.

Borducchi, E.N., Cabral, C., Stephenson, K., Liu, J., Abbink, P., Ng'ang'a, D., Nkolola, J., Brinkman, A., Peter, L.E., Lee, B., Jimenes, J., Mondesir, J., Mojta, S., Chandrashekar, A., Molloy, K., Alter, G., Gerold, J., 2016. Ad26/MVA Therapeutic Vaccination with TLR7 Stimulation in SIV-Infected Rhesus Monkeys. Nature 540, 284–287.

Borges, Á.H., Hoy, J., Florence, E., Sedlacek, D., Stellbrink, H., Uzdaviniene, V., Tomazic, J., 2017. Antiretrovirals , Fractures , and Osteonecrosis in a Large International HIV Cohort. Clin. Infect. Dis. 64, 1413–1421.

Boritz, E.A., Darko, S., Swaszek, L., Wolf, G., Wells, D., Wu, X., Henry, A.R., Laboune, F., Hu, J., Ambrozak, D., Hughes, M.S., Hoh, R., Casazza, J.P., Vostal, A., Bunis, D., Nganou-Makamdop, K., Lee, J.S., Migueles, S.A., Koup, R.A., Connors, M., Moir, S., Schacker, T., Maldarelli, F., Hughes, S.H., Deeks, S.G., Douek, D.C., 2016. Multiple Origins of Virus Persistence during Natural Control of HIV Infection. Cell 166, 1004–1015.

Bosque, A., Famiglietti, M., Weyrich, A.S., Goulston, C., Planelles, V., 2011. Homeostatic proliferation fails to efficiently reactivate HIV-1 latently infected central memory CD4+ T cells. PLoS Pathog. 7, e1002288.

Brady, M.T., Oleske, J.M., Williams, P.L., Elgie, C., Mofenson, L.M., Dankner, W.M., Van Dyke, R.B., Team, P.A.C.T.G., 2010. Declines in Mortality Rates and Changes in Causes of Death in HIV-1-Infected Children during the HAART Era. J Acquir Immune Defic Syndr. 53, 86–94.

Brenchley, J.M., Schacker, T.W., Ruff, L., Price, D.A., Taylor, J., Beilman, G., Nguyen, P., Khoruts, A., Larson, M., Haase, A., Douek, D.C., 2004. CD4 + T Cell Depletion during all Stages of HIV Disease Occurs Predominantly in the Gastrointestinal Tract. J. Exp. Med. 200, 749–759.

Brooks, D.G., Kitchen, S.G., Kitchen, C.M.R., Scripture-Adams, D.D., Zack, J.A., 2001. Generation of HIV latency during thymopoiesis. Nat. Med. 7, 459–464.

Bruner, K.M., Murray, A.J., Pollack, R.A., Soliman, M.G., Laskey, S.B., Capoferri, A.A., Lai, J., Strain, M.C., Lada, S.M., Hoh, R., Ho, Y.C., Richman, D.D., Deeks, S.G., Siliciano, J.D., Siliciano, R.F., 2016. Defective proviruses rapidly accumulate during acute HIV-1 infection. Nat. Med. 22, 1043–1049.

Bruner, K.M., Wang, Z., Simonetti, F.R., Bender, A., Kwon, K.J., Sengupta, S., Fray, E., Beg, S.A., Antar, A., Jenike, K., Bertagnolli, L., Capoferri, A.A., Kufera, J., Timmons, A., Nobles, C.L., Nikolas, J., Ho, Y.-C., Zhang, H., Margolick, J.B., Blankson, J.N., Deeks, S.G., Bushman, F.D., Siliciano, J.D., Laird, G.M., Siliciano, R.F., 2019. A quantitative approach for measuring the reservoir of latent HIV-1 proviruses. Nature 566, 120–125.

Bui, J.K., Sobolewski, M.D., Keele, B.F., Spindler, J., Musick, A., Wiegand, A., Luke, B.T., Shao, W., Hughes, S.H., Coffin, J.M., Kearney, M.F., Mellors, J.W., 2017. Proviruses with identical sequences comprise a large fraction of the replication-competent HIV reservoir. PLoS Pathog. 13, 1–18.

Bull, M.E., Learn, G.H., McElhone, S., Hitti, J., Lockhart, D., Holte, S., Dragavon, J., Coombs, R.W., Mullins, J.I., Frenkel, L.M., 2009. Monotypic human immunodeficiency virus type 1 genotypes across the uterine cervix and in blood suggest proliferation of cells with provirus. J. Virol. 83, 6020–8.

Bullen, C.K., Laird, G.M., Durand, C.M., Siliciano, J.D., Siliciano, R.F., 2014. Novel ex vivo approaches distinguish effective and ineffective single agents for reversing HIV-1 latency in vivo. Nat. Med. 20, 425–429.

Burton, G.F., Keele, B.F., Estes, J.D., Thacker, T.C., Gartner, S., 2002. Follicular dendritic cell contributions to HIV pathogenesis. Semin. Immunol. 14, 275–284.

Busby, E., Whale, A.S., Bridget Ferns, R., Grant, P.R., Morley, G., Campbell, J., Foy, C.A., Nastouli, E., Huggett, J.F., Garson, J.A., 2017. Instability of 8E5 calibration standard revealed by digital PCR risks inaccurate quantification of HIV DNA in clinical samples by qPCR. Sci. Rep. 7, 1–7.

Butler, K.M., Gavin, P., Coughlan, S., Rochford, A., Mc Donagh, S., Cunningham, O., Poulsom, H., Watters, S.A., Klein, N., 2015. Rapid viral rebound after 4 years of suppressive therapy in a seronegative HIV-1 infected infant treated from birth. Pediatr. Infect. Dis. J. 34, e48–e51.

Buzon, M, Martin-gayo, E., Pereyra, F., Ouyang, Z., Sun, H., Li, J.Z., Piovoso, M., Shaw, A., Dalmau, J., Zangger, N., Martinez-picado, J., Zurakowski, R., Yu, X.G., Telenti, A., Walker, B.D., Rosenberg, E.S., 2014. Long-Term Antiretroviral Treatment Initiated at Primary HIV-1 Infection Affects the Size , Composition , and Decay Kinetics of the Reservoir of HIV-1-Infected CD4 T Cells. J. Virol. 88, 10056–10065.

Buzon, M., Sun, H., Li, C., Shaw, A., Seiss, K., Ouyang, Z., Martin-Gayo, E., Leng, J., Henrich, T., Li, J., Pereyra, F., Zurakowski, R., Walker, B., Rosenberg, E., Yu, X., Lichterfeld, M., 2014. HIV-1 persistence in CD4+ T cells with stem cell-like properties. Nat. Med. 20, 139–142.

Buzon, M.J., Massanella, M., Llibre, J., Esteve, A., Dahl, V., Puertas, M.C., Gatell, J., Domingo, P., Paredes, R., Sharkey, M., Palmer, S.E., Stevenson, M., Clotet, B., Blanco, J., Martinez-Picado, J., 2010. HIV-1 replication and immune dynamics are affected by raltegravir intensification of HAART-suppressed subjects. Nat. Med. 16, 460–465.

Bygrave, H., Mtangirwa, J., Ncube, K., Ford, N., Kranzer, K., 2012. Antiretroviral Therapy Outcomes among Adolescents and Youth in Rural Zimbabwe. PLoS One 7, e52856.

Cannon, P., June, C., 2011. CCR5 knockout strategies. Curr. Opin. HIV AIDS 6, 74–79.

Caskey, M., Klein, F., Lorenzi, J.C.C., Seaman, M.S., West, A.P., Buckley, N., Kremer, G., Nogueira, L., Braunschweig, M., Scheid, J.F., Horwitz, J.A., Shimeliovich, I., Ben Avraham-Shulman, S., Witmer-Pack, M., Platten, M., Lehmann, C., Burke, L.A., Hawthorne, T., Gorelick, R.J., Walker, B.D., Keler, T., Gulick, R.M., Fätkenheuer, G., Schlesinger, S.J., Nussenzweig, M.C., 2015. 3BNC117 a Broadly Neutralizing Antibody Suppresses Viremia in HIV-1-Infected Humans. Nature 522, 487–491.

Cassol, E., Alfano, M., Biswas, P., Poli, G., 2006. Monocyte-derived macrophages and myeloid cell lines as targets of HIV-1 replication and persistence. J. Leukoc. Biol. 80, 1018–1030.

Castilla, J., Del Romero, J., Hernando, V., Marincovich, B., García, S., Rodríguez, C., 2005. Effectiveness of highly active antiretroviral therapy in reducing heterosexual transmission of HIV. J. Acquir. Immune Defic. Syndr. 40, 96–101.

Cesana, D., Sio, F.R.S. De, Rudilosso, L., Gallina, P., Calabria, A., Beretta, S., Merelli, I., Bruzzesi, E., Passerini, L., Nozza, S., Vicenzi, E., Poli, G., Gregori, S., Tambussi, G., Montini, E., 2017. HIV-1-mediated insertional activation of STAT5B and BACH2 trigger viral reservoir in T regulatory cells. Nat. Commun. 8, 1–11.

Chan, D.C., Kim, P.S., 1998. HIV Entry and Its Inhibition. Cell 93, 681–684.

Chiang, K., Sung, T.-L., Rice, A.P., 2012. Regulation of Cyclin T1 and HIV-1 Replication by MicroRNAs in Resting CD4+ T Lymphocytes. J. Virol. 86, 3244–3252.

Chomont, N., El-far, M., Ancuta, P., Trautmann, L., Procopio, F.A., Yassine-diab, B., Boucher, G., Boulassel, R., Ghattas, G., Brenchley, J.M., Schacker, T.W., Hill, B.J., Douek, D.C., Routy, J., Haddad, E.K., 2010. HIV reservoir size and persistence are driven by T cell survival and homeostatic proliferation. Nat. Med. 15, 893–900.

Chun, T., Carruth, L.M., Finzi, D., Shen, X., DiGiuseppe, J., Taylor, H., Hermankova, M., Chadwick, K., Margolick, J.B., Quinn, T.C., Kuo, Y.-H., Brookmeyer, R., Zeiger, M., Barditch-Crovo, P., Siliciano, R.F., 1997a. Quantification of latent tissue reservoirs and total body viral loads in HIV-1 infection. Nature 387, 183–188.

Chun, T., Engel, D., Berrey, M., Shea, T., Corey, L., Fauci, A.S., 1998. Early establishment of a pool of latently infected, resting CD4 T cells during primary HIV-1 infection. Proc. Natl. Acad. Sci. 95, 8869–8873.

Chun, T., Justement, J.S., Moir, S., Hallahan, C.W., Maenza, J., Mullins, J.I., Collier, A.C., Corey, L., Fauci, A.S., 2007. Decay of the HIV Reservoir in Patients Receiving Antiretroviral Therapy for Extended Periods : Implications for Eradication of Virus. J. Infect. Dis. 195, 1762–1764.

Chun, T., Nickle, D.C., Justement, S., Large, D., Semerjian, A., Curlin, M.E., O'Shea, A., Hallahan, C.W., Daucher, M., Ward, D.J., Moir, S., Mullins, J.I., Kovacs, C., Fauci, A.S., 2005. HIV-infected individuals receiving effective antiviral therapy for extended periods of time continually replenish their viral reservoir. J. Clin. Invest. 115, 3250–3255.

Chun, T., Stuyver, L., Mizell, S.B., Ehler, L.A., Mican, J.A.M., Baseler, M., Lloyd, A.L., Nowak, M.A., Fauci, A.S., 1997b. Presence of an inducible HIV-1 latent reservoir during highly active antiretroviral therapy. Proc. Natl. Acad. Sci. 94, 13193–13197.

Churchill, M.J., Gorry, P.R., Cowley, D., Lal, L., Sonza, S., Purcell, D.F.J., Thompson, K.A., Gabuzda, D., McArthur, J.C., Pardo, C.A., Wesselingh, S.L., 2006. Use of laser capture microdissection to detect integrated HIV-1 DNA in macrophages and astrocytes from autopsy brain tissues. J. Neurovirol. 12, 146–152.

Cillo, A.R., Sobolewski, M.D., Bosch, R.J., Fyne, E., Piatak, M., Coffin, J.M., Mellors, J.W., 2014a. Quantification of HIV-1 latency reversal in resting CD4+ T cells from patients on suppressive antiretroviral therapy. Proc. Natl. Acad. Sci. 111, 7078–7083.

Cillo, A.R., Vagratian, D., Bedison, M.A., Anderson, E.M., Kearney, M.F., Fyne, E., Koontz, D., Coffin, J.M., Piatak, M., Mellors, J.W., 2014b. Improved single-copy assays for quantification of persistent HIV-1 viremia in patients on suppressive antiretroviral therapy. J. Clin. Microbiol. 52, 3944–3951.

Ciuffi, A., Bushman, F.D., 2006. Retroviral DNA integration: HIV and the role of LEDGF/p75. Trends Genet. 22, 388–395.

Clarridge, K.E., Blazkova, J., Einkauf, K., Petrone, M., Refsland, E.W., Justement, J.S., Shi, V., Huiting, E.D., Seamon, C.A., Lee, G.Q., Yu, X.G., Moir, S., Sneller, M.C., Lichterfeld, M., Chun, T.W., 2018. Effect of analytical treatment interruption and reinitiation of antiretroviral therapy on HIV reservoirs and immunologic parameters in infected individuals. PLoS Pathog. 14, 1–16.

Coffin, J., Swanstrom, R., 2013. HIV Pathogenesis : Dynamics and Genetics of Viral Populations and Infected Cells. Cold Spring Harb. Perspect. Med. 3, a012526.

Cohn, L.B., Silva, I.T., Jankovic, M., Nussenzweig, M.C., Cohn, L.B., Silva, I.T., Oliveira, T.Y., Rosales, R.A., Parrish, E.H., Learn, G.H., Hahn, B.H., Czartoski, J.L., Mcelrath, M.J., Lehmann, C., Klein, F., Caskey, M., Walker, B.D., Siliciano, J.D., Siliciano, R.F., Jankovic, M., Nussenzweig, M.C., 2015. HIV-1 Integration Landscape during Latent and Active Infection. Cell 160, 420–432.

Coleman, C.M., Wu, L., 2009. HIV interactions with monocytes and dendritic cells: Viral latency and reservoirs. Retrovirology 6, 1–12.

Coombs, R.W., Reichelderfer, P.S., Landay, A.L., 2003. Recent observations on HIV type-1 infection in the genital tract of men and women. Aids 17, 455–480.

Corneli, A., Vaz, L., Dulyx, J., Omba, S., Rennie, S., Behets, F., 2009. The role of disclosure in relation to assent to participate in HIV-related research among HIV-infected youth : a formative study. J. Int. AIDS Soc. 12, 1–10.

Cory, T.J., Schacker, T.W., Stevenson, M., Fletcher, C. V., 2013. Overcoming pharmacologic sanctuaries. Curr. Opin. HIV AIDS 8, 190–195.

Costiniuk, C.T., Salahuddin, S., Farnos, O., Olivenstein, R., Pagliuzza, A., Orlova, M., Schurr, E., De Castro, C., Bourbeau, J., Routy, J.P., Ancuta, P., Chomont, N., Jenabian, M.A., 2018. HIV persistence in mucosal CD4+ T cells within the lungs of adults receiving long-term suppressive antiretroviral therapy. AIDS 32, 2279–2289.

Cotton, M.F., Violari, A., Otwombe, K., Panchia, R., Dobbels, E., Rabie, H., Josipovic, D., Liberty, A., Lazarus, E., Innes, S., van Rensburg, A.J., Pelser, W., Truter, H., Madhi, S.A., Handelsman, E., Jean-Philippe, P., McIntyre, J.A., Gibb, D.M., Babiker, A.G., 2013. Early time-limited antiretroviral therapy versus deferred therapy in South African infants infected with HIV: results from the children with HIV early antiretroviral (CHER) randomised trial. Lancet (London, England) 382, 1555–63.

Coull, J.J., Romerio, F., Sun, J., Volker, J.L., Galvin, K.M., Davie, J.R., Shi, Y., Hansen, U., Margolis, D.M., 2000. The Human Factors YY1 and LSF Repress the Human Immunodeficiency Virus Type 1 Long Terminal Repeat via Recruitment of Histone Deacetylase 1 The Human Factors YY1 and LSF Repress the Human Immunodeficiency Virus Type 1 Long Terminal Repeat via Recruitment. J. Virol. 74, 6790–6799.

Craigie, R., Bushman, F.D., 2012. HIV DNA integration. Cold Spring Harb. Perspect. Med. 2, 1–18.

Cribbs, S.K., Lennox, J., Caliendo, A.M., Brown, L.A., Guidot, D.M., 2015. Healthy HIV-1-Infected Individuals on Highly Active Antiretroviral Therapy Harbor HIV-1 in Their Alveolar Macrophages. AIDS Res. Hum. Retroviruses 31, 64–70.

Crooks, A.M., Bateson, R., Cope, A.B., Dahl, N.P., Griggs, M.K., Kuruc, J.A.D., Gay, C.L., Eron, J.J., Margolis, D.M., Bosch, R.J., Archin, N.M., 2015. Precise quantitation of the latent HIV-1 reservoir: Implications for eradication strategies. J. Infect. Dis. 212, 1361–1365.

Crowe, S., Zhu, T., Muller, W., 2003. The contribution of monocyte infection and trafficking to viral persistence, and maintenance of the viral reservoir in HIV infection. J. Leukoc. Biol. 74, 635–641.

Cummins, N.W., Sainski, A.M., Dai, H., Natesampillai, S., Pang, Y.-P., Bren, G.D., de Araujo Correia, M.C.M., Sampath, R., Rizza, S.A., O'Brien, D., Yao, J.D., Kaufmann, S.H., Badley, A.D., 2016. Prime, Shock, and Kill: Priming CD4 T Cells from HIV Patients with a BCL-2 Antagonist before HIV Reactivation Reduces HIV Reservoir Size. J. Virol. 90, 4032–4048.

Davey, R.T., Bhat, N., Yoder, C., Chun, T., Metcalf, J.A., Dewar, R., Natarajan, V., Lempicki, R.A., Adelsberger, J.W., Miller, K.D., Kovacs, J.A., Polis, M.A., Walker, R.E., Falloon, J., Masur, H., Gee, D., Baseler, M., Dimitrov, D.S., Fauci, A.S., Lane, H.C., 1999. HIV-1 and T cell dynamics after interruption of highly active antiretroviral therapy (HAART) in patients with a history of sustained viral suppression. Proc. Natl. Acad. Sci. 96, 15109–15114.

Davies, M., Boulle, A., Fakir, T., Nuttall, J., Eley, B., 2008. Adherence to antiretroviral therapy in young children in Cape Town , South Africa , measured by medication return and caregiver self-report : a prospective cohort study. BMC Pediatr. 8, 1–12.

De Oliveira, M.F., Gianella, S., Letendre, S., Scheffler, K., Pond, S.L.K., Smith, D.M., Strain, M., Ellis, R.J., 2015. Comparative analysis of cell-associated HIV DNA levels in cerebrospinal fluid and peripheral blood by droplet digital PCR. PLoS One 10, e0139510.

De Rossi, A., Walker, A.S., Klein, N., De Forni, D., King, D., Gibb, D.M., 2002. Increased thymic output after initiation of antiretroviral therapy in human immunodeficiency virus type 1-infected children in the Paediatric European Network for Treatment of AIDS (PENTA) 5 Trial. J. Infect. Dis. 186, 312–20.

Debyser, Z., Vansant, G., Bruggemans, A., Janssens, J., Christ, F., 2018. Insight in HIV Integration Site Selection Provides a Block-and-Lock Strategy for a Functional Cure of HIV Infection. Viruses 11, 1–12.

Deleage, C., Turkbey, B., Estes, J.D., 2016a. IMAGING LYMPHOID TISSUES IN NONHUMAN PRIMATES TO UNDERSTAND SIV PATHOGENESIS AND PERSISTENCE. Curr. Opin. Virol. 19, 77–84.

Deleage, C., Wietgrefe, S.W., Del Prete, G., Morock, D., Pei Hao, X., Piatak Jr, M., Bess, J., Anderson, J., Perkey, K., Reilly, C., Mccune, J.M., Haase, A., Lifson, J., Schacker, T.W., Estes, J.D., 2016b. Defining HIV and SIV Reservoirs in Lymphoid Tissues. Pathog. Immun. 1, 68–106.

Deng, K., Pertea, M., Rongvaux, A., Wang, L., Durand, C.M., Ghiaur, G., Lai, J., Mchugh, H.L., Hao, H., Zhang, H., Joseph, B., Gurer, C., Murphy, A.J., Valenzuela, D.M., George, D., Flavell, R.A., Shan, L., Siliciano, R.F., 2015. Broad CTL response is required to clear latent HIV-1 due to dominance of escape mutations. Nature 517, 381–385.

Department of Health Republic of South Africa, 2013. Revised Anti-Retroviral Treatment Guideline Update For Frontline Clinical Health Professionals.

Diem, K., Nickle, D.C., Motoshige, A., Fox, A., Ross, S., Mullins, J.I., Corey, L., Coombs, R.W., Krieger, J.N., 2008. Male Genital Tract Compartmentalization of Human Immunodeficiency Virus Type 1 (HIV). AIDS Res. Hum. Retroviruses 24, 561–571.

Dinoso, J.B., Kim, S.Y., Wiegand, A.M., Palmer, S.E., Gange, S.J., Cranmer, L., Shea, A.O., Callender, M., 2009. Treatment intensification does not reduce residual HIV-1 viremia in patients on highly active antiretroviral therapy. Proc. Natl. Acad. Sci. U. S. A. 106, 9403–9408.

Douek, D.C., 2018. HIV Infection : Advances Toward a Cure. HIV cure 25, 121–125.

Douek, D.C., Brenchley, J.M., Betts, M.R., Ambrozak, D.R., Hill, B.J., Okamoto, Y., Casazza, J.P., Kuruppu, J., Kunstman, K., Wolinsky, S., Grossman, Z., Dybul, M., Oxenius, A., Price, D.A., Connors, M., Koup, R.A., 2002. HIV preferentially infects HIV-specific CD4+ T cells. Nature 417, 2–5.

Ebina, H., Kanemura, Y., Misawa, N., Sakuma, T., Kobayashi, T., Yamamoto, T., Koyanagi, Y., 2015. A high excision potential of TALENs for integrated DNA of HIV-based lentiviral vector. PLoS One 10, e0120047.

Ebina, H., Misawa, N., Kanemura, Y., Koyanagi, Y., 2013. Harnessing the CRISPR/Cas9 system to disrupt latent HIV-1 provirus. Sci. Rep. 3, 1–7.

Einkauf, K., Lee, G.Q., Gao, C., Sharaf, R., Sun, X., Hua, S., Chen, S., Jiang, C., Lian, X., Chowdhury, F.Z., Rosenberg, E.S., Chun, T.-W., Li, J.Z., Yu, X.G., Lichterfeld, M., 2019. Intact HIV-1 proviruses accumulate at distinct chromosomal positions during prolonged antiretroviral therapy. J. Clin. Invest. 129, 988–998.

Elliott, J.H., McMahon, J.H., Chang, C.C., Lee, S.A., Hartogensis, W., Bumpus, N., Savic, R., Roney, J., Hoh, R., Solomon, A., Piatak, M., Gorelick, R.J., Lifson, J., Bacchetti, P., Deeks, S.G., Lewin, S.R., 2015. Short-term Disulfiram to Reverse Latent HIV Infection: A Phase 2 Dose Escalation Study. lancet. HIV 2, e520–e529.

Elliott, J.H., Wightman, F., Solomon, A., Ghneim, K., Ahlers, J., Cameron, M.J., Smith, M.Z., Spelman, T., McMahon, J., Velayudham, P., Brown, G., Roney, J., Watson, J., Prince, M.H., Hoy, J.F., Chomont, N., Fromentin, R., Procopio, F.A., Zeidan, J., Palmer, S., Odevall, L., Johnstone, R.W., Martin, B.P., Sinclair, E., Deeks, S.G., Hazuda, D.J., Cameron, P.U., Sékaly, R.P., Lewin, S.R., 2014. Activation of HIV Transcription with Short-Course Vorinostat in HIV-Infected Patients on Suppressive Antiretroviral Therapy. PLoS Pathog. 10, e1004473.

Eriksson, S., Graf, E.H., Dahl, V., Strain, M.C., Yukl, S. a, Lysenko, E.S., Bosch, R.J., Lai, J., Chioma, S., Emad, F., Abdel-Mohsen, M., Hoh, R., Hecht, F., Hunt, P., Somsouk, M., Wong, J., Johnston, R., Siliciano, R.F., Richman, D.D., O'Doherty, U., Palmer, S., Deeks, S.G., Siliciano, J.D., 2013. Comparative analysis of measures of viral reservoirs in HIV-1 eradication studies. PLoS Pathog. 9, e1003174.

Eugenin, E., Berman, J.W., 2013. Cytochrome c dysregulation induced by HIV infection of astrocytes results in bystander apoptosis of uninfected astrocytes by an IP3 and calcium-dependent mechanism. J. Neurochem. 127, 644–651.

Evans, V.A., Van Der Sluis, R.M., Solomon, A., Dantanarayana, A., McNeil, C., Garsia, R., Palmer, S., Fromentin, R., Chomont, N., Sékaly, R.P., Cameron, P.U., Lewin, S.R., 2018. Programmed cell death-1 contributes to the establishment and maintenance of HIV-1 latency. AIDS 32, 1491–1497.

Evering, T.H., Mehandru, S., Racz, P., Tenner-Racz, K., Poles, M. a, Figueroa, A., Mohri, H., Markowitz, M., 2012. Absence of HIV-1 evolution in the gut-associated lymphoid tissue from patients on combination antiviral therapy initiated during primary infection. PLoS Pathog. 8, e1002506.

Fernandez-Fernandez, B., Montoya-Ferrer, A., Sanz, A.B., Sanchez-Nino, M.D., Izquiero, M.C., Poveda, J., Sainz-Prestel, V., Ortiz-Martin, N., Parra-Rodriquez, A., Selgas, R., Ruiz-Ortega, M., Egido, J., Ortiz, A., 2011. Tenofovir Nephrotoxicity: 2011 Update Beatriz. AIDS Res. Treat. 2011, 1–11.

Fetzer, B.C., Mupenda, B., Lusiama, J., Kitetele, F., Golin, C., Behets, F., 2011. Barriers to and Facilitators of Adherence to Pediatric Antiretroviral Therapy in a Sub-Saharan Setting : Insights from a Qualitative Study. AIDS Patient Care STDS 25, 611–621.

Finzi, D., Blankson, J., Siliciano, J.D., Margolick, J.B., Chadwick, K., Pierson, T., Smith, K., Lisziewicz, J., Lori, F., Flexner, C., Quinn, T.C., Chaisson, R.E., Rosenberg, E., Walker, B., Gange, S., Gallant, J., Siliciano, R.F., 1999. Latent infection of CD4+T cells provides a mechanism for lifelong persistence of HIV-1, even in patients on effective combination therapy. Nat. Med. 5, 512–517.

Fischer, M., Joos, B., Niederöst, B., Kaiser, P., Hafner, R., von Wyl, V., Ackermann, M., Weber, R., Günthard, H.F., 2008. Biphasic decay kinetics suggest progressive slowing in turnover of latently HIV-1 infected cells during antiretroviral therapy. Retrovirology 5, 1–16.

Fletcher, C. V., Staskus, K., Wietgrefe, S.W., Rothenberger, M., Reilly, C., Chipman, J.G., Beilman, G.J., Khoruts, A., Thorkelson, A., Schmidt, T.E., Anderson, J., Perkey, K., Stevenson, M., Perelson, A.S., Douek, D.C., Haase, A.T., Schacker, T.W., 2014. Persistent HIV-1 replication is associated with lower antiretroviral drug concentrations in lymphatic tissues. Proc. Natl. Acad. Sci. 111, 2307–2312.

Foster, C., Pace, M., Kaye, S., Hopkins, E., Jones, M., Robinson, N., Mant, C., 2017. Early antiretroviral therapy reduces HIV DNA following perinatal HIV infection. AIDS 31, 1847–1851.

Frange, P., Faye, A., Avettand-Fenoël, V., Bellaton, E., Descamps, D., Angin, M., David, A., Caillat-Zucman, S., Peytavin, G., Dollfus, C., Le Chenadec, J., Warszawski, J., Rouzioux, C., Sáez-Cirión, A., 2016. HIV-1 virological remission lasting more than 12 years after interruption of early antiretroviral therapy in a perinatally infected teenager enrolled in the French ANRS EPF-CO10 paediatric cohort: A case report.

Lancet HIV 3, e49–e54.

Frankel, A.D., 1992. Activation of HIV transcription by Tat. Curr. Opin. Genet. Dev. 2, 293–298.

Freed, E., 1998. HIV-1 Gag Proteins: Diverse Functions in the Virus Life Cycle. Virology 251, 1–15.

Fromentin, R., Bakeman, W., Lawani, M.B., Khoury, G., Hartogensis, W., DaFonseca, S., Killian, M., Epling, L., Hoh, R., Sinclair, E., Hecht, F.M., Bacchetti, P., Deeks, S.G., Lewin, S.R., Sékaly, R.P., Chomont, N., 2016. CD4+ T Cells Expressing PD-1, TIGIT and LAG-3 Contribute to HIV Persistence during ART. PLoS Pathog. 12, 1–19.

Fukazawa, Y., Lum, R., Okoye, A.A., Park, H., Matsuda, K., Bae, J.Y., Hagen, S.I., Shoemaker, R., Deleage, C., Lucero, C., Morcock, D., Swanson, T., Legasse, A.W., Axthelm, M.K., Hesselgesser, J., Geleziunas, R., Hirsch, V.M., Edlefsen, P.T., Piatak, M., Estes, J.D., Lifson, J.D., Picker, L.J., 2015. A B cell sanctuary permits productive persistent infection in SIV elite controllers. Nat. Med. 21, 132–139.

Gandhi, R.T., Coombs, R.W., Chan, E.S., Bosch, R.J., Zheng, L., Margolis, D.M., Read, S., Kallungal, B., Chang, M., Goecker, E.A., Wiegand, A., Kearney, M., Jacobson, J.M., D'Aquila, R., Lederman, M.M., Mellors, J.W., Eron, J.J., 2012. No effect of raltegravir intensification on viral replication markers in the blood of HIV-1-infected patients receiving antiretroviral therapy. J. Acquir. Immune Defic. Syndr. 59, 229–235.

García, F., Vidal, C., Cruceta, A., Brien, W.A.O., Pantaleo, G., Pumarola, T., Gallart, T., Miró, J.M., Gatell, J.M., 1999. Dynamics of viral load rebound and immunological changes after stopping effective antiretroviral therapy. AIDS 13, F79–F86.

Gardiner, D., Lalezari, J., Lawitz, E., DiMicco, M., Ghalib, R., Reddy, K.R., Chang, K.M., Sulkowski, M., Marro, S.O., Anderson, J., He, B., Kansra, V., McPhee, F., Wind-Rotolo, M., Grasela, D., Selby, M., Korman, A.J., Lowy, I., 2013. A Randomized, Double-Blind, Placebo-Controlled Assessment of BMS-936558, a Fully Human Monoclonal Antibody to Programmed Death-1 (PD-1), in Patients with Chronic Hepatitis C Virus Infection. PLoS One 8, e63818.

Gattinoni, L., Lugli, E., Ji, Y., Pos, Z., Paulos, C., Quigley, M., Almeida, J., Gostick, E., Yu, Z., Carpentino, C., Wang, E., Douek, D., Price, D.A., June, C.H., Marincola, F., Roederer, M., Restifo, N., 2012. A human memory T-cell subset with stem cell-like properties. Nat. Med. 17, 1290–1297.

Golden, M., Muhire, B.M., Semegni, Y., Martin, D.P., 2014. Patterns of recombination in HIV-1M are influenced by selection disfavouring the survival of recombinants with disrupted genomic RNA and protein structures. PLoS One 9, 1–8.

Gona, P., Van Dyke, R.B., Williams, P.L., Dankner, W.M., Chernoff, M.C., Nachman, S.A., Seage, G.R., 2006. Incidence of opportunistic and other infections in HIV-infected children in the HAART era. J. Am. Med. Assoc. 296, 292–300.

Gortmaker, S.L., Hughes, M., Cervia, J., Brady, M., Johnson, G.M., Seage, G.R., Song, L.Y., Dankner, W.M., Oleske, J.M., 2001. Effect of Combination Therapy Including Protease Inhibitors on Mortality among Children and Adolescents Infected with HIV-1. N. Engl. J. Med. 345, 1522–1528.

Granich, R., Crowley, S., Vitoria, M., Smyth, C., Kahn, J.G., Bennett, R., Lo, Y., Souteyrand, Y., Williams, B., 2010. Highly active antiretroviral treatment as prevention of HIV transmission: Review of scientific evidence and update. Curr Opin HIV AIDS 5, 298–304.

Grau-Expósito, J., Serra-Peinado, C., Miguel, L., Navarro, J., Curran, A., Burgos, J., Ocaña, I., Ribera, E., Torrella, A., Planas, B., Badía, R., Castellví, J., Falcó, V., Crespo, M., Buzon, M.J., 2017. A novel single-cell FISH-flow assay identifies effector memory CD4+T cells as a major niche for HIV-1 transcription in HIV-infected patients. MBio 8, 1–18.

Groot, F., Welsch, S., Sattentau, Q.J., 2008. Efficient HIV-1 transmission from macrophages to T cells across transient virological synapses. Blood 111, 4660–4663.

Gupta, R.K., Abdul-jawad, S., Mccoy, L.E., Mok, H.P., Peppa, D., Salgado, M., Martinez-picado, J., Nijhuis, M., Wensing, A.M.J., Lee, H., Grant, P., Nastouli, E., Lambert, J., Pace, M., Salasc, F., Monit, C., Innes, A., Muir, L., Waters, L., Frater, J., Lever, A.M.L., Edwards, S.G., Gabriel, I.H., Olavarria, E., 2019. HIV-1

remission following CCR5Δ32/Δ32 haematopoietic stem-cell transplantation. Nature 4, 1–20.

Gupta, S., Neogi, U., Srinivasa, H., Shet, A., 2013. High concordance of genotypic coreceptor prediction in plasma-viral RNA and proviral DNA of HIV-1 subtype C: Implications for use of whole blood DNA in resource-limited settings. J. Antimicrob. Chemother. 68, 2003–2006.

Gutierrez, C., Serrano-Villar, S., Madrid-Elena, N., Perez-Elias, M., Barbas, C., Ruiperez, J., Munoz, E., 2016. Bryostatin-1 for latent virus reactivation in HIV-infected patients on antiretroviral therapy. Aids 30, 1385–1392.

Halper-Stromberg, A., Lu, C.L., Klein, F., Horwitz, J.A., Bournazos, S., Nogueira, L., Eisenreich, T.R., Liu, C., Gazumyan, A., Schaefer, U., Furze, R.C., Seaman, M.S., Prinjha, R., Tarakhovsky, A., Ravetch, J. V., Nussenzweig, M.C., 2014. Broadly neutralizing antibodies and viral inducers decrease rebound from HIV-1 latent reservoirs in humanized mice. Cell 158, 989–999.

Han, Y., Lin, Y.B., An, W., Xu, J., Yang, H., Connell, K.O., Dordai, D., Boeke, J.D., Siliciano, J.D., Siliciano, R.F., 2008. Orientation-dependent Regulation of Integrated HIV-1 Expression by Host Gene Transcriptional Readthrough. Cell Host Microbe 4, 134–146.

Hansen, S., Ford, J., Lewis, M., Ventura, A., Hughes, C., Coyne-Johnson, L., Whizin, N., Oswald, K., Shemaker, R., Swanson, T., Legasse, A., Chuichiolo, M., Parks, C., Axthelm, M., 2011. Profound early control of highly pathogenic SIV by an effector memory T-cell vaccine. Nature 473, 523–527.

Hansen, S., Piatak, M., Ventura, A., Hughes, C., Gilbride, R., Ford, J., Oswald, K., Shoemaker, R., Li, Y., Lewis, M., Gilliam, A., Xu, G., Whizin, N., Burwitz, B., Planer, S., Turner, J., Legasse, A., Axthelm, M., Nelson, J., 2013. Immune Clearance of highly pathogenic SIV infection. Nature 502, 100–104.

Harris, R.S., Bishop, K.N., Sheehy, A.M., Craig, H.M., Petersen-Mahrt, S.K., Watt, I.N., Neuberger, M.S., Malim, M.H., 2003. DNA deamination mediates innate immunity to retroviral infection. Cell 113, 803–809.

Hatano, H., Delwart, E.L., Norris, P.J., Lee, T., Torsten, B., Kelley, C.F., Hunt, P.W., Hoh, R., Linnen, J.M., Jeffrey, N., Busch, M.P., Deeks, S.G., 2011. Evidence of persistent Low-level Viremia in Long-term HAART-suppressed, HIV-Infected Individuals. AIDS 24, 2535–2539.

Haworth, K.G., Schefter, L.E., Norgaard, Z.K., Ironside, C., Adair, J.E., Kiem, H., 2018. HIV infection results in clonal expansions containing integrations within pathogenesis-related biological pathways. J. Clin. Invest. 3, 1–18.

Hellerstein, M.K., Hoh, R.A., Hanley, M.B., Cesar, D., Lee, D., Neese, R.A., Mccune, J.M., 2003. Subpopulations of long-lived and short-lived T cells in advanced HIV-1 infection. J. Clin. Invest. 112, 956–966.

Henrich, T.J., 2018. Dolutegravir intensification and HIV persistence: 3 + 1 = 3. Lancet 5, E201–E202.

Henrich, T.J., Gallien, S., Li, J.Z., Pereyra, F., Kuritzkes, D.R., 2012. Low-Level Detection and Quantitation of Cellular HIV-1 DNA and 2-LTR Circles Using Digital PCR. J. Virol. Methods 186, 68–72.

Henrich, T.J., Hanhauser, E., Marty, F.M., Sirignano, M.N., Keating, S., Lee, T., Robles, Y.P., Davis, B.T., Jonathan, Z., Heisey, A., Hill, A.L., Busch, M.P., Armand, P., Robert, J., 2014. Antiretroviral-Free HIV-1 Remission and Viral Rebound Following Allogeneic Stem Cell Transplantation: A Report of Two Cases. Ann. Intern. Med. 161, 319–327.

Hiener, B., Horsburgh, B.A., Eden, J.S., Barton, K., Schlub, T.E., Lee, E., von Stockenstrom, S., Odevall, L., Milush, J.M., Liegler, T., Sinclair, E., Hoh, R., Boritz, E.A., Douek, D., Fromentin, R., Chomont, N., Deeks, S.G., Hecht, F.M., Palmer, S., 2017. Identification of Genetically Intact HIV-1 Proviruses in Specific CD4+T Cells from Effectively Treated Participants. Cell Rep. 21, 813–822.

Hill, A.L., Rosenbloom, D.I.S., Fu, F., Nowak, M. a, Siliciano, R.F., 2014. Predicting the outcomes of treatment to eradicate the latent reservoir for HIV-1. Proc. Natl. Acad. Sci. 111, 13475–13480.

Hill, M., Tachedjian, G., Johnson, M., 2005. The Packaging and Maturation of the HIV-1 Pol Proteins. Curr. HIV Res. 3, 73–85.

Ho, D.D., Rota, T.R., Hirsch, M.S., 1986. Infection of monocyte/macrophages by human T lymphocyte virus

type III. J. Clin. Invest. 77, 1712–1715.

Ho, Y.-C., Shan, L., Hosmane, N.N., Wang, J., Laskey, S.B., Rosenbloom, D.I.S., Lai, J., Blankson, J.N., Siliciano, J.D., Siliciano, R.F., 2013. Replication-competent noninduced proviruses in the latent reservoir increase barrier to HIV-1 cure. Cell 155, 540–51.

Hoffmann, C., Welz, T., Sabranski, M., Kolb, M., Wolf, E., Stellbrink, H., Wyen, C., 2017. Higher rates of neuropsychiatric adverse events leading to dolutegravir discontinuation in women and older patients. HIV Med. 18, 56–63.

Hong, F., Aga, E., Cillo, A., Yates, A.L., Besson, G., Fyne, E., Koontz, D.L., Jennings, C., Zheng, L., Mellors, J.W., 2016. Novel assays to measure total cell-associated HIV-1 DNA and RNA. J. Clin. Microbiol. 54, 902–911.

Horiike, M., Iwami, S., Kodama, M., Sato, A., Watanabe, Y., Yasui, M., Ishida, Y., Kobayashi, T., Miura, T., Igarashi, T., 2012. Lymph nodes harbor viral reservoirs that cause rebound of plasma viremia in SIV-infected macaques upon cessation of combined antiretroviral therapy. Virology 423, 107–118.

Hosmane, N.N., Kwon, K.J., Bruner, K.M., Capoferri, A.A., Beg, S., Rosenbloom, D.I.S., Keele, B.F., Ho, Y.-C., Siliciano, J.D., Siliciano, R.F., 2017. Proliferation of latently infected CD4 $^{+}$ T cells carrying replication-competent HIV-1: Potential role in latent reservoir dynamics. J. Exp. Med. 214, 959–972.

Huang, J., Wang, F., Argyris, E., Chen, K., Liang, Z., Tian, H., Huang, W., Squires, K., Verlinghieri, G., Zhang, H., 2007. Cellular microRNAs contribute to HIV-1 latency in resting primary CD4+T lymphocytes. Nat. Med. 13, 1241–1247.

Huang, S.-H., Walker, B.D., Jones, R.B., 2018. Latent HIV reservoirs exhibit inherent resistance to elimination by CD8 + T cells The Journal of Clinical Investigation. J. Clin. Invest. 128, 876–889.

Huang, Y., Hoque, M.T., Jenabian, M.A., Vyboh, K., Whyte, S.K., Sheehan, N.L., Brassard, P., Bélanger, M., Chomont, N., Fletcher, C. V., Routy, J.P., Bendayan, R., 2016. Antiretroviral drug transporters and metabolic enzymes in human testicular tissue: Potential contribution to HIV-1 sanctuary site. J. Antimicrob. Chemother. 71, 1954–1965.

Hudson, R.R., Boos, D.D., Kaplan, N.L., 1992. A statistical test for detecting geographic subdivision. Mol. Biol. Evol. 9, 138–151.

Hutter, G., Nowak, D., Mossner, M., Ganepola, S., Mubig, A., Allers, K., Schneider, T., Hofmann, J., Kucherer, C., Blau, O., Blau, I.W., Hofmann, W.K., Thiel, E., 2009. Long-Term Control of HIV by CCR5 Delta32/Delta32 Stem-Cell Transplantation. N. Engl. J. Med. 7, 692–698.

Ikeda, T., Shibata, J., Yoshimura, K., Koito, A., Matsushita, S., 2007. Recurrent HIV-1 Integration at the BACH2 Locus in Resting CD4 + T Cell Populations during Effective Highly Active Antiretroviral Therapy. J. Infect. 195, 716–725.

Imamichi, H., Dewar, R.L., Adelsberger, J.W., Rehm, C.A., Doherty, U.O., Paxinos, E.E., 2016. Defective HIV-1 proviruses produce novel protein- coding RNA species in HIV-infected patients on combination antiretroviral therapy. Proc. Natl. Acad. Sci. 113, 8783–8788.

Imamichi, H., Natarajan, V., Adelsberger, J.W., Rehm, C.A., Lempicki, R.A., Das, B., Hazen, A., Imamichi, T., Lane, H.C., 2014. Lifespan of effector memory CD4 R T cells determined by replication-incompetent integrated HIV-1 provirus. AIDS 28, 1091–1099.

Jain, V., Hartogensis, W., Bacchetti, P., Hunt, P.W., Hatano, H., Sinclair, E., Epling, L., Lee, T., Busch, M.P., Mccune, J.M., Pilcher, C.D., Hecht, F.M., Deeks, S.G., 2013. Antiretroviral Therapy Initiated Within 6 Months of HIV Infection Is Associated With Lower T-Cell Activation and Smaller HIV Reservoir Size. J. Infect. Dis. 208, 1202–1211.

Jenuwein, T., Allis, C.D., 2001. Translating the Histone Code. Science (80-.). 293, 1074–1081.

Joos, B., Fischer, M., Kuster, H., Pillai, S.K., Wong, J.K., Boni, J., Hirschel, B., Weber, R., Trkola, A., Gunthard, H.F., 2008. HIV rebounds from latently infected cells, rather than from continuing low-level replication. Proc. Natl. Acad. Sci. 105, 16725–16730.

Josefsson, L., von Stockenstrom, S., Faria, N.R., Sinclair, E., Bacchetti, P., Killian, M., Epling, L., Tan, A., Ho, T., Lemey, P., Shao, W., Hunt, P.W., Somsouk, M., Wylie, W., Douek, D.C., Loeb, L., Custer, J., Hoh, R., Poole, L., Deeks, S.G., Hecht, F., Palmer, S., 2013. The HIV-1 reservoir in eight patients on long-term suppressive antiretroviral therapy is stable with few genetic changes over time. Proc. Natl. Acad. Sci. 110, E4987–E4996.

Joseph, S.B., Kincer, L.P., Bowman, N.M., Evans, C., Vinikoor, M.J., Lippincott, C.K., Gisslén, M., Spudich, S., Menezes, P., Robertson, K., Archin, N., Kashuba, A., Eron, J.J., Price, R.W., Swanstrom, R., 2018. HIV-1 RNA Detected in the CNS after Years of Suppressive Antiretroviral Therapy Can Originate from a Replicating CNS Reservoir or Clonally Expanded Cells. Clin. Infect. Dis. ciy1066.

Jourdain, G., Mary, J.-Y., Coeur, S. Le, Ngo-Giang-Huong, N., Yuthavisuthi, P., Limtrakul, A., Traisathit, P., McIntosh, K., Lallemant, M., 2007. Risk factors for in utero or intrapartum mother-to-child transmission of human immunodeficiency virus type 1 in Thailand. J. Infect. Dis. 196, 1629–1636.

Judd, A., Doerholt, K., Tookey, P.A., Sharland, M., Riordan, A., Menson, E., Novelli, V., Lyall, E.G.H., Masters, J., Tudor-Williams, G., Duong, T., Gibb, D.M., 2007. Morbidity, Mortality, and Response to Treatment by Children in the United Kingdom and Ireland with Perinatally Acquired HIV Infection during 1996-2006: Planning for Teenage and Adult Care. Clin. Infect. Dis. 45, 918–924.

Kaminski, R., Bella, R., Yin, C., Otte, J., Ferrante, P., Gendelman, H.E., Li, H., Booze, R., Gordon, J., Hu, W., Khalili, K., 2016. Excision of HIV-1 DNA by Gene Editing: A Proof-of-Concept In Vivo Study. Gene Ther. 23, 690–695.

Kao, S., Calman, A., Luciw, P., Peterlin, M., 1987. Anti-termination of transcription within the long terminal repeat of HIV-1 by tat gene product. Nature 330, 489–493.

Katlama, C., Deeks, S.G., Autran, B., Martinez-Picado, J., van Lunzen, J., Rouzioux, C., Miller, M., Vella, S., Schmitz, J.E., Ahlers, J., Richman, D.D., Sekaly, R.P., 2013. Barriers to a cure for HIV: new ways to target and eradicate HIV-1 reservoirs. Lancet 381, 2109–17.

Kearney, M., Maldarelli, F., Shao, W., Margolick, J.B., Daar, E.S., Mellors, J.W., Rao, V., Coffin, J.M., Palmer, S., 2009. Human immunodeficiency virus type 1 population genetics and adaptation in newly infected individuals. J. Virol. 83, 2715–2727.

Kearney, M., Palmer, S., Maldarelli, F., Shao, W., Polis, M.A., Rock-kress, D., Margolick, J.B., Coffin, J.M., Mellors, J.W., 2008. Frequent polymorphism at drug resistance sites in HIV-1 protease and reverse transcriptase. AIDS 22, 497–501.

Kearney, M.F., Anderson, E.M., Coomer, C., Smith, L., Shao, W., Johnson, N., Kline, C., Spindler, J., Mellors, J.W., Coffin, J.M., Ambrose, Z., 2015. Well-mixed plasma and tissue viral populations in RT-SHIV-infected macaques implies a lack of viral replication in the tissues during antiretroviral therapy. Retrovirology 12, 1–17.

Kearney, M.F., Spindler, J., Shao, W., Yu, S., Anderson, E.M., O'Shea, A., Rehm, C., Poethke, C., Kovacs, N., Mellors, J.W., Coffin, J.M., Maldarelli, F., 2014. Lack of detectable HIV-1 molecular evolution during suppressive antiretroviral therapy. PLoS Pathog. 10, e1004010.

Kearney, M.F., Wiegand, A., Shao, W., Coffin, J.M., Mellors, J.W., Lederman, M., Gandhi, R.T., Keele, B.F., Li, J.Z., 2016. Origin of Rebound Plasma HIV Includes Cells with Identical Proviruses That Are Transcriptionally Active before Stopping of Antiretroviral Therapy. J. Virol. 90, 1369–1376.

Kearney, M.F., Wiegand, A., Shao, W., McManus, W.R., Bale, M.J., Luke, B., Maldarelli, F., Mellors, J.W., Coffin, J.M., 2017. Ongoing HIV Replication During ART Reconsidered. Open Forum Infect. Dis. 4, 4–8.

Kelly, J., Beddall, M., Yu, D., Iyer, S., Marsh, J., Wu, Y., 2008. Human Macrophages Support Persistent Transcription From Unintegrated HIV-1 DNA. Virology 372, 300–312.

Kessing, C.F., Nixon, C.C., Li, C., Tsai, P., Takata, H., Mousseau, G., Ho, P.T., Honeycutt, J.B., Fallahi, M., Trautmann, L., Garcia, J.V., Valente, S.T., 2017. In Vivo Suppression of HIV Rebound by Didehydro-Cortistatin A, a "Block-and-Lock" Strategy for HIV-1 Treatment. Cell Rep. 21, 600–611.

Kieffer, T.L., Kwon, P., Nettles, R.E., Han, Y., Ray, S.C., Siliciano, R.F., 2005. G-A Hypermutation in Protease and Reverse Transcriptase Regions of Human Immunodeficiency Virus Type 1 Residing in Resting CD4+ T Cells In Vivo. J. Virol. 79, 1975–1980.

Kim, M., Siliciano, R.F., 2016. Reservoir expansion by T-cell proliferation may be another barrier to curing HIV infection Homeostatic proliferation. Proc. Natl. Acad. Sci. 113, 1692–1694.

Kiselinova, M., Pasternak, A.O., De Spiegelaere, W., Vogelaers, D., Berkhout, B., Vandekerckhove, L., 2014. Comparison of droplet digital PCR and seminested real-time PCR for quantification of cell-associated HIV-1 RNA. PLoS One 9, e85999.

Kitchen, S.G., Levin, B.R., Bristol, G., Rezek, V., Kim, S., Aguilera-Sandoval, C., Balamurugan, A., Yang, O.O., Zack, J.A., 2012. In vivo suppression of HIV by antigen specific T cells derived from engineered hematopoietic stem cells. PLoS Pathog. 8, e1002649.

Klein, N., Palma, P., Luzuriaga, K., Pahwa, S., Nastouli, E., Gibb, D.M., Rojo, P., Borkowsky, W., Bernardi, S., Zangari, P., Calvez, V., Compagnucci, A., Wahren, B., Foster, C., Munoz-fernández, M.Á., Rossi, A. De, Maraňon, G., 2015. Early antiretroviral therapy in children perinatally infected with HIV : a unique opportunity to implement immunotherapeutic approaches to prolong viral remission. Lancet 3099, 1–7.

Klein, N., Sefe, D., Mosconi, I., Zanchetta, M., Castro, H., Jacobsen, M., Jones, H., Bernardi, S., Pillay, D., Giaquinto, C., Walker, a S., Gibb, D.M., De Rossi, A., 2013. The immunological and virological consequences of planned treatment interruptions in children with HIV infection. PLoS One 8, e76582.

Koelsch, K.K., Lui, L., Haubrich, R., May, S., Havlir, D., Gunthard, H.F., Ignacio, C.C., Campos-Soto, P., Little, S.J., Shafer, R., Robbins, G., D'Aquila, R., Kawano, Y., Young, K., Dao, P., Spina, C., Richman, D.D., Wong, J.K., 2008. Dynamics of total, linear nonintegrated, and integrated HIV-1 DNA in vivo and in vitro. J. Infect. Dis. 197, 411–419.

Koenig, S., Gendelman, H.E., Orenstein, J.M., Canto, M.C., Pezeshkpour, H., Yungbluth, M., Janotta, F., Aksamit, A., Martin, M.A., Fauci, A.S., 1986. Detection of AIDS Virus in Macrophages in Brain Tissue from AIDS Patients with Encephalopathy. Science (80-.). 233, 1089–1093.

Korber, B.T., Foley, B.T., Kuiken, C.L., Pillai, S.K., Sodroski, J.G., 1998. Numbering positions in HIV relative to HXB2CG. Hum. retroviruses AIDS 3, 102–111.

Kordelas, L., Verheyen, J., Esser, S., 2014. Shift of HIV Tropism in Stem-Cell Transplantation with *CCR5* Delta32 Mutation. N. Engl. J. Med. 371, 880–882.

Kovari, H., Weber, R., 2011. Influence of antiretroviral therapy on liver disease. Curr. Opin. HIV AIDS 6, 272–277.

Kumar, A., Herbein, G., 2014. The macrophage: a therapeutic target in HIV-1 infection. Mol. Cell. Ther. 2, 1–15.

Lai, S., Bartlett, J., Lai, H., Moore, R., Cofrancesco, J., Pannu, H., Tong, W., Meng, W., Sun, H., Fishman, E.K., 2009. Long-Term Combination Antiretroviral Therapy Is Associated with the Risk of Coronary Plaques in African Americans with HIV Infection. AIDS Patient Care STDS 23, 815–824.

Lee, G.Q., Orlova-Fink, N., Einkauf, K., Chowdhury, F.Z., Sun, X., Harrington, S., Kuo, H.H., Hua, S., Chen, H.R., Ouyang, Z., Reddy, K., Dong, K., Ndung'U, T., Walker, B.D., Rosenberg, E.S., Yu, X.G., Lichterfeld, M., 2017. Clonal expansion of genome-intact HIV-1 in functionally polarized Th1 CD4+T cells. J. Clin. Invest. 127, 2689–2696.

Lenasi, T., Contreras, X., Peterlin, B.M., 2008. Transcriptional Interference Antagonizes Proviral Gene Expression to Promote HIV Latency. Cell Host Microbe 4, 123–133.

Leroy, V., Newell, M.L., Dabis, F., Peckham, C., Van de Perre, P., Bulterys, M., Kind, C., Simonds, R.J., Wiktor, S., Msellati, P., 1998. International multicentre pooled analysis of late postnatal mother-to-child transmission of HIV-1 infection. Ghent International Working Group on Mother-to-Child Transmission of HIV. Lancet 352, 597–600.

Li, J.Z., Etemad, B., Ahmed, H., Aga, E., Bosch, R.J., John, W., Kuritzkes, D.R., Lederman, M.M., Para, M., Gandhi, R.T., Hospital, G., 2016. The Size of the Expressed HIV Reservoir Predicts Timing of Viral Rebound after Treatment Interruption. AIDS 30, 343–353.

Li, L., Liang, S., Chen, L., Lui, W., Li, H., Lui, Y., Bao, Z., Wang, Z., Zhuang, D., Lui, S., Li, J., 2010. Genetic Characterization of 13 Subtype CRF01_AE Near Full-Length Genomes in Guangxi, China. AIDS Res. Hum. Retroviruses 26, 699–704.

Li, S., Juarez, J., Alali, M., Dwyer, D., Collman, R., Cunningham, A., Naif, H.M., 1999. Persistent CCR5 Utilization and Enhanced Macrophage Tropism by Primary Blood Human Immunodeficiency Virus Type 1 Isolates from Advanced Stages of Disease and Comparison to Tissue-Derived Isolates. J. Virol. 73, 9741–9755.

Lilian, R., Kalk, E., Technau, K., Sherman, G., 2013. Birth diagnosis of HIV infection in infants to reduce infant mortality and monitor for elimination of mother-to-child transmission. Pediatr. Infect. Dis. J. 32, 1080–1085.

Lisziewicz, J., Toke, E., 2013. Nanomedicine applications towards the cure of HIV. Nanomedicine 9, 28–38.

Lorenzi, J.C., Cohen, Y. z, Cohn, L.B., Kreider, E.F., Barton, J.P., Learn, G.H., Oliveira, T., Lavine, C.L., Joshua, A., Settler, A., Jankovic, M., Seaman, M.S., Arup, K., Hahn, B.H., Caskey, M., Michel, C., 2017. Paired quantitative and qualitative assessment of the replication-competent HIV-1 reservoir and comparison with integrated proviral DNA. Proc. Natl. Acad. Sci. 114, E648–E649.

Lorenzo-Redondo, R., Fryer, H.R., Bedford, T., Kim, E.Y., Archer, J., Kosakovsky Pond, S.L., Chung, Y.S., Penugonda, S., Chipman, J.G., Fletcher, C. V., Schacker, T.W., Malim, M.H., Rambaut, A., Haase, A.T., McLean, A.R., Wolinsky, S.M., 2016. Persistent HIV-1 replication maintains the tissue reservoir during therapy. Nature 530, 51–56.

Lu, C., Murakowski, D.K., Bournazos, S., Schoofs, T., Halper-stromberg, A., Horwitz, J.A., Nogueira, L., Golijanin, J., Gazumyan, A., Ravetch, J. V, Caskey, M., Chakraborty, A.K., Nussenzweig, M.C., 2016. Enhanced clearance of HIV-1-infected cells by anti-HIV-1 broadly neutralizing antibodies in vivo. Science (80-.). 352, 1001–1004.

Lusic, M., Marcello, A., Cereseto, A., Giacca, M., 2003. Regulation of HIV-1 gene expression by histone acetylation and factor recruitment at the LTR promoter. Eur. Mol. Biol. Organ. 22, 6550–6561.

Luzuriaga, K., Gay, H., Ziemniak, C., Sanborn, K., Somasundaran, M., Rainwater-Lovett, K., Mellors, J.W., Rosenbloom, D.I.S., Persaud, D., 2015. Viremic Relapse Following Prolonged Antiretroviral-Free HIV-1 Remission in a Perinatally Infected Child. N. Engl. J. Med. 372, 786–788.

Luzuriaga, K., Manus, M.M.C., Catalina, M., Mayack, S., Sharkey, M., Stevenson, M., Sullivan, J.L., The, F.O.R., Investigators, P., 2000. Early Therapy of Vertical Human Immunodeficiency Virus Type 1 (HIV-1) Infection : Control of Viral Replication and Absence of Persistent HIV-1-Specific Immune Responses. J. Virol. 74, 6984–6991.

Luzuriaga, K., Tabak, B., Garber, M., Chen, Y.H., Ziemniak, C., McManus, M.M., Murray, D., Strain, M.C., Richman, D.D., Chun, T.W., Cunningham, C.K., Persaud, D., 2014. HIV Type 1 (HIV-1) Proviral reservoirs decay continuously under sustained Virologic control in HIV-1-infected children who received early treatment. J. Infect. Dis. 210, 1529–1538.

Lynch, H., Goldberg, G., Chidgey, A., Van den Brink, M., Boyd, R., Sempowski, G., 2011. Thymic involution and immune reconstitution. Trends Immunol. 30, 366–373.

Ma, Q., Vaida, F., Wong, J., Sanders, C.A., Kao, Y., Croteau, D., Clifford, D.B., Collier, A.C., Gelman, B.B., Marra, C.M., Mcarthur, J.C., Morgello, S., Simpson, D.M., Heaton, R.K., Grant, I., Letendre, S.L., Group, C., 2016. Long-term efavirenz use is associated with worse neurocognitive functioning in HIV-infected patients. J. Neurovirol. 22, 170–178.

Maldarelli, F., Palmer, S., King, M.S., Wiegand, A., Polis, M.A., Mican, J.A., Kovacs, J.A., Davey, R.T., Rock-Kress, D., Dewar, R., Liu, S., Metcalf, J.A., Rehm, C., Brun, S.C., Hanna, G.J., Kempf, D.J., Coffin, J.M., Mellors, J.W., 2007. ART suppresses plasma HIV-1 RNA to a stable set point predicted by pretherapy

viremia. PLoS Pathog. 3, 484–488.

Maldarelli, F., Wu, X., Su, L., Simonetti, F.R., Shao, W., Hill, S., Spindler, J., Ferris, A.L., Mellors, J.W., Kearney, M.F., Coffin, J.M., Hughes, S.H., 2014. Specific HIV integration sites are linked to clonal expansion and persistence of infected cells. Science (80-.). 345, 179–183.

Mangeat, B., Turelli, P., Caron, G., Friedli, M., Perrin, L., Trono, D., 2003. Broad antiretroviral defence by human APOBEC3G through lethal editing of nascent reverse transcripts. Nature 424, 99–103.

Margolis, D.M., Garcia, J.V., Hazuda, D., Haynes, B.F., 2016. Latency reversal and viral clearance to cure HIV-1. Science (80-.). 353.

Martínez-bonet, M., Puertas, M.C., Fortuny, C., Ouchi, D., Mellado, M.J., Rojo, P., 2015. Establishment and Replenishment of the Viral Reservoir in Perinatally HIV-1-infected Children Initiating Very Early Antiretroviral Therapy. Clin. Infect. Dis. 61, 1169–1178.

Mascio, M. Di, Paik, C.H., Carrasquillo, J.A., Maeng, J., Jang, B., Shin, I.S., Srinivasula, S., Byrum, R., Neria, A., Kopp, W., Catalfamo, M., Nishimura, Y., Reimann, K., Martin, M., Lane, H.C., 2009. Non-Invasive In Vivo Imaging of CD4 Cells in simian-human immunodeficiency virus (SHIV)- Infected nonhuman primates. Blood 114, 328–338.

Massanella, M., Yek, C., Shefa, N., Lada, S.M., Strain, M.C., Richman, D.D., 2016. Improved assays to measure the inducible latent HIV reservoir. In: Keystone Synposia: HIV Persistence Pathogenesis and Eradication. CA:Olympic Valley.

McMahon, D., Jones, J., Wiegand, A., Gange, S.J., Kearney, M., Palmer, S., McNulty, S., Metcalf, J.A., Acosta, E., Rehm, C., Coffin, J.M., Mellors, J.W., Maldarelli, F., 2010. Short-Course Raltegravir Intensification Does Not Reduce Persistent Low-Level Viremia in Patients with HIV-1 Suppression during Receipt of Combination Antiretroviral Therapy. Clin. Infect. Dis. 50, 912–919.

McManus, M., Mick, E., Hudson, R., Mofenson, L.M., Sullivan, J.L., Somasundaran, M., Luzuriaga, K., 2016. Early combination antiretroviral therapy limits exposure to HIV-1 replication and cell-associated HIV-1 DNA levels in infants. PLoS One 11, 1–10.

McManus, W.R., Bale, M.J., Spindler, J., Wiegand, A., Musick, A., Wu, X., Wells, D., Hughes, S.H., Keele, B.F., Hoh, R.A., Milush, J.M., Coffin, J.M., Mellors, J.W., Deeks, S.G., Kearney, M.F., 2018. No evidence for ongoing HIV replication in lyphm nodes during suppressive ART. In: Conference on Retroviruses and Opportunistic Infections. Boston Massachusetts, p. 70.

Mehandru, S., Poles, M.A., Tenner-Racz, K., Horowitz, A., Hurley, A., Hogan, C., Boden, D., Racz, P., Markowitz, M., 2004. Primary HIV-1 Infection Is Associated with Preferential Depletion of CD4 $^{+}$ T Lymphocytes from Effector Sites in the Gastrointestinal Tract. J. Exp. Med. 200, 761–770.

Mellins, C., Tassiopoulos, K., Malee, K., Moscicli, A.-B., Patton, D., Smith, R., Usitalo, A., Allison, S., Van Dyke, R., Seage, G.R., 2011. Behavioral Health Risks in Perinatally HIV-Exposed Youth : to Antiretroviral Treatment. AIDS Patient Care STDS 25, 413–422.

Mellins, C.A., Brackis-Cott, E., Dolezal, C., Abrams, E.J., 2004. The role of psychosocial and family factors in adherence to antiretroviral treatment in human immunodeficiency virus-infected children. Pediatr. Infect. Dis. J. 23, 1035–1041.

Metcalf Pate, K.A., Pohlmeyer, C.W., Walker-Sperling, V.E., Foote, J.B., Najarro, K.M., Cryer, C.G., Salgado, M., Gama, L., Engle, E.L., Shirk, E.N., Queen, S.E., Chioma, S., Vermillion, M.S., Bullock, B., Li, M., Lyons, C.E., Adams, R.J., Zink, M.C., Clements, J.E., Mankowski, J.L., Blankson, J.N., 2015. A murine viral outgrowth assay to detect residual HIV type 1 in patients with undetectable viral loads. J. Infect. Dis. 212, 1387–1396.

Miller, V., Sabin, C., Hertogs, K., Bloor, S., Martinez-Picado, J., D'Aquila, R., Larder, B., Lutz, T., Gute, P., Weidmann, E., Rabenau, H., Phillips, A., Staszewski, S., 2000. Virological and immunological effects of treatment interruptions in HIV-1 infected patients with treatment failure. AIDS 14, 2857–67.

Mitchell, R.S., Beitzel, B.F., Schroder, A.R.W., Shinn, P., Chen, H., Berry, C.C., Ecker, J.R., Bushman, F.D., 2004.

Retroviral DNA integration: ASLV, HIV, and MLV show distinct target site preferences. PLoS Biol. 2, e234.

Mok, H.P., Norton, N.J., Hirst, J.C., Fun, A., Bandara, M., Wills, M.R., Lever, A.M.L., 2018. No evidence of ongoing evolution in replication competent latent HIV-1 in a patient followed up for two years. Sci. Rep. 8, 1–6.

Montalto, G.J., Sawe, F.K., Miruka, A., Maswai, J., Kiptoo, I., Aoko, A., Oreyo, C., Obiero, E., Korir, S., Bii, S.K., Song, K.X., Kunz, A.N., 2017. Diagnosis disclosure to adolescents living with HIV in rural Kenya improves antiretroviral therapy adherence and immunologic outcomes : A retrospective cohort study. PLoS One 12, 1–11.

Murray, J., McBride, K., Boesecke, C., Bailey, M., Amin, J., Suzuki, K., Baker, D., Zaunders, J., Emery, S., Cooper, D.A., Koelsch, K.K., Kelleher, A.D., 2012. Integrated HIV DNA accumulates prior to treatment while episomal HIV DNA records ongoing transmission afterwards. AIDS 26, 543–550.

Mylvaganam, G.H., Silvestri, G., Amara, R.R., National, Y., 2016. HIV Therapeutic Vaccines: Moving towards a Functional Cure. Curr. Opin. Immunol. 1–8.

Narasipura, S., Henderson, L.J., Fu, S.W., Chen, L., Kashanchi, F., Al-Harthi, L., 2012. Role of B Catenin and TCF/LEF Family Members in Transcriptional Activity of HIV in Astrocytes. J. Virol. 86, 1911–1921.

Newell, M.L., Coovadia, H., Cortina-Borja, M., Rollins, N., Gaillard, P., Dabis, F., 2004. Mortality of infected and uninfected infants born to HIV-infected mothers in Africa: a pooled analysis. Lancet 364, 1236–1243.

Nishimura, Y., Sadjadpour, R., Mattapallil, J.J., Igarashi, T., Lee, W., Buckler-white, A., Roederer, M., Chun, T., Martin, M.A., 2009. High frequencies of resting CD4 + T cells containing integrated viral DNA are found in rhesus macaques during acute lentivirus infections. Proc. Natl. Acad. Sci. 106, 8015–8020.

Offersen, R., Nissen, S.K., Tolstrupa, M., 2016. A Novel Toll-Like Receptor 9 Agonist, MGN1703, Enhances HIV-1 Transcription and NK Cell-Mediated Inhibition of HIV-1-Infected Autologous CD4 T Cells. J. Virol. 90, 4441–4453.

Olivares-Villagómez, D., Van Kaer, L., 2018. Intestinal Intraepithelial Lymphocytes: Sentinels of the Mucosal Barrier. Trends Immunol. 39, 264–275.

Pace, M., Williams, J., Kurioka, A., Gerry, A.B., Jakobsen, B., Klenerman, P., Nwokolo, N., Fox, J., Fidler, S., Frater, J., 2016. Histone Deacetylase Inhibitors Enhance CD4 T Cell Susceptibility to NK Cell Killing but Reduce NK Cell Function. PLoS Pathog. 12, e1005782.

Paillart, J.C., Berthoux, L., Ottmann, M., Darlix, J.L., Marquet, R., Ehresmann, B., Ehresmann, C., 1996. A dual role of the putative RNA dimerization initiation site of human immunodeficiency virus type 1 in genomic RNA packaging and proviral DNA synthesis. J. Virol. 70, 8348–54.

Palella, F.J., Delaney, K.M., Moorman, A.C., Loveless, M.O., Fuhrer, J., Satten, G.A., Aschman, D.J., Holmberg, S.D., 1998. Declining morbidity and mortality among patients with advanced Human Immunodeficiency Virus infection. N. Engl. J. Med. 339, 853–860.

Pallikkuth, S., Sharkey, M., Babic, D.Z., Gupta, S., Stone, G.W., Fischl, M.A., Stevenson, M., Pahwa, S., 2016. Peripheral T Follicular Helper Cells Are the Major HIV Reservoir within Central Memory CD4 T Cells in Peripheral Blood from Chronically HIV-Infected Individuals on Combination Antiretroviral Therapy. J. Virol. 90, 2718–2728.

Palmer, S., Kearney, M., Maldarelli, F., Elias, K., Bixby, C.J., Bazmi, H., Rock, D., Jr, R.T.D., Dewar, R.L., Julia, A., Hammer, S., Mellors, J.W., Coffin, J.M., Halvas, E.K., Falloon, J., Davey, R.T., Metcalf, J.A., 2005. Multiple , Linked Human Immunodeficiency Virus Type 1 Drug Resistance Mutations in Treatment-Experienced Patients Are Missed by Standard Genotype Analysis Multiple , Linked Human Immunodeficiency Virus Type 1 Drug Resistance Mutations in Treatment-Experie. J. Clin. Microbiol. 43, 403.

Palmer, S., Wiegand, A.P., Maldarelli, F., Bazmi, H., Mican, J.M., Polis, M., Dewar, R.L., Planta, A., Liu, S., Metcalf, J.A., Mellors, J.W., Coffin, J.M., Al, P.E.T., Icrobiol, J.C.L.I.N.M., 2003. New Real-Time Reverse Transcriptase-Initiated PCR Assay with Single-Copy Sensitivity for Human Immunodeficiency Virus Type

1 RNA in Plasma. J. Clin. Microbiol. 41, 4531–4536.

Parikh, U.M., McCormick, K., Van Zyl, G., Mellors, J.W., 2017. Future technologies for monitoring HIV drug resistance and cure. Curr. Opin. HIV AIDS 12, 182–189.

Park, J., Morrow, C.D., 1991. Overexpression of the gag-pol Precursor from Human Immunodeficiency Virus Type 1 Proviral Genomes Results in Efficient Proteolytic Processing in the Absence of Virion Production. J. Virol. 65, 5111–5117.

Payne, H., Mkhize, N., Otwombe, K., Lewis, J., Panchia, R., Callard, R., Morris, L., Babiker, A., Violari, A., Cotton, M.F., Klein, N.J., Gibb, D.M., 2015. Reactivity of routine HIV antibody tests in children who initiated antiretroviral therapy in early infancy as part of the Children with HIV Early Antiretroviral Therapy (CHER) trial: a retrospective analysis. Lancet Infect. Dis. 15, 803–809.

Perreau, M., Savoye, A.-L., De Crignis, E., Corpataux, J.-M., Cubas, R., Haddad, E.K., De Leval, L., Graziosi, C., Pantaleo, G., 2013. Follicular helper T cells serve as the major CD4 T cell compartment for HIV-1 infection, replication, and production. J. Exp. Med. 210, 143–156.

Persaud, D., Gay, H., Ziemniak, C., Chen, Y.H., Piatak, M., Chun, T.-W., Strain, M., Richman, D., Luzuriaga, K., 2013. Absence of detectable HIV-1 viremia after treatment cessation in an infant. N. Engl. J. Med. 369, 1828–35.

Persaud, D., Palumbo, P.E., Ziemniak, C., Hughes, M.D., Alvero, C.G., Luzuriaga, K., Yogev, R., Capparelli, E. V, Chadwick, E.G., 2012. Dynamics of the resting CD4(+) T-cell latent HIV reservoir in infants initiating HAART less than 6 months of age. AIDS 26, 1483–90.

Persaud, D., Patel, K., Karalius, B., Rainwater-Lovett, K., Ziemniak, C., Ellis, A., Chen, Y.H., Richman, D.D., Siberry, G.K., Van Dyke, R., Burchett, S., Seage, G., Luzuriaga, K., 2014. Age at Virologic Control Influences Peripheral Blood HIV Reservoir Size and Serostatus in Perinatally-Infected Adolescents. JAMA Pediatr. 168, 1138–1146.

Persaud, D., Ray, S.C., Kajdas, J., Ahonkhai, A., Siberry, G.K., Ferguson, K., Ziemniak, C., Quinn, T.C., Casazza, J.P., Zeichner, S., Gange, S.J., Watson, D.C., 2007. Slow human immunodeficiency virus type 1 evolution in viral reservoirs in infants treated with effective antiretroviral therapy. AIDS Res. Hum. Retroviruses 23, 381–90.

Persaud, D., Siberry, G.K., Ahonkhai, A., Kajdas, J., Monie, D., Hutton, N., Watson, D.C., Quinn, T.C., Ray, S.C., Siliciano, R.F., 2004. Continued production of drug-sensitive human immunodeficiency virus type 1 in children on combination antiretroviral therapy who have undetectable viral loads. J. Virol. 78, 968–79.

Phelps, R., Rakhmanina, N., 2011. Antiretroviral Drugs in Pediatric HIV-Infected Patients Pharmacokinetic and Practical Challenges. Pediatr. Drugs 13, 175–192.

Pinzone, M.R., Vanbelzen, D.J., Weissman, S., Bertuccio, M.P., Cannon, L., Hwang, W., Sherman, B., Doherty, U.O., 2018. Proviral sequencing suggests the majority of the HIV reservoir is expressed over time but significant decay is obscured by clonal expansion. bioRxiv 1–26.

Pollack, R.A., Jones, B.R., Pertea, M., Bruner, K.M., Martin, A.R., Thomas, A.S., Capoferri, A.A., Beg, S.A., Huang, S.-H., Karandish, S., Hao, H., Halper-Stromberg, E., Yong, P.C., Kovacs, C., Benko, E., Siliciano, R.F., Ho, Y.-C., 2017. Defective HIV-1 proviruses are expressed and can be recognized by cytotoxic T lymphocytes which shapes the proviral landscape. Cell Host Microbe 21, 494–506.

Procopio, F.A., Fromentin, R., Kulpa, D.A., Brehm, J.H., Bebin, A.G., Strain, M.C., Richman, D.D., O'Doherty, U., Palmer, S., Hecht, F.M., Hoh, R., Barnard, R.J.O., Miller, M.D., Hazuda, D.J., Deeks, S.G., Sékaly, R.P., Chomont, N., 2015. A Novel Assay to Measure the Magnitude of the Inducible Viral Reservoir in HIV-infected Individuals. EBioMedicine 2, 874–883.

Qu, X., Wang, P., Ding, D., Li, L., Wang, H., Ma, L., Zhou, X., Liu, Shaohui, Lin, S., Wang, X., Zhang, G., Liu, Sijie, Liu, L., Wang, J., Zhang, F., Lu, D., Zhu, H., 2013. Zinc-finger-nucleases mediate specific and efficient excision of HIV-1 proviral DNA from infected and latently infected human T cells. Nucleic Acids Res. 41, 7771–7782.

Quayle, A.J., Xu, C., Mayer, K.H., Anderson, D.J., Pantaleo, G., Soudeyns, H., Demarest, J.F., Vaccarezza, M., Graziosi, C., Paolucci, S., Daucher, M., Cohen, O.J., Denis, F., Biddison, W.E., Sekaly, R.P., Fauci, A.S., Chun, T.W., Stuyver, L., Mizell, S.B., Ehler, L.A., Mican, J.A., Baseler, M., Lloyd, A.L., Nowak, M.A., 1997. T lymphocytes and macrophages, but not motile spermatozoa, are a significant source of human immunodeficiency virus in semen. J. Infect. Dis. 176, 960–968.

Rainwater-Lovett, K., Ziemniak, C., Watson, D., Luzuriaga, K., Siberry, G., Petru, A., Chen, Y.H., Uprety, P., Mcmanus, M., Ho, Y.C., Lamers, S.L., Persaud, D., 2017. Paucity of intact non-induced provirus with early, long-Term antiretroviral therapy of perinatal HIV infection. PLoS One 12, 1–15.

Ranki, A., Lagerstedt, A., Ovod, V., Aavik, E., Krohn, K., 1994. Expression kinetics and subcellular localization of HIV-1 regulatory proteins Nef, Tat and Rev in acutely and chronically infected lymphoid cell lines. Arch. Virol. 139, 365–378.

Rasmussen, T.A., Lewin, S.R., 2016. Shocking HIV out of hiding: Where are we with clinical trials of latency reversing agents? Curr. Opin. HIV AIDS 11, 394–401.

Rasmussen, T.A., McMahon, J.H., Chang, J.J., Audsley, J., Rhodes, A., Tennakoon, S., Dantanarayana, A., Spelman, T., Schmidt, T., Kent, S.J., Morcilla, V., Palmer, S., Elliott, J.H., Lewin, S.R., 2018. The effect of antiretroviral intensification with dolutegravir on residual virus replication in HIV-infected individuals: a randomised, placebo-controlled, double-blind trial. Lancet HIV 5, e221–e230.

Rasmussen, T.A., Tolstrup, M., Brinkmann, C.R., Olesen, R., Erikstrup, C., Solomon, A., Winckelmann, A., Palmer, S., Dinarello, C., Buzon, M., Lichterfeld, M., Lewin, S.R., Ostergaard, L., Søgaard, O.S., 2014. Panobinostat, a histone deacetylase inhibitor, for latent virus reactivation in HIV-infected patients on suppressive antiretroviral therapy: A phase 1/2, single group, clinical trial. Lancet HIV 1, e13–e21.

Reeves, D.B., Duke, E.R., Wagner, T.A., Palmer, S.E., Spivak, A.M., Schiffer, J.T., 2018. A majority of HIV persistence during antiretroviral therapy is due to infected cell proliferation. Nat. Commun. 9, 4811.

Robertson, D., Anderson, J., Bradac, J., Carr, J.K., Foley, B.T., Funkhouser, R., Gao, F., Hahn, B.H., Kuiken, C.L., Learn, G.H., Leitner, T., McCutchan, F., Osmanov, S., Peeters, M., Pieniazek, D., Kalish, M., Salminen, M., Sharp, P., Wolinsky, S., Korber, B.T., 2000. HIV-1 Nomenclature Proposal. Science (80-.). 288, 55–65.

Rose, R., Lamers, S.L., Nolan, D.J., Maidji, E., Faria, N.R., Pybus, O.G., Dollar, J.J., Maruniak, S.A., McAvoy, A.C., Salemi, M., Stoddart, C.A., Singer, E.J., McGrath, M.S., 2016. HIV Maintains an Evolving and Dispersed Population in Multiple Tissues during Suppressive Combined Antiretroviral Therapy in Individuals with Cancer. J. Virol. 90, 8984–8993.

Rosenbloom, D.I.S., Elliott, O., Hill, A.L., Henrich, T.J., Siliciano, J.M., Siliciano, R.F., 2015. Designing and Interpreting Limiting Dilution Assays: General Principles and Applications to the Latent Reservoir for Human Immunodeficiency Virus-1. Open Forum Infect. Dis. 1–9.

Rosenbloom, D.I.S., Hill, A.L., Laskey, S.B., Siliciano, R.F., 2017. Re-evaluating evolution in the HIV reservoir. Nature 551, E6–E9.

Rouzine, I.M., Coffin, J.M., 2010. Multi-site adaptation in the presence of infrequent recombination. Theor. Popul. Biol. 77, 189–204.

Sabin, C.A., 2013. Do people with HIV infection have a normal life expectancy in the era of combination antiretroviral therapy? BMC Med. 11, 1–7.

Sabin, C.A., Reiss, P., Ryom, L., Phillips, A.N., Weber, R., Law, M., Fontas, E., Mocroft, A., Wit, S. De, Smith, C., Dabis, F., Monforte, A., 2016. Is there continued evidence for an association between abacavir usage and myocardial infarction risk in individuals with HIV ? A cohort collaboration. BMC Med. 14, 1–14.

Sáez-Cirión, A., Bacchus, C., Hocqueloux, L., Avettand-Fenoel, V., Girault, I., Lecuroux, C., Potard, V., Versmisse, P., Melard, A., Prazuck, T., Descours, B., Guergnon, J., Viard, J.P., Boufassa, F., Lambotte, O., Goujard, C., Meyer, L., Costagliola, D., Venet, A., Pancino, G., Autran, B., Rouzioux, C., 2013. Post-Treatment HIV-1 Controllers with a Long-Term Virological Remission after the Interruption of Early Initiated Antiretroviral Therapy ANRS VISCONTI Study. PLoS Pathog. 9, e1003211.

Salazar-Gonzalez, J.F., Bailes, E., Pham, K.T., Salazar, M.G., Guffey, M.B., Keele, B.F., Derdeyn, C. a, Farmer, P., Hunter, E., Allen, S., Manigart, O., Mulenga, J., Anderson, J. a, Swanstrom, R., Haynes, B.F., Athreya, G.S., Korber, B.T.M., Sharp, P.M., Shaw, G.M., Hahn, B.H., 2008. Deciphering human immunodeficiency virus type 1 transmission and early envelope diversification by single-genome amplification and sequencing. J. Virol. 82, 3952–70.

Salminen, M.O., Koch, C., Sanders-Buell, E., Ehrenberg, P.K., Michael, N.L., Carr, J.K., Burke, D.S., McCutchan, F.E., 1995. Recovery of Virtually Full-Length HIV-1 Provirus of Diverse Subtypes from Primary Virus Cultures Using the Polymerase Chain Reaction. Virology 213, 80–86.

Sanchez, G., Xu, X., Chermann, J.C., Hirsch, I., 1997. Accumulation of defective viral genomes in peripheral blood mononuclear cells of human immunodeficiency virus type 1-infected individuals. J. Virol. 71, 2233–40.

Sarkar, I., Hauber, I., Hauber, J., Buchholz, F., 2007. HIV-1 proviral DNA excision using an evolved recombinase. Science (80-.). 316, 1912–1915.

Scheid, J.F., Horwitz, J.A., Bar-on, Y., Kreider, E.F., Lu, L., Lorenzi, J.C.C., Feldmann, A., Braunschweig, M., Nogueira, L., Oliveira, T., Shimeliovich, I., Patel, R., Burke, L., Cohen, Y.Z., Hadrigan, S., Settler, A., Witmer-pack, M., Jr, A.P.W., Juelg, B., Keler, T., Hawthorne, T., Zingman, B., Gulick, R.M., Pfeifer, N., Gerald, H., Seaman, M.S., Bjorkman, P.J., Klein, F., Sarah, J., Walker, B.D., Hahn, B.H., Nussenzweig, M.C., Caskey, M., Hospital, G., Algorithmics, A., 2016. HIV-1 antibody 3BNC117 suppresses viral rebound in humans during treatment interruption. Nature 535, 556–560.

Scherzer, R., Estrella, M., Li, Y., Deeks, S., Grunfeld, C., Shlipak, M., 2012. Association of Tenofovir Exposure with Kidney Disease Risk in HIV Infection. AIDS 26, 867–875.

Schlatter, A.F., Deathe, A.R., Vreeman, R.C., 2016. The Need for Pediatric Formulations to Treat Children with HIV. AIDS Res. Treat. 2016, 1–8.

Schuetz, A., Deleage, C., Sereti, I., Rerknimitr, R., Phanuphak, N., Phuang-Ngern, Y., Estes, J.D., Sandler, N.G., Sukhumvittaya, S., Marovich, M., Jongrakthaitae, S., Akapirat, S., Fletscher, J.L.K., Kroon, E., Dewar, R., Trichavaroj, R., Chomchey, N., Douek, D.C., O'Connell, R.J., Ngauy, V., Robb, M.L., Phanuphak, P., Michael, N.L., Excler, J.L., Kim, J.H., de Souza, M.S., Ananworanich, J., 2014. Initiation of ART during Early Acute HIV Infection Preserves Mucosal Th17 Function and Reverses HIV-Related Immune Activation. PLoS Pathog. 10, e1004543.

Sethi, A.K., Celentano, D.D., Gange, S.J., Moore, R.D., Gallant, J.E., 2003. Association between Adherence to Antiretroviral Therapy and Human Immunodeficiency Virus Drug Resistance. Clin. Infect. Dis. 37, 1112–1118.

Shan, L., Deng, K., Shroff, N.S., Durand, C.M., Rabi, S.A., Yang, H.-C., Zhang, H., Margolick, J.B., Blankson, J.N., Siliciano, R.F., 2012. Stimulation of HIV-1-specific cytolytic T lymphocytes facilitates elimination of latent viral reservoir after virus reactivation. Immunity 36, 491–501.

Sharova, N., Swingler, C., Sharkey, M., Stevenson, M., 2005. Macrophages archive HIV-1 virions for dissemination in trans. EMBO J. 24, 2481–2489.

Shetty, R., Velu, V., Titanji, K., Bosinger, S., Freeman, G., Silvestri, G., Amara, R.R., 2012. PD-1 blockade during chronic SIV infection reduces hyperimmune activation and microbial translocation in rhesus macaques. J. Clin. Invest. 122, 1712–6.

Siliciano, J.D., Kajdas, J., Finzi, D., Quinn, T.C., Chadwick, K., Margolick, J.B., Kovacs, C., Gange, S.J., Siliciano, R.F., 2003. Long-term follow-up studies confirm the stability of the latent reservoir for HIV-1 in resting CD4+ T cells. Nat. Med. 9, 727–728.

Siliciano, J.D., Siliciano, R.F., 2005. Enhanced culture assay for detection and quantitation of latently infected, resting CD4+ T-cells carrying replication-competent virus in HIV-1-infected individuals. Methods Mol. Biol. 304, 3–15.

Siliciano, R.F., Greene, W.C., 2011. HIV latency. Cold Spring Harb. Perspect. Med. 1, 1–19.

Simonetti, F., 2015. Residual Viremia caused by clonally expanded tumor-infiltrating CD4+ cells. Conf. Retroviruses Opportunistic Infect. Seattle, W.

Simonetti, F.R., Sobolewski, M.D., Fyne, E., Shao, W., Spindler, J., Hattori, J., Halvas, E.K., Besson, G., Penrose, K.J., Yang, Z., Kwan, R.W., Waes, C. Van, Piatak, M., Keele, B.F., Kearney, M.F., Coffin, J.M., Hughes, S.H., Mellors, J.W., Maldarelli, F., 2016. Clonally expanded CD4 + T cells can produce infectious HIV-1 in vivo. Proc. Natl. Acad. Sci. 113, 1883–1888.

Søgaard, O.S., Graversen, M.E., Leth, S., Olesen, R., Brinkmann, C.R., Nissen, S.K., Kjaer, A.S., Schleimann, M.H., Denton, P.W., Hey-Cunningham, W.J., Koelsch, K.K., Pantaleo, G., Krogsgaard, K., Sommerfelt, M., Fromentin, R., Chomont, N., Rasmussen, T.A., Østergaard, L., Tolstrup, M., 2015. The Depsipeptide Romidepsin Reverses HIV-1 Latency In Vivo. PLoS Pathog. 11, e1005142.

Spiegel, H., Herbst, H., Niedobitek, G., Foss, H.D., Stein, H., 1992. Follicular dendritic cells are a major reservoir for human immunodeficiency virus type 1 in lymphoid tissues facilitating infection of CD4+ T-helper cells. Am. J. Pathol. 140, 15–22.

Spivak, A.M., Andrade, A., Eisele, E., Hoh, R., Bacchetti, P., Bumpus, N.N., Emad, F., Buckheit, R., Ccance-Katz, E.F., Lai, J., Kennedy, M., Chander, G., Siliciano, R.F., Siliciano, J.D., Deeks, S.G., 2014. A pilot study assessing the safety and latency-reversing activity of disulfiram in HIV-1-infected adults on antiretroviral therapy. Clin. Infect. Dis. 58, 883–890.

Steingrover, R., Pogány, K., Fernandez Garcia, E., Jurriaans, S., Brinkman, K., Schuitemaker, H., Miedema, F., Lange, J.M., Prins, J.M., 2008. HIV-1 viral rebound dynamics after a single treatment interruption depends on time of initiation of highly active antiretroviral therapy. Aids 22, 1583–1588.

Stellenbosch University, HEALTH RESEARCH ETHICS COMMITTEE, 2015. Guideline for Paediatric Blood Volume for Research Purposes, Health Research Ethics Committee (HREC).

Strain, M.C., Lada, S.M., Luong, T., Rought, S.E., Gianella, S., Terry, V.H., Spina, C.A., Woelk, C.H., Richman, D.D., 2013. Highly Precise Measurement of HIV DNA by Droplet Digital PCR. PLoS One 8, e55943.

Strain, M.C., Little, S.J., Daar, E.S., Havlir, D. V, Gunthard, H.F., Lam, R.Y., Daly, O. a, Nguyen, J., Ignacio, C.C., Spina, C. a, Richman, D.D., Wong, J.K., 2005. Effect of treatment, during primary infection, on establishment and clearance of cellular reservoirs of HIV-1. J. Infect. Dis. 191, 1410–8.

Strongin, Z., Sharaf, R., VanBelzen, D.J., Jacobson, J.M., Connick, E., Volberding, P., Skiest, D.J., Gandhi, R.T., Kuritzkes, D.R., O'Doherty, U., Li, J.Z., 2018. Effect of Short-Term Art Interruption on Levels of Integrated Hiv Dna. J. Virol. 92, JVI.00285-18.

Suzuki, K., Hattori, S., Marks, K., Ahlenstiel, C., Maeda, Y., Ishida, T., Millington, M., Boyd, M., Symonds, G., Cooper, D.A., Okada, S., Kelleher, A.D., 2013. Promoter Targeting shRNA Suppresses HIV-1 Infection In vivo Through Transcriptional Gene Silencing. Mol. Ther. - Nucleic Acids 2, e137.

Tateishi, H., Monde, K., Anraku, K., Koga, R., Hayashi, Y., Ciftci, H.I., Demirci, H., Higashi, T., Motoyama, K., Arima, H., Otsuka, M., Fujita, M., 2017. A clue to unprecedented strategy to HIV eradication: "Lock-in and apoptosis." Sci. Rep. 7, 1–8.

Teasdale, C., Marais, B., Abrams, E., 2011. HIV: prevention of mother-to-child transmission. Clin. Evid. (Online). 1, 1–33.

Tebas, P., Stein, D., Tang, W., Frank, I., Wang, S., Lee, G., Spratt, K., Surosky, R., Giedlin, M., Nichol, M., 2014. Gene Editing of CCR5 in Autologous CD4 T Cells of Persons Infected with HIV. N. Engl. J. Med. 370, 901–910.

Temin, H.M., 1993. Retrovirus variation and reverse transcription: abnormal strand transfers result in retrovirus genetic variation. Proc. Natl. Acad. Sci. U. S. A. 90, 6900–6903.

Thompson, K.A., Cherry, C.L., Bell, J.E., McLean, C.A., 2011. Brain cell reservoirs of latent virus in presymptomatic HIV-infected individuals. Am. J. Pathol. 179, 1623–1629.

Tobin, N.H., Learn, G.H., Holte, S.E., Wang, Y., Melvin, A.J., McKernan, J.L., Pawluk, D.M., Mohan, K.M., Lewis, P.F., Mullins, J.I., Frenkel, L.M., 2005. Evidence that low-level viremias during effective highly active

antiretroviral therapy result from two processes: expression of archival virus and replication of virus. J. Virol. 79, 9625–9634.

Treisman, G.J., Kaplin, A.I., 2002. Neurologic and psychiatric complications of antiretroviral agents. AIDS 16, 1201–1215.

Tsai, A., Irrinki, A., Kaur, J., Cihlar, T., Kukolj, G., Sloan, D.D., Murry, J.P., 2017. Toll-Like Receptor 7 Agonist GS-9620 Induces HIV Expression and HIV-Specific Immunity in Cells from HIV-Infected Individuals on Suppressive Antiretroviral Therapy. J. Virol. 91, e02166-16.

UNAIDS, 2018a. 2017 Global HIV Statistics.

UNAIDS, 2018b. Global AIDS Monitoring 2018: Indicators for monitoring the 2016 United Nations Political Declaration on Ending AIDS.

Valentin, A., Rosati, M., Patenaude, D.J., Hatzakis, A., Kostrikis, L.G., Lazanas, M., Wyvill, K.M., Yarchoan, R., Pavlakis, G.N., 2002. Persistent HIV-1 infection of natural killer cells in patients receiving highly active antiretroviral therapy. Proc. Natl. Acad. Sci. 99, 7015–7020.

van Zyl, G., Bale, M.J., Kearney, M.F., 2018. HIV evolution and diversity in ART-treated patients. Retrovirology 15, 1–12.

Van Zyl, G.U., Bedison, M.A., Janse van Rensburg, A., Laughton, B., Cotton, M.F., Mellors, J.W., 2014. Early antiretroviral therapy in South African children reduces HIV-1 infected cells and cell-associated HIV-1 RNA in blood mononuclear cells. J Infect Dis 1–5.

Veazey, R.S., DeMaria, M.A., Chalifoux, L. V., Shvetz, D.E., Pauley, D.R., Knight, H.L., Rosenzweig, M., Johnson, R.P., Desrosiers, R.C., Lackner, A.A., 1998. Gastrointestinal tract as a major site of CD4+T cell depletion and viral replication in SIV infection. Science (80-.). 280, 427–431.

Veenhuis, R.T., Bushman, F.D., Joel, N., Veenhuis, R.T., Kwaa, A.K., Garliss, C.C., Latanich, R., Salgado, M., Pohlmeyer, C.W., Nobles, C.L., Gregg, J., Scully, E.P., Bailey, J.R., Bushman, F.D., Blankson, J.N., 2018. Long-term remission despite clonal expansion of replication-competent HIV-1 isolates Find the latest version : Long-term remission despite clonal expansion of replication-competent HIV-1 isolates. J. Clin. Invest. 3, e122795.

Veldsman, K.A., Maritz, J., Isaacs, S., Katusiime, M.G., Janse Van Rensburg, A., Laughton, B., Mellors, J.W., Cotton, M.F., Van Zyl, G.U., 2018. Rapid decline of HIV-1 DNA and RNA in infants starting very early antiretroviral therapy may pose a diagnostic challenge. Aids 32, 629–634.

Velu, V., Shetty, D.D., Larsson, M., Shankar, E.M., 2015. Role of PD-1 co-inhibitory pathway in HIV infection and potential therapeutic options. Retrovirology 12, 1–17.

Velu, V., Titanji, K., Zhu, B., Husain, S., Lai, L., Vanderford, T.H., Chennareddi, L., Freeman, G.J., Ahmed, R., Amara, R.R., 2009. Enhancing SIV-Specific Immunity In Vivo by PD-1 Blockade. Nature 458, 206–210.

Venter, W.F., Kaiser, B., Pillay, Y., Conradie, F., Gomez, G.B., Clayden, P., Matsolo, M., Amole, C., Rutter, L., Abdullah, F., Abrams, E.J., Casas, C.P., Barnhart, M., Pillay, A., Pozniak, A., Hill, A., Fairlie, L., Boffito, M., Moorhouse, M., Chersich, M., Serenata, C., Quevedo, J., Loots, G., 2017. Cutting the cost of South African antiretroviral therapy using newer, safer drugs. South African Med. J. 107, 28–30.

Verdin, E., Paras, P., Van Lint, C., 1993. Chromatin disruption in the promoter of human immunodeficiency virus type 1 during transcriptional activation. EMBO J. 12, 3249–59.

Vibholm, L., Schleimann, M.H., Højen, J.F., Benfield, T., Offersen, R., Rasmussen, K., Olesen, R., Dige, A., Agnholt, J., Grau, J., Buzon, M., Wittig, B., Lichterfeld, M., Petersen, A.M., Deng, X., Abdel-Mohsen, M., Pillai, S.K., Rutsaert, S., Trypsteen, W., De Spiegelaere, W., Vandekerchove, L., Østergaard, L., Rasmussen, T.A., Denton, P.W., Tolstrup, M., Søgaard, O.S., 2017. Short-course toll-like receptor 9 agonist treatment impacts innate immunity and plasma viremia in individuals with human immunodeficiency virus infection. Clin. Infect. Dis. 64, 1686–1695.

Violari, A., Cotton, M.F., Kuhn, L., Schramm, D.B., Paximadis, M., Loubser, S., Shalekoff, S., Da, B., Dias, C., Otwombe, K., Liberty, A., Mcintyre, J., Babiker, A., Gibb, D., Tiemessen, C.T., 2019. A child with perinatal

HIV infection and long-term sustained virological control following antiretroviral treatment cessation. Nat. Commun. 10, 1–11.

Wada, N.I., Jacobson, L.P., Margolick, J.B., Breen, E.C., Macatangay, B., Penugonda, S., Martínez-maza, O., Bream, J.H., Hopkins, J., Maryland, N.I.W., 2015. The effect of HAART-induced HIV suppression on circulating markers of inflammation and immune activation. AIDS 29, 463–471.

Wagner, T. a, McKernan, J.L., Tobin, N.H., Tapia, K. a, Mullins, J.I., Frenkel, L.M., 2013. An increasing proportion of monotypic HIV-1 DNA sequences during antiretroviral treatment suggests proliferation of HIV-infected cells. J. Virol. 87, 1770–8.

Wagner, T.A., McLaughlin, S., Garg, K., Cheung, C.Y.K., Larsen, B.B., Styrchak, S., Huang, H.C., Edlefsen, P.T., Mullins, J.I., Frenkel, L.M., 2014. Proliferation of cells with HIV integrated into cancer genes contributes to persistent infection. Science (80-.). 345, 570–573.

Walensky, R.P., Paltiel, A.D., Losina, E., Mercincavage, L.M., Schackman, B.R., Sax, P.E., Weinstein, M.C., Freedberg, K.A., 2006. The Survival Benefits of AIDS Treatment in the United States. J. Infect. Dis. 194, 11–19.

Wang, F.X., Xu, Y., Sullivan, J., Souder, E., Argyris, E.G., Acheampong, E.A., Fisher, J., Sierra, M., Thomson, M.M., Najera, R., Frank, I., Kulkosky, J., Pomerantz, R.J., Nunnari, G., 2005. IL-7 is a potent and proviral strain-specific inducer of latent HIV-1 cellular reservoirs of infected individuals on virally suppressive HAART. J. Clin. Invest. 115, 128–137.

Wang, P., Qu, X., Zhou, X., Shen, Y., Ji, H., Fu, Z., Deng, J., Lu, P., Yu, W., Lu, H., Zhu, H., 2015. Two cellular microRNAs, miR-196b and miR-1290, contribute to HIV-1 latency. Virology 486, 228–238.

Wang, Z., Gurule, E.E., Brennan, T.P., Gerold, J.M., Kwon, K.J., Hosmane, N.N., Kumar, M.R., Beg, S.A., Capoferri, A.A., Ray, S.C., Ho, Y.-C., Hill, A.L., Siliciano, J.D., Siliciano, R.F., 2018. Expanded cellular clones carrying replication-competent HIV-1 persist, wax, and wane. Proc. Natl. Acad. Sci. 1–10.

Westermann, J., Pabst, R., 1992. Distribution of lymphocyte subsets and natural killer cells in the human body. Clin. Investig. 70, 539–544.

Whitney, J.B., Hill, A.L., Sanisetty, S., Penaloza-macmaster, P., Liu, J., Shetty, M., Parenteau, L., Cabral, C., Shields, J., Blackmore, S., Smith, J.Y., Brinkman, A.L., Peter, L.E., Mathew, S.I., Smith, K.M., Borducchi, E.N., Rosenbloom, D.I.S., Lewis, M.G., Hattersley, J., Li, B., Hesselgesser, J., Geleziunas, R., Robb, M.L., Kim, J.H., Michael, N.L., Barouch, D.H., 2014. Rapid seeding of the Viral reservoir prior to SIV viraemia in rhesus monkeys. Nature 512, 74–77.

WHO, 2015. PMTCT Strategic Vision 2010–2015 Preventing mother-to-child transmission of HIV to reach the UNGASS and Millennium Development Goals.

Wiegand, A., Spindler, J., Hong, F.F., Shao, W., Cyktor, J.C., Cillo, A.R., Halvas, E.K., 2017. Single-cell analysis of HIV-1 transcriptional activity reveals expression of proviruses in expanded clones during ART. Proc. Natl. Acad. Sci. E3659–E3668.

Williams, J.P., Hurst, J., Stöhr, W., Robinson, N., Brown, H., Fisher, M., Kinloch, S., Cooper, D., Schechter, M., Tambussi, G., Fidler, S., Carrington, M., Babiker, A., Weber, J., Koelsch, K.K., Kelleher, A.D., Phillips, R.E., Frater, J., 2014. HIV-1 DNA predicts disease progression and post-treatment virological control. Elife 3, e03821.

Williams, K.C., Corey, S., Westmoreland, S. V, Pauley, D., Knight, H., DeBakker, C., Alvarez, X., Lackner, A.A., 2001. Perivascular macrophages are the primary cell type productively infected by simian immunodeficiency virus in the brains of macaques: implications for the neuropathogenesis of AIDS. J. Exp. Med. 193, 905–915.

Williams, L.D., Ofek, G., Schätzle, S., Mcdaniel, J.R., Lu, X., Nicely, N.I., Wu, L., Lougheed, C.S., Bradley, T., Mark, K., Mckee, K., Bailer, R.T., Dell, S.O., Georgiev, I.S., Michael, S., Parks, R.J., Marshall, D.J., Anasti, K., Yang, G., Nie, X., Tumba, N.L., Wiehe, K., Wagh, K., Korber, B., Kepler, T.B., 2017. Potent and broad HIV-neutralizing antibodies in memory B cells and plasma. Sci. Immunol. 2, 1–34.

Williams, P.L., Storm, D., Montepiedra, G., Nichols, S., Kammerer, B., Sirois, P.A., Farley, J., Malee, K., 2006. Predictors of Adherence to Antiretroviral Medications in Children and Adolescents With HIV Infection. Pediatrics 118, e1745–e1757.

Wu, X., Li, Y., Crise, B., Burgess, S.M., 2003. Transcription Start Regions in the Human Genome Are Favored Targets for MLV Integration. Science (80-.). 300, 1749–1751.

Xing, S., Bullen, C.K., Shroff, N.S., Shan, L., Yang, H.-C., Manucci, J.L., Bhat, S., Zhang, H., Margolick, J.B., Quinn, T.C., Margolis, D.M., Siliciano, J.D., Siliciano, R.F., 2011. Disulfiram Reactivates Latent HIV-1 in a Bcl-2-Transduced Primary CD4+ T Cell Model without Inducing Global T Cell Activation. J. Virol. 85, 6060–6064.

Yin, C., Zhang, T., Qu, X., Zhang, Y., Putatunda, R., Xiao, X., Li, F., Xiao, W., Zhao, H., Dai, S., Qin, X., Mo, X., Young, W. Bin, Khalili, K., Hu, W., 2017. In Vivo Excision of HIV-1 Provirus by saCas9 and Multiplex Single-Guide RNAs in Animal Models. Mol. Ther. 25, 1168–1186.

Ylisastigui, L., Coull, J.J., Rucker, V.C., Melander, C., Bosch, R.J., Brodie, S.J., Corey, L., Sodora, D.L., Dervan, P.B., Margolis, D.M., 2004. Polyamides reveal a role for repression in latency within resting T cells of HIV-infected donors. J. Infect. Dis. 190, 1429–1437.

Yukl, S.A., Kaiser, P., Kim, P.S., Li, P., 2016. Investigating the Mechanisms that Control HIV Transcription and Latency In Vivo. In: Conference on Retroviruses and Opportunistic Infections.

Yukl, S.A., Shergill, A.K., Ho, T., Killian, M., Girling, V., Epling, L., Li, P., Wong, L.K., Crouch, P., Deeks, S.G., Havlir, D. V., McQuaid, K., Sinclair, E., Wong, J.K., 2013. The distribution of HIV DNA and RNA in cell subsets differs in gut and blood of HIV-positive patients on ART: Implications for viral persistence. J. Infect. Dis. 208, 1212–1220.

Zhang, J., Perelson, A.S., 2013. Contribution of follicular dendritic cells to persistent HIV viremia. J. Virol. 87, 7893–901.

Zhen, A., Kamata, M., Rezek, V., Rick, J., Levin, B.R., Kasparian, S., Chen, I., Yang, O., Zack, J.A., Kitchen, S.G., 2015. HIV-specific Immunity Derived From Chimeric Antigen Receptor-engineered Stem Cells. Mol. Ther. 23, 1358–1367.

Zhuang, J., Jetzt, A.E., Sun, G., Yu, H., Klarmann, G., Ron, Y., Preston, B.D., Dougherty, J.P., 2002. Human immunodeficiency virus type 1 recombination: rate, fidelity, and putative hot spots. J. Virol. 76, 11273–82.